Carriers of a VEGFA enhancer polymorphism selectively binding chop/ddit3 are predisposed to increased circulating levels of thyroid stimulating hormone

Ahluwalia, Tarunveer Singh; Troelsen, Jesper; Balslev-Harder, Marie; Bork-Jensen, Jette; Thuesen, Betina Heinsbæk; Cerqueira, Charlotte; Linneberg, Allan; Grarup, Niels; Pedersen, Oluf; Hansen, Torben; Dalgaard, Louise Torp

Published in:
Journal of Medical Genetics

DOI:
10.1136/jmedgenet-2016-104084

Publication date:
2017

Document Version
Peer reviewed version

Journal of
Medical Genetics

CARRIERS OF A VEGFA ENHANCER POLYMORPHISM SELECTIVELY BINDING CHOP/DDIT3 ARE PREDISPOSED TO INCREASED CIRCULATING LEVELS OF THYROID STIMULATING HORMONE

Journal:	*Journal of Medical Genetics*
Manuscript ID	jmedgenet-2016-104084.R1
Article Type:	Original Article
Date Submitted by the Author:	n/a

Complete List of Authors:	Ahluwalia, Tarunveer; University of Copenhagen, The Novo Nordisk Foundation Center for Basic Metabolic Research, Section of Metabolic Genetics, Faculty of Health and Medical Sciences; Steno Diabetes Center AS Troelsen, Jesper; Roskilde Universitet, Department of Science and Environment Balslev-Harder, Marie; University of Copenhagen, 1The Novo Nordisk Foundation Center for Basic Metabolic Research, Section of Metabolic Genetics, Faculty of Health and Medical Sciences Bork-Jensen, Jette; University of Copenhagen, The Novo Nordisk Foundation Center for Basic Metabolic Research, Section of Metabolic Genetics, Faculty of Health and Medical Sciences Thuesen, Betina; Research Centre for Prevention and Health Cerqueira, Charlotte; Research Centre for Prevention and Health Linneberg, Allan; Research Centre for Prevention and Health Grarup, Niels; Kobenhavns Universitet Sundhedsvidenskabelige Fakultet, The Novo Nordisk Foundation Center for Basic Metabolic Research Pedersen, Oluf; Kobenhavns Universitet Sundhedsvidenskabelige Fakultet, The Novo Nordisk Foundation Center for Basic Metabolic Research Hansen, Torben; Kobenhavns Universitet Sundhedsvidenskabelige Fakultet, The Novo Nordisk Foundation Center for Basic Metabolic Research Dalgaard, Louise; Roskilde Universitet, Department of Science and Environment
Keywords:	thyroíd, Molecular genetics, Metabolic disorders, insulin resistance, transcription factor

CARRIERS OF A *VEGFA* ENHANCER POLYMORPHISM SELECTIVELY BINDING CHOP/DDIT3 ARE PREDISPOSED TO INCREASED CIRCULATING LEVELS OF THYROID STIMULATING HORMONE

Running title: Circulating TSH association with a *VEGFA* functional polymorphism

Tarunveer Singh Ahluwalia[1,2], Jesper Thorvald Troelsen[3], Marie Balslev-Harder[1], Jette Bork-Jensen[1], Betina Heinsbæk Thuesen[4], Charlotte Cerqueira[4], Allan Linneberg[4,5,6], Niels Grarup[1], Oluf Pedersen[1], Torben Hansen[1,7], Louise Torp Dalgaard[3]

[1]The Novo Nordisk Foundation Center for Basic Metabolic Research, Section of Metabolic Genetics, Faculty of Health and Medical Sciences, University of Copenhagen, Copenhagen, Denmark
[2]Steno Diabetes Center, Gentofte, Denmark
[3]Department of Science and Environment, Roskilde University, Roskilde, Denmark
[4]Research Centre for Prevention and Health, The Capital Region, Glostrup, Denmark
[5]Department of Clinical Experimental Research, Rigshospitalet, Copenhagen, Denmark
[6] Department of Clinical Medicine, Faculty of Health and Medical Sciences, University of Copenhagen, Copenhagen, Denmark
[7]Faculty of Health Sciences, University of Southern Denmark, Odense, Denmark

Address correspondence to:

Associate professor Louise Torp Dalgaard, MSc, PhD, Department of Science and Environment, Roskilde University, Universitetsvej 1, DK-4000 Roskilde, Denmark. E-mail: ltd@ruc.dk, phone: +4546742713

Word counts: Text: 4136, Abstract: 250, References: 49, Tables: 2, Supplementary tables: 7

Figures: 4, Supplementary figures: 4

KEYWORDS

thyroid, genetics, metabolic disorders, insulin resistance, transcription factor

ABSTRACT

Background: Levels of serum thyroid stimulating hormone (TSH) indicate thyroid function, because thyroid hormone negatively controls TSH release. Genetic variants in the vascular endothelial growth factor A (*VEGFA*) gene are associated with TSH levels. The aim was to characterize the association of *VEGFA* variants with TSH in a Danish cohort and to identify and characterize functional variants.

Methods: We performed an association study of the *VEGFA* locus for circulating TSH levels in 8445 Danish individuals. Lead variants were tested for allele-specific effects *in vitro* using luciferase reporter and gel-shift assays.

Results: Four SNPs in *VEGFA* were associated with circulating TSH (rs9472138, rs881858, rs943080 and rs4711751). For rs881858, the presence of each G allele was associated with a corresponding decrease in TSH levels of 2.3% (P=8.4×10-9) and an increase in circulating free T4 levels (P=0.0014). Rs881858 is located in a binding site for CHOP (C/EBP homology protein) and C/EBPβ (ccaat enhancer binding protein β). Reporter-gene analysis showed increased basal enhancer activity of the rs881858 A-allele versus the G-allele (34.5±9.9% (average±SEM), P=0.0012), while co-expression of CHOP effectively suppressed the rs881858 A-allele activity. The A-allele showed stronger binding to CHOP in gel-shift assays.

Conclusions: VEGF is an important angiogenic signal required for tissue expansion. We show that *VEGFA* variation giving allele-specific response to transcription factors with overlapping binding sites associate closely with circulating TSH levels. Because CHOP is induced by several types of intracellular stress, this indicates that cellular stress could be involved in the normal or pathophysiological response of the thyroid to TSH.

ABBREVIATIONS

TSH thyroid stimulating hormone, VEGFA vascular endothelial growth factor A, CHOP c/EBP homology protein, c/EBPβ ccaat enhancer binding protein β, CEBPB *C/EBPβ* gene symbol, SNP single nucleotide polymorphism, Chr chromosome, EAF effect allele frequency, BS binding site, ds double-stranded, DTT dithiothreitol, GWAS genome wide association study, BMI body mass index, eQTL expressed quantitative trait locus

INTRODUCTION

The thyroid gland is an essential regulator whole body energy expenditure and metabolic rate. Circulating levels and activities of thyroid hormones, their activating enzymes (deiodinases) and the regulating hormones TSH (thyrotropin/thyroid stimulating hormone) and TRH (thyrotropin releasing hormone) are precisely balanced to ensure the euthyroid state. Circulating levels of TSH comprise a clinically valuable indicator of thyroid function, and in the absence of pituitary or hypothalamic failure, an increased level of TSH is a very sensitive marker of decreased thyroid function. Clinical reference levels for TSH define elevated TSH levels above 4mU/L as being associated with clinically decreased thyroid function[1]. However, there is a marked inter-individual, while low intra-individual variability in circulating TSH levels, as well as in the hypothalamic-pitutary-thyroid axis[2], which appears to be highly heritable as evidenced by heritability estimates of 65% derived from twin studies[3-5].

Subclinical hypothyroidism (TSH above 4mU/L with T4 levels within the reference range) is associated with an impaired metabolic phenotype, cardiovascular risk factors, elevated blood total cholesterol and blood pressure increase, decreased glomerular filtration rate and bone fractures[6]. However, association between TSH within the reference range and obesity is not well established. A meta-analysis encompassing 29 studies, found 18 of these to report a positive association[7]. There have been reports of positive correlations between TSH levels and BMI in obese or over-weight individuals, suggesting decreased thyroid function in these subjects[8-10], but also cross sectional population-based reports have been made for the association between increased TSH levels and BMI[11-13].

Recent genome wide association studies (GWAS) for circulating serum TSH levels have focused on common variants (minor allele frequency (MAF) > 5%) and have identified at least 26 genomic loci to date[14-17] of which one was the Vascular Endothelial Growth Factor A gene (*VEGFA*) (Fig. 1A).

Both the VEGF protein and its receptor, KDR (Kinase Insert Domain Receptor), are highly expressed in the thyroid gland[18]. *In vivo*, TSH administration increases VEGF release from the thyroid gland[19] and treatment of isolated, cultured thyrocytes with TSH also stimulates VEGF release[20]. Variants regulating the activity of the *VEGFA* locus are likely contributors to the observed TSH association[14], because TSH levels indicate thyroid function.

In order to investigate the molecular and genetic mechanisms in the *VEGFA* locus controlling circulating levels of TSH, we performed an association study using densely spaced SNPs of the *VEGFA* genomic region in three population-based cohorts from Denmark comprising 8,445 individuals and meta-analysed them. The lead variants were further investigated to identify allele specific effects using *in vitro* cell based assays to elucidate the molecular mechanism supporting the observed clinical findings.

METHODS

Genetic association analysis

Study participants

The study was conducted in accordance with the Helsinki declaration and approved by the Danish Data Protection Board and by the Ethical Committee of Copenhagen County. Informed written consent was obtained from all subjects before participation. The genetic association analyses were performed in three Danish study cohorts (Inter99, Health2006 and Health2008) that have been described previously elsewhere[21]: 1) The study (ClinicalTrials.gov ID-no: NCT00289237) is a population-based study for ischemic heart disease[22], 2) The Health 2006 Study (Ethical committee approval number: KA20060011) is a population based study comprising individuals aged between 18-69 years from the South Western part of greater Copenhagen area[23]. This study was designed to address chronic health issues, 3) The Health 2008 Study (Ethical committee approval number: KA20060011) is a cross sectional population based study[24].

Biochemical and anthropometric measurements

The biochemical and anthropometric information on and phenotypical characterization of study participants is described in Table S1 and Table S2 and has been presented previously[22-24].

Genotyping, variant calling and quality checks

DNA extraction, genotyping and genotype call processing has been described previously[21 25]. A total of 8,445 individuals ($n_{Inter99}$:5,420, $n_{Health2006}$:2,442, $n_{Health2008}$:583) with complete phenotype and genotype data participated for the serum TSH association analyses. The genotyping platform was Illumina Human Exome 12v1.0 containing 263.894 SNPs (including 16.024 custom SNPs identified from a recent exome sequencing study in Danes[21 25]) post quality control.

SNP Selection

SNPs from the *VEGFA* gene region (6:43737946-6:43754224 GRCh37) and within the adjoining flanking region (±75 Kb) were selected covering a total of 166.2 kb (6:43662946-6:43829224 GRCh37) region. After removing SNPs with a MAF<0.005 a total of 15 non-coding SNPs were available from the *VEGFA* gene region for this study. Based on this SNP selection, a Bonferroni corrected *p* value corresponding 0.0033 was set as the significance threshold for SNP-TSH association testing.

SNP-TSH association testing and meta-analyses

The association testing between the SNPs and the serum TSH levels was performed individually for each cohort using the additive linear regression model adjusting for gender, age and first five principal components as covariates. The fasting circulating measures of TSH were transformed to natural log scale before the association testing to control for non-normalised data. Prior to the association testing, individuals with known thyroid pathologies and those with out of range TSH values (<0.4 mIU/L and >4.0 mU/L) were removed. The method for meta-analyses was as previously described[21].

SNP metabolic traits association

Associations between a SNP and metabolic traits were tested among normal glucose tolerant (NGT) individuals from the Inter99 cohort using the general linear model assuming an additive genetic effect for the SNP. Association was tested with baseline measures and changes during follow-up (Δ values: *Follow up – baseline measurements*) and was adjusted for gender and age. A *p*-value of $p<0.05$ was considered significant for the follow-up and single SNP-metabolic trait testing. All association analyses were performed using PLINK v1.07 (http://pngu.mgh.harvard.edu/purcell/plink/), and R version 3.1.1 (http://www.r-project.org/).

Linkage Disequilibria (LD) estimations

LD estimation and proxy search was performed using 1000 genomes project data and an LD heat-map depicting pairwise r^2 values is available in Fig. S1. Non-genotyped SNPs in LD with TSH-associated SNPs were retrieved from the ENSEMBL genome browser and SNPs with LD≥0.8 were inspected for evidence of differential allele effects using Genome Browser (https://genome.ucsc.edu/) (Table S3).

In vitro molecular biology studies

Reporter gene analysis

The *VEGFA* proximal promoter (hg19, chr6:43737097-43738057), corresponding to 849bp of promoter and 252bp of the first intron, was cloned into pGL4.10. Genomic regions containing rs881858 and rs9472138 were amplified by PCR from homozygous carriers and cloned into *VEGFA* pro/GL4.10 down-stream of the *luc* gene to generate rs88 A/GL4.10, rs88 G/GL4.10, rs94 C/GL4.10 and rs94 T/GL4.10. All constructs were confirmed by sequencing. Plasmid DNA was prepared using Qiagen Maxi Prep kit (Qiagen, Copenhagen Ø, Denmark) and ethanol precipitated. Transfections were made in human embryonic kidney cells (HEK)-293 cells (American Tissue Type Culture Collection, Rockville, MD, U.S.A.) using polyethylene imine (PEI25). Cells were harvested after 24hrs for luciferase assays (Dual Light, Thermofisher Scientific, Copenhagen Ø, Denmark).

Expression vectors for C/EBPβ and CHOP10 were a gift from Peter Johnson (Addgene plasmid #12557) and David Ron (Addgene plasmid # 21899), respectively.

Electrophoretic mobility shift assay (EMSA)

Nuclear extracts from HEK293 cells were prepared as described previously[26]. Some extracts were prepared following incubation of cells with 1mM dithiothreitol (DTT) for 16hrs to induce CHOP10 via the unfolded protein response[27]. Complementary oligos representing the SNPs rs881858 were annealed and labelled with α-^{32}P-dATP (3000 Ci/mmol) by Klenow fill-in and purified using NICK columns (GE Healthcare, Brøndby, Denmark). Binding reactions were made as described previously[26], separated with non-denaturing polyacrylamide gel-electrophoresis and visualized on phosphor-imager screen. Screens were scanned using a Molecular Dynamics Storm Scanner and the protein/DNA complexes analyzed using Image-Quant Software version 3.5. Oligonucleotides used for cloning and EMSA are listed in Table S3.

Statistics for molecular biology experiments

Results are expressed as mean value ± SEM. Statistical analysis was performed in GraphPad Prism software. Effects of SNP constructs were tested using ANOVA with post-hoc t-test and Bonferroni correction. Differences between treatments were considered significant at a P-value<0.05 (two-tailed).

RESULTS

VEGFA and TSH association analyses

We investigated three population-based Danish cohort studies for association analyses of the VEGFA locus with circulating TSH: The Inter99, the Health2006 and Health2008 cohorts[23 24] (Table S1). We searched for genotyped SNPs located up to 75kb up- and downstream of the *VEGFA* transcription start site (TSS) (*VEGFA*: Chr6:43737946-43754224). This region was defined based on the localization of chromatin marks within this region (Chromatin Interaction Analysis by paired-end

sequencing, ChIA-PET indicating interaction with the *VEGFA* gene and localization of nearby transcripts MRPS18A (upstream of VEGFA) and LOC100132354 and C6orf223 downstream of VEGFA) and we identified 15 SNPs in this region (Table 1, Table S4).

Table 1: *VEGFA* SNPs significantly associated with circulating levels of thyroid stimulating hormone (TSH)

SNP name	Position (build 37/hg19)	Location wrt *VEGFA*	Alleles (effect/ other)	EAF	Inter99 *n*=5,420		Health2006 *n*=2,442		Health2008 *n*=583		Combined		
					Effect	*P*	Effect	*P*	Effect	*P*	*N*	*P*	I^2 (P_{HET})
#rs9472138*	43,811,762	Downstream	T/C	0.27	-0.046	4.4×10^{-6}	-0.051	1.0×10^{-3}	-0.041	0.15	8,443	5.9×10^{-9}	0 (0.94)
#rs881858*	43,806,609	Downstream	G/A	0.28	-0.046	2.9×10^{-6}	-0.047	1.9×10^{-3}	-0.038	0.18	8,445	8.4×10^{-9}	0 (0.96)
#rs943080**	43,826,672	Downstream	T/C	0.51	-0.024	0.0053	-0.012	0.35	-0.040	0.12	8,440	0.0016	0 (0.59)
#rs4711751**	43,828,582	Downstream	T/C	0.51	-0.023	0.0089	-0.012	0.32	-0.043	0.09	8,402	0.002	0 (0.58)

#SNPs in LD (r^2>0.4). *SNPs in strong LD (r^2: 0.73, D':0.94). **SNPs in strong LD (r^2: 1.0, D': 1.0). EAF: Effect allele frequency. *VEGFA*: Vascular endothelial growth factor A. I^2: heterozygosity at meta-analyses level. P_{HET}: P value for heterozygosity. List of SNPs not reaching study wide association with circulating TSH-levels is given in Suppl. Table S4.

Four *VEGFA* region SNPs (rs9472138, rs881858, rs943080, and rs4711751) associated with fasting serum TSH levels at a study-wide significance level ($P_{combined}$<0.0033), (Table 1, Fig. 1A and Fig. S2) in up to 8445 individuals following combined-meta analysis of the three cohorts. All four SNPs were in LD with each other (r^2>0.4), and one SNP was a known signal (*VEGFA* rs9472138)[14] for circulating TSH. All the significantly associating SNPs were common (MAF>0.05).

Genomic marks qualifying VEGFA SNPs for further investigation

Common SNPs in high LD (r^2>0.8) (proxy SNPs) with the four significant SNPs in *VEGFA*: rs9472138, rs881858, rs943080 and rs4711751 was obtained from the ENSEMBL browser yielding 12 common SNPs linked with rs9472138 and rs881858 and 3 SNPs with rs943080 and rs4711751 (Table S5, Fig. S1), previously genotyped in the 1000genomes project. These SNPs were considered functional candidates to explain the observed genetic association, because they are common and in high LD with the lead SNPs. Using ENCODE data-tracks on Genome Browser (GRCh37/hg19[28] these SNPs were evaluated based on presence of open chromatin structure (DNase seq), conservation, marks of H3K27Ac (Histone 3, Lysine 27 acetylation) and H3K4Me1 (Histone 3, Lysine 4 mono-methylation) and indication of protein binding to the SNP region by ChIP-seq. Furthermore, it was also assessed if the SNP altered the binding site for factors shown to bind the region by ChIP (Table S5, Fig.1B). From this, it was evident that rs881858 was highly conserved with G being the ancestral allele. Furthermore, rs881858 was located in a region showing marks characteristic of active regulatory elements (*H3K27Ac* and *H3K4Me1* and displaying evidence of close three dimensional proximity to the *VEGFA* promoter (Chromosome Interaction Analysis-Paired End Tags (ChIA-PET). The region was also DNase hypersensitive suggesting an open chromatin structure (Fig. 1B).

Moreover, rs881858 was directly located in a site bound by the transcription factor c/EBPβ (encoded by *CEBPB*) (by ChIP-seq) in multiple cell lines, and predicted to be bound by CHOP. Thus, for rs881858 there is strong evidence of an allele-specific regulatory role. Performing the same analysis

for the other SNPs did not reveal equal evidence of regulatory activity, conservation or protein binding to their vicinity (Table S5, Fig. S3). Rs881858 is located at the 3' end of the c/EBPβ binding site BS in a position, which does not confer specificity to the c/EBPβ binding according to the position weight matrix (PWM) for c/EBPβ (Fig. 1C)[29], whereas the BS for CHOP is predicted to prefer the A-allele of the rs881858 compared with the G-allele. Thus, based on ENSEMBL and ENCODE data and differential predicted binding affinities to c/EBPβ and CHOP, the A and G alleles of rs881858 could confer differential responses.

Association of G-allele of VEGFA rs881858 with decreased circulating TSH, increased thyroid hormone levels and metabolic traits

The effect size of rs881858 on circulating TSH levels was -0.092 ($P=2.2\times10^{-11}$) for the G-allele corresponding to an additive 2.3% decrease in TSH level per allele. Furthermore, free T4 levels were correspondingly increased in GG subjects compared with AA or AG subjects (GG: 15.4 (14.2-16.6) vs AA: 15.0 (13.8-16.3) pmol/L, P=0.0014), indicating a slightly increased thyroid function in GG individuals and an altered set point for the TSH/T4 axis (Table 2). There was no available information on circulating levels of total T3 or thyroid hormone binding globulin for these subjects.

Table 2: Associations between *VEGFA* rs881858 G-allele and metabolic traits in 4,373 normal glucose tolerant (NGT) Danish subjects (Inter99) at baseline

***VEGFA* rs881858**	**GG**	**GA**	**AA**	***Effect**	**SE**	***P***
n	347	1,754	2,272	-	-	-
Age (years)	45 (40-50)	45 (40-50)	45 (40-50)	-	-	-
TSH (mIU/L)	1.11 (0.77-1.56)	1.23 (0.88-1.75)	1.29 (0.90-1.85)	-0.092	0.013	**2.2×10^{-11}**
Free T4 (pmol/L)	15.4 (14.2-16.6)	15.0 (13.9-16.3)	15.0 (13.8-16.3)	0.009	0.002	**1.4×10^{-3}**
BMI (kg/m^2)	25.1 (22.8-28.2)	24.9 (22.8-27.6)	24.9 (22.7-27.5)	0.14	0.095	0.11
Leptin (ng/ml)	5.5 (2.5-10.9)	5.3 (2.4-11.0)	5.3 (2.4-11.3)	0.01	0.022	0.62
HbA1c (%)	5.8 (5.5-6.1)	5.8 (5.5-6.0)	5.8 (5.5-6.0)	0.016	0.008	0.056
Fasting plasma glucose (mmol/L)	5.4 (5.1-5.6)	5.3 (5.0-5.6)	5.3 (5.0-5.6)	0.021	0.008	**0.016**
2-hour glucose during OGTT (mmol/L)	5.6 (4.8-6.4)	5.6 (4.7-6.4)	5.5 (4.7-6.3)	0.072	0.026	**6.1×10^{-3}**
Fasting serum insulin (pmol/L)	32 (23-47.5)	31 (22-45)	31 (21-44)	0.023	0.013	0.073
2-hour insulin during OGTT (pmol/L)	133 (86-221)	131 (83-202)	134 (83-204)	0.013	0.017	0.43
$ISI_{Matsuda}$	3.03 (2.2-4.2)	3.15 (2.24-4.44)	3.19 (2.25-4.47)	-0.02	0.012	0.12
HOMA-IR	1.25 (0.92-1.92)	1.20 (0.83-1.81)	1.20 (0.82-1.76)	0.027	0.013	**0.041**
Insulinogenic index	85.2 (53.3-137.2)	76.0 (47.6-125.1)	77.0 (49.7-129.2)	0.013	0.017	0.45
Disposition index	227.0 (169.3-339.8)	226.0 (159.6-341.0)	231.6 (162.7-352.7)	-0.006	0.015	0.68

Values correspond to median (interquartile range) in non-transformed traits. * G allele as the effect allele assuming an additive genetic model for log transformed traits. ISI Matsuda, HOMA-IR, Insulinogenic index and Disposition index were calculated as described in Supplementary Table S3. *P* values in bold indicate significant results ($P<0.05$).

Since increased circulating TSH levels are associated with an impaired metabolic phenotype, it was tested if rs881858 associated with measures of glucose tolerance. The GG genotype of rs881858 was associated with slightly increased fasting and 2-hour post OGTT plasma glucose levels (P=0.016 and 6.1×10^{-3}) (Table 2) and increased HOMA-IR values (P=0.041) among glucose-tolerant subjects. Body mass index, HbA1c and circulating leptin levels were not associated with carrier-status of the rs881858. Moreover, we investigated measures of insulin release derived from OGTT data in relation to rs881858, but the insulinogenic index and the disposition index were not different between genotypes (Table 2).

Association of G-allele of VEGFA rs881858 with fasting circulating TSH, thyroid hormone levels and metabolic traits after 5-yr follow-up

We studied changes in metabolic traits over the 5 yr follow-up period were studied among glucose tolerant individuals from the Inter99 cohort (Table S2, Table S6). Glucose (HbA1c: 0.66% and fasting plasma glucose: 0.86%) and insulin measures (fasting serum insulin: 3.2%; HOMA-IR: 4.1%) improved over a mean follow-up time of 5.4 years (Table S2). However, none of these measures were associated with the *VEGFA* rs881858 polymorphism. Moreover, changes in BMI, circulating TSH and T4 levels were also not associated with *VEGFA* rs881858 (Table S6). This indicates that the variant could act by modulating a given set point for TSH, since the phenotype of carriers appears to be stable during follow-up.

Reporter-gene analysis of VEGFA rs881858 and rs9472138 alleles

To determine if the most significant TSH associated *VEGFA* SNPs rs881858 or rs9472138 could confer functional changes to the *VEGFA* promoter activity, luciferase reporter vectors representing the SNPs were tested by transfection in HEK293 cells followed by luciferase assays (Fig. 2). Basal activity of the *VEGFA* minimal promoter was very high in HEK293 cells (not shown). The activity of the rs881858 A allele was significantly higher than the G-allele (P=0.0012) (Fig. 2A), while there was no difference between the C and the T-allele of *VEGFA* rs9472138.

The A-allele of *VEGFA* rs881858 is predicted to create a novel binding site for the transcription factor CHOP. To test the response of this site to CHOP, HEK293 cells were transfected with increasing amounts of CHOP expression vector in the presence of either rs881858 A- or G-allele reporter vector (Fig. 2B). With no CHOP over-expression the *VEGFA* A-allele had increased activity compared with the G-allele (as in Fig. 2A). Low amounts of CHOP expression vector increased the G-allele reporter activity, while there was no difference in the activity of the A-allele. Furthermore,

increasing amounts of CHOP activity resulted in significantly decreased activity of the A-allele, indicating that the activity of this site is repressed by CHOP. Thus, the main action of CHOP on the predicted binding site created by rs881858 A was to decrease reporter gene activity, which is in line with CHOP being a transcriptional repressor[30]. When over-expressing c/EBPβ both the *VEGFA* A- and the G-alleles of rs881858 responded by increasing luciferase activities 25% ($P<0.05$) at low levels of c/EBPβ while decreasing at higher amounts of c/EBPβ (Fig. 2C). Since the rs881858 is not located in the core binding site of c/EBPβ (Fig. 1B), this is compatible with an equal response to c/EBPβ by either SNP allele.

The interaction between different amounts of c/EBPβ and CHOP was tested by co-transfection experiments in which varying ratios of c/EBPβ and CHOP were used with reporter vectors. For all combinations of CHOP in the presence of c/EBPβ, CHOP repressed the A-allele luciferase activity, while having no effect on the G-allele (Fig. 2D). Thus, based on reporter-gene assays, the A-allele of *VEGFA* rs881858 creates a novel response element of CHOP effectively repressing the minimal promoter activity of *VEGFA*, while this has no effect on the response to c/EBPβ. Furthermore, the A-allele confers higher reporter-gene activity in the basal state compared to the G-allele.

Binding affinities of VEGFA rs881858 (A/G) alleles

Electrophoretic mobility shift assays (EMSA) were made assess *in vitro* transcription factor binding of *VEGFA* rs881858. Double-stranded (ds)-oligos representing the A-allele and the G-allele and encompassing both the c/EBPβ and the CHOP binding sites were compared with known c/EBPβ and the CHOP binding sites. Labeled 'A' and 'G' oligos formed two strong binding complexes (lane 1 and 6) of which the double band could be removed by competition (COMP) with unlabelled A and G-oligos, as well as with un-labeled CHOP (lane 2 and 9) and c/EBPβ (lane 5) oligos (Fig. 3A). This complex contains CHOP as well as c/EBPβ protein, because of the efficient competition by corresponding unlabelled oligos, and the reduction in band intensity, when adding C/EBPβ antibody

to the binding reaction (lane 10, 'supershift'). Moreover, the intensity of the CHOP complex was increased for the A oligo compared with G, indicating stronger binding of the A probe to CHOP protein (Fig. 3A, lane 1 vs. lane 6, Fig. 3B, lane 5 vs. 6 and 9 vs. 10). One complex was specific for A and G oligos as these efficiently out-compete the radio-labeled probes (Fig. 3A and 3B, arrow), whereas competition using oligos containing known CHOP or c/EBPβ sites did not remove the complex (Fig. 3A, lane 1 vs. 2, 5 vs. 6, 5 vs. 9 and Fig. 3B, lane 1 vs. 2). Thus, both A and G versions of rs881858 can bind CHOP and c/EBPβ *in vitro.*

We also compared A and G oligos with oligos representing known CHOP or C/EBPβ binding sites[30] [31] (Fig. 3B). CHOP and C/EBPβ oligos form complexes with the same mobility shift as A and G oligos. The same lower complex formed with either the CHOP or C/EBPβ probe, consistent with CHOP and C/EBPβ forming heterodimers. UPR induction increased C/EBPβ, A and G complex quantity (Fig. 3B). Furthermore, excess unlabelled CHOP oligo efficiently removed the VEGFA A and G probe binding at the lower complex, but not the top complex (arrow, Fig. 3B). The A oligo consistently formed more lower complex than the G oligo, indicating increased binding strength of this probe. The top complex, specific for the rs881858 site (Fig. 3A and 3B, arrows) suggests that additional proteins may bind the *VEGFA* rs881858 site.

The c/EBPβ probe formed a faint complex (lane 3 and 7 Fig. 3B, lanes 1-3, Fig. 3C), most likely c/EBPβ homo-dimer, because it was super-shifted with c/EBPβ antibody and competed with un-labeled c/EBPβ probe. The known CHOP binding site of the *TRIB3* promoter was used as probe for EMSA (Fig. 3C, lane 4-10). As expected the formed complex formed contained CHOP, shown by efficient competition by unlabelled CHOP ds-oligo (lane 4, Fig. 3C) and decreased complex formation with addition of CHOP antibody (lane 5, Fig. 3C). However, since excess of A or G did not remove TRIB3 probe binding, this indicates that the investigated *VEGFA* binding site has lower affinity for CHOP than the TRIB3 site with no difference between the A-allele and the G-allele of

the rs881858. In summary, the *VEGFA* rs881858 site forms a binding site for both CHOP and c/EBPβ, where the A-allele forms more CHOP complex compared with the G-allele, but where this site measured against a well-characterized CHOP binding site has lower affinity for CHOP.

Public eQTL databases were search in order to determine, if base-line thyroid *VEGFA* mRNA levels correlated with the SNPs significantly associated with TSH. Data from the GTEX database[32] is shown in Figure S4 indicating that base-line thyroid *VEGFA* transcript levels do not depend on genotypes of the SNPs rs881858, rs9472138, rs943080 or rs4711751.

DISCUSSION AND CONCLUSIONS

We focused on the genetic and molecular characterization of the *VEGFA* locus with the aim to identify the functional variant(s) explaining the association with circulating TSH levels[14-17]. We performed a dense association-mapping for *VEGFA* SNPs using data from 8445 Danish individuals, and identified 4 SNPs significantly associated with circulating TSH levels, all of which were located more than 50kb 3' of the coding region. Among the top hits we identified *VEGFA* rs881858, in high LD to the *VEGFA* GWAS SNP rs9472138[14]. The carriers of *VEGFA* rs881858 G allele had a 2.3% decrease in circulating TSH levels in an additive manner. Moreover, the identified SNP rs881858 provided functional evidence of allele specific effects at a VEGFA regulatory region binding CHOP and C/EBPβ proteins, thus connecting cellular stress activated pathways with *VEGFA* gene regulatory activity and thyroid function, because CHOP production is activated by several types of cellular stress, such as endoplasmic reticulum stress, nutrient deprivation or oxidative stress[33].

Thus, data here and elsewhere[14] support that common variation in the *VEGFA* locus is an important determinant of circulating TSH levels. For the *VEGFA* locus, the variants most highly associated with TSH, rs881858 and rs9472138 are located >50kb 3' of the *VEGFA* coding region, and equally

close to a long non-coding RNA (Loc100132354), the function of which is not characterized. However, chromosomal interaction analysis identified contact points between the rs881858 SNP region and the promoter of *VEGFA* indicating control of *VEGFA* gene activity (Fig. 1A).

VEGFA is important for angiogenesis, homeostatic responses and organ growth in multiple tissues or cell types (white adipose tissue [34 35], islets of Langerhans[36 37]), and has also been shown to control T4 to T3 conversion in hypothalamic tanycytes and thereby the feedback control of thyroid hormones to TRH and TSH release[38 39]. *VEGFA* rs881858 is also a known GWAS locus for chronic kidney disease (CKD) and kidney function[40] suggesting a possibility that this SNP controls responses in multiple organs, also as *VEGFA* is expressed ubiquitously. Since T4 levels were correspondingly increased in G-allele carriers, whose TSH levels were decreased, rs881858 seem to act primarily on the thyroid gland.

The G-allele is associated with increased VEGFA response to TSH, an increased T4 release, and presumably increased T3 conversion in the hypothalamus and therefore resulting in decreased TSH release as a hypothalamic-pituitary response. However, it is also a possibility that the action of rs881858 can be on both *VEGFA* expression in the thyroid gland as well as on the hypothalamic tanycytes. Consistent with CHOP being a repressor[41] A-allele carriers have lower T4 and increased TSH: For A-carriers the induction of ER-stress may result in an impaired response to stimulate thyroid growth via *VEGFA* due to increased CHOP binding (Fig.4). Since thyroid VEGF is increased by TSH[19], this is consistent with rs881858 being more important in thyroid than in hypothalamus. Moreover, CHOP deficient mice have increased angiogenesis, showing that CHOP normally acts to limit angiogenesis[42].

Interestingly, the genomic region containing rs881858 and rs9472138 is only modestly associated with levels of circulating VEGF, while regions situated both 5' of the *VEGFA* coding regions and further 3' in the C6orf223 locus are highly associated with circulating VEGF levels[43 44]. There is

little or no LD between these regions and the LD block harbouring the SNPs associated with circulating TSH in the current study (rs881858, rs94772138, rs943080 and rs4711751) and these signals appear to be independent. Thus, it is conceivable that several regions in or near the *VEGFA* locus control different aspects of VEGF regulation and releaseIt seems reasonable that regulatory mechanisms operating in thyroid tissue to govern for example stress induced VEGF production could different from the molecular mechanisms contributing to the regulation of circulating VEGF levels. Although we do not know the contribution of the thyroid gland to the sVEGF pool it is likely to be only a minor contributor compared with endothelial-released VEGF.

Although we present evidence for differential effects of alleles of *VEGFA* rs881858 by both reporter assays and direct binding, and have retrieved and inspected SNPs with high LD to this allele; we have not performed an extensive investigation of all linked SNPs in the *VEGFA* region for evidence of regulatory activity, and thus cannot exclude that additional functional SNPs may exist. Another limitation of our study is that we have no available data to show association between rs881858 alleles and levels of *VEGFA* mRNA transcript, protein levels or TSH stimulated VEGF release. Data from public eQTL databases shows no association between the investigated SNPs and thyroid *VEGFA* mRNA levels (Fig. S4).

When examining metabolic traits association with *VEGFA* rs881858 GG homozygous subjects were slightly more insulin resistant, while having similar measures of obesity and similar insulin secretion capacity (Table 2). Adipose tissue-specific knock-out of *Vegfa* results in inability to expand the adipose tissue, when demands for fat storage increases, exemplified by high-fat feeding[34]. Our results indicate that in the human setting the A-allele of *VEGFA* rs881858 via CHOP binding generates lower reporter-gene activity suggesting a decreased *VEGFA* response to cellular stress. This would result in an impaired angiogenic response of the A-allele, which is consistent with increased TSH levels. However, this is seemingly at odds with the GG-homozygous subjects being more insulin

resistant, because in mouse models insulin resistance is observed when the angiogenic response and therefore adipogenesis is impaired[34 35]. Thus, further studies are necessary to determine the tissue-specific effects of VEGFA and genetic variation on different human tissues. The *VEGFA* SNP rs9472138 has previously been associated with visceral obesity and insulin resistance in women[45], further underlining the importance of genetic variation in *VEGFA* also for human adipose tissue expansion. Of note, increased circulating TSH is associated with obesity and impaired cardio-metabolic health, which could indirectly affect the observed associations between insulin resistance and *VEGFA* rs881858. Mendelian randomization studies in large population based cohort could potentially resolve this.

ACKNOWLEDGMENTS

This study was supported by the Danish Medical Research Council (grant DFF – 1331-00033), The Novo Nordisk Foundation, the Danish Diabetes Association, the Gerda and Aage Haensch Foundation, the A.P. Møller Foundation for the Advancement of Medical Science, Novo Nordisk A/S, Roskilde University and University of Copenhagen. The Novo Nordisk Foundation Center for Basic Metabolic Research is an independent Research Center at the University of Copenhagen partially funded by an unrestricted donation from the Novo Nordisk Foundation (www.metabol.ku.dk). Further, this work is supported by the European Commission as an integrated project under the 6th Framework Programme (LSHM-CT-2005-018734, HepAdip). The Danish Obesity Research Centre (DanORC; www.danorc.dk) is supported by The Danish Council for Strategic Research (grant 2101-06-0005). TSA was funded by the Gene Diet Interactions in Obesity (GENDINOB, www.gendinob.dk) project and acknowledges the same. The authors wish to thank Christa Persson, Annemette Forman, Tina Lorentzen, and Marianne Stendal for technical assistance, Arne Nielsen for data management, and Grete Lademann and Trine Toldsted for secretarial support.

References

1. Laurberg P, Andersen S, Carle A, Karmisholt J, Knudsen N, Pedersen IB. The TSH upper reference limit: where are we at? Nat Rev Endocrinol 2011;**7**(4):232-9.
2. Andersen S, Pedersen KM, Bruun NH, Laurberg P. Narrow individual variations in serum T(4) and T(3) in normal subjects: a clue to the understanding of subclinical thyroid disease. J Clin Endocrinol Metab 2002;**87**(3):1068-72.
3. Hansen PS, Brix TH, Bennedbaek FN, Bonnema SJ, Kyvik KO, Hegedus L. Genetic and environmental causes of individual differences in thyroid size: a study of healthy Danish twins. J Clin Endocrinol Metab 2004;**89**(5):2071-7.
4. Hansen PS, Brix TH, Sorensen TI, Kyvik KO, Hegedus L. Major genetic influence on the regulation of the pituitary-thyroid axis: a study of healthy Danish twins. J Clin Endocrinol Metab 2004;**89**(3):1181-7.

5. Panicker V, Wilson SG, Spector TD, Brown SJ, Falchi M, Richards JB, Surdulescu GL, Lim EM, Fletcher SJ, Walsh JP. Heritability of serum TSH, free T4 and free T3 concentrations: a study of a large UK twin cohort. Clin Endocrinol (Oxf) 2008;**68**(4):652-9.
6. Taylor PN, Razvi S, Pearce SH, Dayan CM. Clinical review: A review of the clinical consequences of variation in thyroid function within the reference range. J Clin Endocrinol Metab 2013;**98**(9):3562-71.
7. de Moura Souza A, Sichieri R. Association between serum TSH concentration within the normal range and adiposity. Eur J Endocrinol 2011;**165**(1):11-5.
8. Chikunguwo S, Brethauer S, Nirujogi V, Pitt T, Udomsawaengsup S, Chand B, Schauer P. Influence of obesity and surgical weight loss on thyroid hormone levels. Surg Obes Relat Dis 2007;**3**(6):631-5; discussion 35-6.
9. Iacobellis G, Ribaudo MC, Zappaterreno A, Iannucci CV, Leonetti F. Relationship of thyroid function with body mass index, leptin, insulin sensitivity and adiponectin in euthyroid obese women. Clin Endocrinol (Oxf) 2005;**62**(4):487-91.
10. Sakurai M, Nakamura K, Miura K, Yoshita K, Takamura T, Nagasawa SY, Morikawa Y, Ishizaki M, Kido T, Naruse Y, Nakashima M, Nogawa K, Suwazono Y, Nakagawa H. Association between a serum thyroid-stimulating hormone concentration within the normal range and indices of obesity in Japanese men and women. Intern Med 2014;**53**(7):669-74.
11. Knudsen N, Laurberg P, Rasmussen LB, Bulow I, Perrild H, Ovesen L, Jorgensen T. Small differences in thyroid function may be important for body mass index and the occurrence of obesity in the population. J Clin Endocrinol Metab 2005;**90**(7):4019-24.
12. Asvold BO, Bjoro T, Vatten LJ. Association of serum TSH with high body mass differs between smokers and never-smokers. J Clin Endocrinol Metab 2009;**94**(12):5023-7.
13. Fox CS, Pencina MJ, D'Agostino RB, Murabito JM, Seely EW, Pearce EN, Vasan RS. Relations of thyroid function to body weight: cross-sectional and longitudinal observations in a community-based sample. Arch Intern Med 2008;**168**(6):587-92.
14. Porcu E, Medici M, Pistis G, Volpato CB, Wilson SG, Cappola AR, Bos SD, Deelen J, den Heijer M, Freathy RM, Lahti J, Liu C, Lopez LM, Nolte IM, O'Connell JR, Tanaka T, Trompet S, Arnold A, Bandinelli S, Beekman M, Bohringer S, Brown SJ, Buckley BM, Camaschella C, de Craen AJ, Davies G, de Visser MC, Ford I, Forsen T, Frayling TM, Fugazzola L, Gogele M, Hattersley AT, Hermus AR, Hofman A, Houwing-Duistermaat JJ, Jensen RA, Kajantie E, Kloppenburg M, Lim EM, Masciullo C, Mariotti S, Minelli C, Mitchell BD, Nagaraja R, Netea-Maier RT, Palotie A, Persani L, Piras MG, Psaty BM, Raikkonen K, Richards JB, Rivadeneira F, Sala C, Sabra MM, Sattar N, Shields BM, Soranzo N, Starr JM, Stott DJ, Sweep FC, Usala G, van der Klauw MM, van Heemst D, van Mullem A, Vermeulen SH, Visser WE, Walsh JP, Westendorp RG, Widen E, Zhai G, Cucca F, Deary IJ, Eriksson JG, Ferrucci L, Fox CS, Jukema JW, Kiemeney LA, Pramstaller PP, Schlessinger D, Shuldiner AR, Slagboom EP, Uitterlinden AG, Vaidya B, Visser TJ, Wolffenbuttel BH, Meulenbelt I, Rotter JI, Spector TD, Hicks AA, Toniolo D, Sanna S, Peeters RP, Naitza S. A meta-analysis of thyroid-related traits reveals novel loci and gender-specific differences in the regulation of thyroid function. PLoS Genet 2013;**9**(2):e1003266.
15. Malinowski JR, Denny JC, Bielinski SJ, Basford MA, Bradford Y, Peissig PL, Carrell D, Crosslin DR, Pathak J, Rasmussen L, Pacheco J, Kho A, Newton KM, Li R, Kullo IJ, Chute CG, Chisholm RL, Jarvik GP, Larson EB, McCarty CA, Masys DR, Roden DM, de Andrade M, Ritchie MD, Crawford DC. Genetic variants associated with serum thyroid stimulating hormone (TSH) levels in European Americans and African Americans from the eMERGE Network. PLoS One 2014;**9**(12):e111301.
16. Zhan M, Chen G, Pan CM, Gu ZH, Zhao SX, Liu W, Wang HN, Ye XP, Xie HJ, Yu SS, Liang J, Gao GQ, Yuan GY, Zhang XM, Zuo CL, Su B, Huang W, Ning G, Chen SJ, Chen JL, Song HD, China Consortium for Genetics of Autoimmune Thyroid D. Genome-wide association study identifies a novel susceptibility gene for serum TSH levels in Chinese populations. Hum Mol Genet 2014;**23**(20):5505-17.
17. Kwak SH, Park YJ, Go MJ, Lee KE, Kim SJ, Choi HS, Kim TH, Choi SH, Lim S, Kim KW, Park do J, Kim SS, Lee JY, Park KS, Jang HC, Cho NH. A genome-wide association study on thyroid function and anti-thyroid peroxidase antibodies in Koreans. Hum Mol Genet 2014;**23**(16):4433-42.

18. Wu C, Orozco C, Boyer J, Leglise M, Goodale J, Batalov S, Hodge CL, Haase J, Janes J, Huss JW, III, Su AI. BioGPS: an extensible and customizable portal for querying and organizing gene annotation resources. Genome Biol 2009;**10**(11):R130.
19. Sato K, Yamazaki K, Shizume K, Kanaji Y, Obara T, Ohsumi K, Demura H, Yamaguchi S, Shibuya M. Stimulation by thyroid-stimulating hormone and Grave's immunoglobulin G of vascular endothelial growth factor mRNA expression in human thyroid follicles in vitro and flt mRNA expression in the rat thyroid in vivo. J Clin Invest 1995;**96**(3):1295-302.
20. Viglietto G, Romano A, Manzo G, Chiappetta G, Paoletti I, Califano D, Galati MG, Mauriello V, Bruni P, Lago CT, Fusco A, Persico MG. Upregulation of the angiogenic factors PlGF, VEGF and their receptors (Flt-1, Flk-1/KDR) by TSH in cultured thyrocytes and in the thyroid gland of thiouracil-fed rats suggest a TSH-dependent paracrine mechanism for goiter hypervascularization. Oncogene 1997;**15**(22):2687-98.
21. Ahluwalia TS, Allin KH, Sandholt CH, Sparso TH, Jorgensen ME, Rowe M, Christensen C, Brandslund I, Lauritzen T, Linneberg A, Husemoen LL, Jorgensen T, Hansen T, Grarup N, Pedersen O. Discovery of coding genetic variants influencing diabetes-related serum biomarkers and their impact on risk of type 2 diabetes. J Clin Endocrinol Metab 2015;**100**(4):E664-71.
22. Jorgensen T, Borch-Johnsen K, Thomsen TF, Ibsen H, Glumer C, Pisinger C. A randomized non-pharmacological intervention study for prevention of ischaemic heart disease: baseline results Inter99. Eur J Cardiovasc Prev Rehabil 2003;**10**(5):377-86.
23. Thuesen BH, Cerqueira C, Aadahl M, Ebstrup JF, Toft U, Thyssen JP, Fenger RV, Hersoug LG, Elberling J, Pedersen O, Hansen T, Johansen JD, Jorgensen T, Linneberg A. Cohort Profile: the Health2006 cohort, research centre for prevention and health. Int J Epidemiol 2014;**43**(2):568-75.
24. Byberg S, Hansen AL, Christensen DL, Vistisen D, Aadahl M, Linneberg A, Witte DR. Sleep duration and sleep quality are associated differently with alterations of glucose homeostasis. Diabet Med 2012;**29**(9):e354-60.
25. Albrechtsen A, Grarup N, Li Y, Sparso T, Tian G, Cao H, Jiang T, Kim SY, Korneliussen T, Li Q, Nie C, Wu R, Skotte L, Morris AP, Ladenvall C, Cauchi S, Stancakova A, Andersen G, Astrup A, Banasik K, Bennett AJ, Bolund L, Charpentier G, Chen Y, Dekker JM, Doney AS, Dorkhan M, Forsen T, Frayling TM, Groves CJ, Gui Y, Hallmans G, Hattersley AT, He K, Hitman GA, Holmkvist J, Huang S, Jiang H, Jin X, Justesen JM, Kristiansen K, Kuusisto J, Lajer M, Lantieri O, Li W, Liang H, Liao Q, Liu X, Ma T, Ma X, Manijak MP, Marre M, Mokrosinski J, Morris AD, Mu B, Nielsen AA, Nijpels G, Nilsson P, Palmer CN, Rayner NW, Renstrom F, Ribel-Madsen R, Robertson N, Rolandsson O, Rossing P, Schwartz TW, Group DESIRS, Slagboom PE, Sterner M, Consortium D, Tang M, Tarnow L, Tuomi T, van't Riet E, van Leeuwen N, Varga TV, Vestmar MA, Walker M, Wang B, Wang Y, Wu H, Xi F, Yengo L, Yu C, Zhang X, Zhang J, Zhang Q, Zhang W, Zheng H, Zhou Y, Altshuler D, t Hart LM, Franks PW, Balkau B, Froguel P, McCarthy MI, Laakso M, Groop L, Christensen C, Brandslund I, Lauritzen T, Witte DR, Linneberg A, Jorgensen T, Hansen T, Wang J, Nielsen R, Pedersen O. Exome sequencing-driven discovery of coding polymorphisms associated with common metabolic phenotypes. Diabetologia 2013;**56**(2):298-310.
26. Troelsen JT, Mitchelmore C, Spodsberg N, Jensen AM, Noren O, Sjostrom H. Regulation of lactase-phlorizin hydrolase gene expression by the caudal-related homoeodomain protein Cdx-2. Biochem J 1997;**322 (Pt 3)**:833-38.
27. Roybal CN, Yang S, Sun CW, Hurtado D, Vander Jagt DL, Townes TM, Abcouwer SF. Homocysteine increases the expression of vascular endothelial growth factor by a mechanism involving endoplasmic reticulum stress and transcription factor ATF4. J Biol Chem 2004;**279**(15):14844-52.
28. Kent WJ, Sugnet CW, Furey TS, Roskin KM, Pringle TH, Zahler AM, Haussler D. The human genome browser at UCSC. Genome Res 2002;**12**(6):996-1006.
29. Matys V, Kel-Margoulis OV, Fricke E, Liebich I, Land S, Barre-Dirrie A, Reuter I, Chekmenev D, Krull M, Hornischer K, Voss N, Stegmaier P, Lewicki-Potapov B, Saxel H, Kel AE, Wingender E. TRANSFAC and its module TRANSCompel: transcriptional gene regulation in eukaryotes. Nucleic Acids Res 2006;**34**(Database issue):D108-10.
30. Tang QQ, Lane MD. Role of C/EBP homologous protein (CHOP-10) in the programmed activation of CCAAT/enhancer-binding protein-beta during adipogenesis. Proc Natl Acad Sci U S A 2000;**97**(23):12446-50.

31. Ohoka N, Yoshii S, Hattori T, Onozaki K, Hayashi H. TRB3, a novel ER stress-inducible gene, is induced via ATF4-CHOP pathway and is involved in cell death. EMBO J 2005;**24**(6):1243-55.
32. Mele M, Ferreira PG, Reverter F, DeLuca DS, Monlong J, Sammeth M, Young TR, Goldmann JM, Pervouchine DD, Sullivan TJ, Johnson R, Segre AV, Djebali S, Niarchou A, Consortium GT, Wright FA, Lappalainen T, Calvo M, Getz G, Dermitzakis ET, Ardlie KG, Guigo R. Human genomics. The human transcriptome across tissues and individuals. Science 2015;**348**(6235):660-5.
33. Brewer JW. Regulatory crosstalk within the mammalian unfolded protein response. Cell Mol Life Sci 2014;**71**(6):1067-79.
34. Sung HK, Doh KO, Son JE, Park JG, Bae Y, Choi S, Nelson SM, Cowling R, Nagy K, Michael IP, Koh GY, Adamson SL, Pawson T, Nagy A. Adipose vascular endothelial growth factor regulates metabolic homeostasis through angiogenesis. Cell Metab 2013;**17**(1):61-72.
35. Elias I, Franckhauser S, Ferre T, Vila L, Tafuro S, Munoz S, Roca C, Ramos D, Pujol A, Riu E, Ruberte J, Bosch F. Adipose tissue overexpression of vascular endothelial growth factor protects against diet-induced obesity and insulin resistance. Diabetes 2012;**61**(7):1801-13.
36. Brissova M, Aamodt K, Brahmachary P, Prasad N, Hong JY, Dai C, Mellati M, Shostak A, Poffenberger G, Aramandla R, Levy SE, Powers AC. Islet microenvironment, modulated by vascular endothelial growth factor-A signaling, promotes beta cell regeneration. Cell Metab 2014;**19**(3):498-511.
37. Reinert RB, Brissova M, Shostak A, Pan FC, Poffenberger G, Cai Q, Hundemer GL, Kantz J, Thompson CS, Dai C, McGuinness OP, Powers AC. Vascular endothelial growth factor-a and islet vascularization are necessary in developing, but not adult, pancreatic islets. Diabetes 2013;**62**(12):4154-64.
38. Langlet F, Levin BE, Luquet S, Mazzone M, Messina A, Dunn-Meynell AA, Balland E, Lacombe A, Mazur D, Carmeliet P, Bouret SG, Prevot V, Dehouck B. Tanycytic VEGF-A boosts blood-hypothalamus barrier plasticity and access of metabolic signals to the arcuate nucleus in response to fasting. Cell Metab 2013;**17**(4):607-17.
39. Fonseca TL, Correa-Medina M, Campos MP, Wittmann G, Werneck-de-Castro JP, Arrojo e Drigo R, Mora-Garzon M, Ueta CB, Caicedo A, Fekete C, Gereben B, Lechan RM, Bianco AC. Coordination of hypothalamic and pituitary T3 production regulates TSH expression. J Clin Invest 2013;**123**(4):1492-500.
40. Kottgen A, Pattaro C, Boger CA, Fuchsberger C, Olden M, Glazer NL, Parsa A, Gao X, Yang Q, Smith AV, O'Connell JR, Li M, Schmidt H, Tanaka T, Isaacs A, Ketkar S, Hwang SJ, Johnson AD, Dehghan A, Teumer A, Pare G, Atkinson EJ, Zeller T, Lohman K, Cornelis MC, Probst-Hensch NM, Kronenberg F, Tonjes A, Hayward C, Aspelund T, Eiriksdottir G, Launer LJ, Harris TB, Rampersaud E, Mitchell BD, Arking DE, Boerwinkle E, Struchalin M, Cavalieri M, Singleton A, Giallauria F, Metter J, de Boer IH, Haritunians T, Lumley T, Siscovick D, Psaty BM, Zillikens MC, Oostra BA, Feitosa M, Province M, de Andrade M, Turner ST, Schillert A, Ziegler A, Wild PS, Schnabel RB, Wilde S, Munzel TF, Leak TS, Illig T, Klopp N, Meisinger C, Wichmann HE, Koenig W, Zgaga L, Zemunik T, Kolcic I, Minelli C, Hu FB, Johansson A, Igl W, Zaboli G, Wild SH, Wright AF, Campbell H, Ellinghaus D, Schreiber S, Aulchenko YS, Felix JF, Rivadeneira F, Uitterlinden AG, Hofman A, Imboden M, Nitsch D, Brandstatter A, Kollerits B, Kedenko L, Magi R, Stumvoll M, Kovacs P, Boban M, Campbell S, Endlich K, Volzke H, Kroemer HK, Nauck M, Volker U, Polasek O, Vitart V, Badola S, Parker AN, Ridker PM, Kardia SL, Blankenberg S, Liu Y, Curhan GC, Franke A, Rochat T, Paulweber B, Prokopenko I, Wang W, Gudnason V, Shuldiner AR, Coresh J, Schmidt R, Ferrucci L, Shlipak MG, van Duijn CM, Borecki I, Kramer BK, Rudan I, Gyllensten U, Wilson JF, Witteman JC, Pramstaller PP, Rettig R, Hastie N, Chasman DI, Kao WH, Heid IM, Fox CS. New loci associated with kidney function and chronic kidney disease. Nat Genet 2010;**42**(5):376-84.
41. Ron D, Habener JF. CHOP, a novel developmentally regulated nuclear protein that dimerizes with transcription factors C/EBP and LAP and functions as a dominant-negative inhibitor of gene transcription. Genes Dev 1992;**6**(3):439-53.
42. Loinard C, Zouggari Y, Rueda P, Ramkhelawon B, Cochain C, Vilar J, Recalde A, Richart A, Charue D, Duriez M, Mori M, Arenzana-Seisdedos F, Levy BI, Heymes C, Silvestre JS. C/EBP homologous protein-10 (CHOP-10) limits postnatal neovascularization through control of endothelial nitric oxide synthase gene expression. Circulation 2012;**125**(8):1014-26.

43. Choi SH, Ruggiero D, Sorice R, Song C, Nutile T, Vernon Smith A, Concas MP, Traglia M, Barbieri C, Ndiaye NC, Stathopoulou MG, Lagou V, Maestrale GB, Sala C, Debette S, Kovacs P, Lind L, Lamont J, Fitzgerald P, Tonjes A, Gudnason V, Toniolo D, Pirastu M, Bellenguez C, Vasan RS, Ingelsson E, Leutenegger AL, Johnson AD, DeStefano AL, Visvikis-Siest S, Seshadri S, Ciullo M. Six Novel Loci Associated with Circulating VEGF Levels Identified by a Meta-analysis of Genome-Wide Association Studies. PLoS Genet 2016;**12**(2):e1005874.
44. Debette S, Visvikis-Siest S, Chen MH, Ndiaye NC, Song C, Destefano A, Safa R, Azimi NM, Sawyer D, Marteau JB, Xanthakis V, Siest G, Sullivan L, Pfister M, Smith H, Choi SH, Lamont J, Lind L, Yang Q, Fitzgerald P, Ingelsson E, Vasan RS, Seshadri S. Identification of cis- and trans-acting genetic variants explaining up to half the variation in circulating vascular endothelial growth factor levels. Circ Res 2011;**109**(5):554-63.
45. Burgdorf KS, Gjesing AP, Grarup N, Justesen JM, Sandholt CH, Witte DR, Jorgensen T, Madsbad S, Hansen T, Pedersen O. Association studies of novel obesity-related gene variants with quantitative metabolic phenotypes in a population-based sample of 6,039 Danish individuals. Diabetologia 2012;**55**(1):105-13.
46. Bonnefond A, Saulnier PJ, Stathopoulou MG, Grarup N, Ndiaye NC, Roussel R, Nezhad MA, Dechaume A, Lantieri O, Hercberg S, Lauritzen T, Balkau B, El-Sayed Moustafa JS, Hansen T, Pedersen O, Froguel P, Charpentier G, Marre M, Hadjadj S, Visvikis-Siest S. What is the contribution of two genetic variants regulating VEGF levels to type 2 diabetes risk and to microvascular complications? PLoS One 2013;**8**(2):e55921.
47. Fullwood MJ, Han Y, Wei CL, Ruan X, Ruan Y. Chromatin interaction analysis using paired-end tag sequencing. Curr Protoc Mol Biol 2010;**Chapter 21**:Unit 21 15 1-25.
48. Li G, Fullwood MJ, Xu H, Mulawadi FH, Velkov S, Vega V, Ariyaratne PN, Mohamed YB, Ooi HS, Tennakoon C, Wei CL, Ruan Y, Sung WK. ChIA-PET tool for comprehensive chromatin interaction analysis with paired-end tag sequencing. Genome Biol 2010;**11**(2):R22.
49. Daily K, Patel VR, Rigor P, Xie X, Baldi P. MotifMap: integrative genome-wide maps of regulatory motif sites for model species. BMC Bioinformatics 2011;**12**:495.

Legends to figures

Figure 1: A) Schematic representation of SNPs in the *VEGFA* gene associated with circulating TSH, serum VEGF, Type 2 diabetes or insulin resistance. Chromosomal base pair annotations is given for the hg19 assembly. The citations for the articles is: Porcu et al.[14], Debbette et al. [44], Choi et al. [43], Burgdorf et al. [45] and Bonnefond et al. [46]. B) Genomic region surrounding the *VEGFA* gene. Simplified representations of ENCODE sub-tracks from Genome Browser are shown. TSS: transcription start site, PROM: promoter, H3K27AC: Histone 3, Lysine 27 Acetylation (a mark of active and regulatory genomic DNA), H3K4Me1: Histone 3, Lysine 4 Mono-methylation (a mark of active enhancers), Conservation: 24 placental mammals, ChIA-PET: Chromatin Interaction Analysis Paired-End Tags (ChIA-PET) from ENCODE/Genome Institute of Singapore-Ruan[47 48], c/EBP-β binding; Chromatin-immunoprecipitation using antibody directed against C/EBPβ followed by sequencing, DNase HS: DNase hyper sensitivity. Genome browser screen-shots of the area are shown in Suppl. Fig. S3. B) The binding sites for c/EBPβ and CHOP aligned showing the binding preferences of c/EBPβ and CHOP at the position of rs881858. TSS: Transcription start site. UIPAC nucleotide abbreviations N: Any, M: A or C, R: A or G, K: G or T, D: A or G or T. Binding site logos were from http://motifmap.ics.uci.edu/[49].

Figure 2: Reporter gene activities of examined *VEGFA* gene variants: rs881858 A or G, and rs9472138 C or T, respectively, refer to enhancer plasmids containing the VEGFA minimal promoter as well as the DNA regions surrounding rs881858 and rs9472138 and representing the different version of the SNPs. A) Basal activity of VEGFA minimal promoter and SNP-containing regions. Shown are relative luciferase activities of plasmids transfected into HEK203 cells. pGL4.10: promoter-less plasmid. Min pro: VEGFA minimal promoter plasmid. Luciferase activities were normalized to beta-galactosidase activity and are presented relative to the activity of the VEGFA minimal promoter, B) and C) Response of the rs881858 A and G alleles to separate CHOP and c/EBPβ over-expression, respectively. Shown are relative luciferase activities of rs881858 enhancer plasmids harbouring A or G co-transfected with CHOP or c/EBPβ expression plasmids in HEK293 cells. Luciferase activities were normalized to beta-galactosidase activity and are presented relative to the activity of the VEGFA minimal promoter (not shown on graph). D) Response of the rs881858 A and G alleles to varying levels of concurrent CHOP and c/EBPβ over-expression (5ng per well). Relative luciferase activities of rs881858 enhancer plasmids harbouring A or G co-transfected with CHOP and c/EBPβ expression plasmids in HEK293 cells. Experiments were performed 4 times in triplicate. * $P<0.05$, ** $P<0.01$ by t-test for the indicated comparison or compared against the basal activity of the allele.

Figure 3: Electrophoretic Mobility Shift Assay (EMSA) experiments probing the *VEGFA* rs881858 region for binding using HEK293 nuclear extract. A) Lane 1-4: ^{32}P-labeled A-allele as probe ('A'), 5-10: ^{32}P-labeled G-allele as probe ('G'). Nuclear extracts from DTT treated HEK293 in all lanes. B) Comparison of complex formation using probes for the A-allele, G-allele, CHOP and c/EBPβ binding sites. C) Identification of complexes binding to CHOP and C/EBPβ using known binding sites for these proteins. Abbreviations: Probe: ^{32}P-labeled ds-oligo as indicated. COMP: Competition using unlabelled ds-oligo, Ab.: Antibody used for super-shift of complexes. N.E.: Nuclear Extract. CHOP: ds-oligo having the CHOP binding site from the TRIB3 (tribbles pseudokinase 3) gene [31].

CEBP: ds-oligo having the c/EBPβ binding site from the c/EBPα gene promoter [30]. Labels to the left of images indicate formed complexes: c/EBPβ homodimer, CHOP/c/EBPβ heterodimer and arrows indicate rs881858 specific complexes not binding CHOP or c/EBPβ. N.s.: non-specific. Shown are representative blots (n=2-4 of each).

Figure 4: A model illustrating the possible involvement of *VEGFA* rs881858 in regulating thyroid function and the set point of TSH. The rs881858 A-allele is repressed by CHOP, which is activated by the cellular stress, resulting in less VEGFA enhancer activity, with predicted less thyrocyte VEGF produced. The result is predicted to be reduced angiogenesis and less thyroid compensatory expansion. This result will be less T4 production, less feedback inhibition of TRH and TSH release and therefore increased circulating TSH levels. A higher TSH level will result in increased stimulation of the TSH receptor and a higher degree of activation of the ER-stress response. Dashed lines illustrate rs881858 A-allele related effects.

Supplementary Figure legends

Figure S1: Meta-Analysis Forest plot of the association between TSH and the G-allele of *VEGFA* rs881858

The association between TSH and the G-allele of rs881858 of the *VEGFA* locus was meta-analysed in three cohorts: Inter99, Health2006 and Health2008. Shown are the β-values and SE for each cohort with corresponding 95% confidence intervals and overall P-value evaluated using a fixed effect model. A total of 8,445 individuals from three Danish cohorts (Inter99, Health2006, and Health2008) were combined for inverse variance meta-analyses, where weights are proportional to the squared standard errors of the effect estimates. Genomic inflation factor (λ) was at acceptable levels (λTSH = 1.0) after the meta-analyses. A chi-square test for heterogeneity (I) was implemented, to estimate the heterogeneity in effect sizes across different participating cohorts using METAL software (http://csg.sph.umich.edu/abecasis/metal/).

Figure S2. LD Heat Map of pairwise r^2 values of SNPs studied from the *VEGFA* gene region LD estimations and proxy search were performed using 1000 genomes project data implemented in SNP Annotation Proxy search tool (http://www.broadinstitute.org/mpg/snap/). An LD heat-map depicting pairwise r2 values as colors (least correlated r2=0 as dark blue and most correlated r2=1.0 as light shade of blue). Non-genotyped SNPs in LD with TSH associated SNPs were retrieved from the ENSEMBL genome browser (http://grch37.ensembl.org/Homo_sapiens/Info/Index) using CEU data, only SNPs with LD≥0.8 were investigated further for evidence of differential allele effects.

Figure S3: Genome browser (www.genome.ucsc.edu) screen shots of genomic regions containing the SNPs summarized in Table S5.

Figure S4: Expressed quantitative trait locus (eQTL) data for rs9472138, rs881858, rs943080 and rs4711751 for *VEGFA* mRNA in thyroid tissue. The mRNA levels of *VEGFA* are presented according to genotype of each of the SNPs. Data were retrieved from the GTEX portal (www.gtexportal.org)[32].

Figure 1

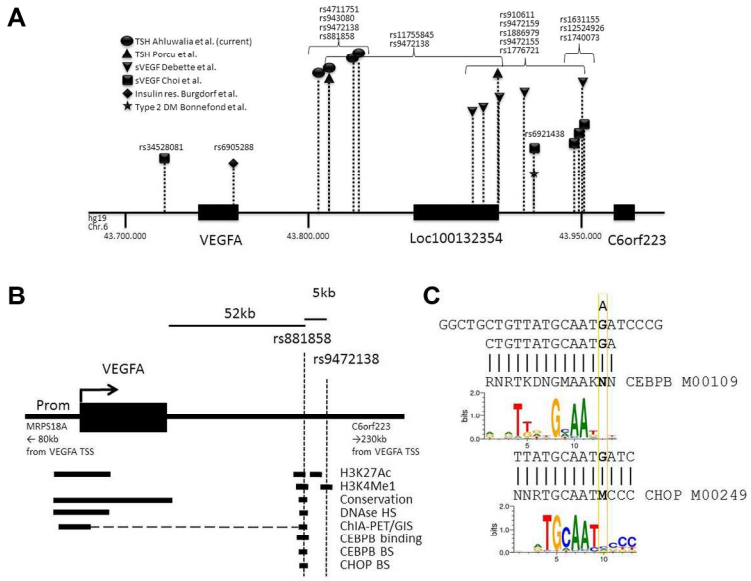

Figure 1: A) Schematic representation of SNPs in the VEGFA gene associated with circulating TSH, serum VEGF, Type 2 diabetes or insulin resistance. Chromosomal base pair annotations is given for the hg19 assembly. The citations for the articles is: Porcu et al.14, Debbette et al. 44, Choi et al. 43, Burgdorf et al. 45 and Bonnefond et al. 46. B) Genomic region surrounding the VEGFA gene. Simplified representations of ENCODE sub-tracks from Genome Browser are shown. TSS: transcription start site, PROM: promoter, H3K27AC: Histone 3, Lysine 27 Acetylation (a mark of active and regulatory genomic DNA), H3K4Me1: Histone 3, Lysine 4 Mono-methylation (a mark of active enhancers), Conservation: 24 placental mammals, ChIA-PET: Chromatin Interaction Analysis Paired-End Tags (ChIA-PET) from ENCODE/Genome Institute of Singapore-Ruan47 48, c/EBP-β binding; Chromatin-immunoprecipitation using antibody directed against C/EBPβ followed by sequencing, DNase HS: DNase hyper sensitivity. Genome browser screen-shots of the area are shown in Suppl. Fig. S3. B) The binding sites for c/EBPβ and CHOP aligned showing the binding preferences of c/EBPβ and CHOP at the position of rs881858. TSS: Transcription start site. UIPAC nucleotide abbreviations N: Any, M: A or C, R: A or G, K: G or T, D: A or G or T. Binding site logos were from

http://motifmap.ics.uci.edu/49.
Fig. 1
209x297mm (300 x 300 DPI)

Figure 2

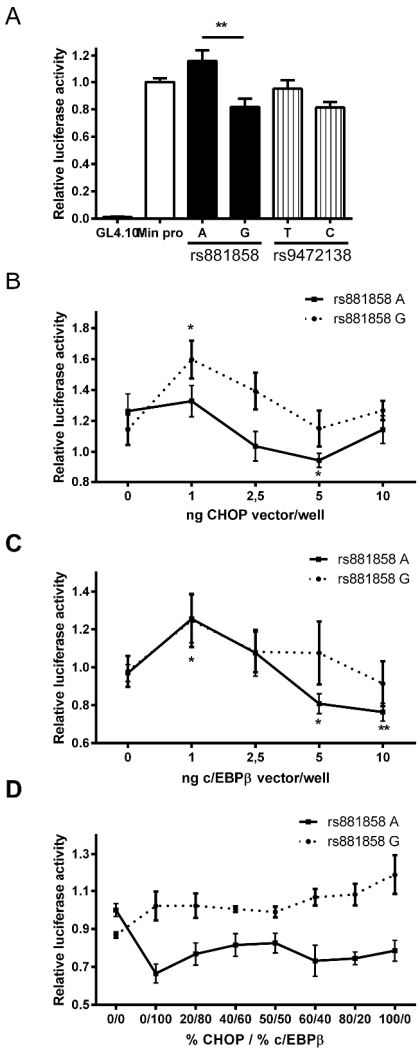

Figure 2: Reporter gene activities of examined VEGFA gene variants: rs881858 A or G, and rs9472138 C or T, respectively, refer to enhancer plasmids containing the VEGFA minimal promoter as well as the DNA regions surrounding rs881858 and rs9472138 and representing the different version of the SNPs. A) Basal activity of VEGFA minimal promoter and SNP-containing regions. Shown are relative luciferase activities of plasmids transfected into HEK203 cells. pGL4.10: promoter-less plasmid. Min pro: VEGFA minimal promoter plasmid. Luciferase activities were normalized to beta-galactosidase activity and are presented relative to the activity of the VEGFA minimal promoter, B) and C) Response of the rs881858 A and G alleles to separate CHOP and c/EBPβ over-expression, respectively. Shown are relative luciferase activities of rs881858 enhancer plasmids harbouring A or G co-transfected with CHOP or c/EBPβ expression plasmids in HEK293 cells. Luciferase activities were normalized to beta-galactosidase activity and are presented relative to the activity of the VEGFA minimal promoter (not shown on graph). D) Response of the rs881858 A and G alleles to varying levels of concurrent CHOP and c/EBPβ over-expression (5ng per well). Relative luciferase activities of rs881858 enhancer plasmids harbouring A or G co-transfected with CHOP and c/EBPβ

expression plasmids in HEK293 cells. Experiments were performed 4 times in triplicate. * P<0.05, **P<0.01 by t-test for the indicated comparison or compared against the basal activity of the allele.

Fig. 2

197x489mm (600 x 600 DPI)

Figure 3

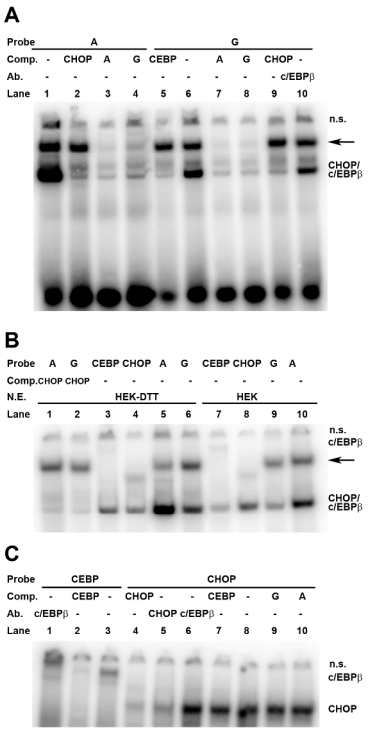

Figure 3: Electrophoretic Mobility Shift Assay (EMSA) experiments probing the VEGFA rs881858 region for binding using HEK293 nuclear extract. A) Lane 1-4: 32P-labeled A-allele as probe ('A'), 5-10: 32P-labeled G-allele as probe ('G'). Nuclear extracts from DTT treated HEK293 in all lanes. B) Comparison of complex formation using probes for the A-allele, G-allele, CHOP and c/EBPβ binding sites. C) Identification of complexes binding to CHOP and C/EBPβ using known binding sites for these proteins. Abbreviations: Probe: 32P-labeled ds-oligo as indicated. COMP: Competition using unlabelled ds-oligo, Ab.: Antibody used for super-shift of complexes. N.E.: Nuclear Extract. CHOP: ds-oligo having the CHOP binding site from the TRIB3 (tribbles pseudokinase 3) gene 31. CEBP: ds-oligo having the c/EBPβ binding site from the c/EBPα gene promoter 30. Labels to the left of images indicate formed complexes: c/EBPβ homodimer, CHOP/c/EBPβ heterodimer and arrows indicate rs881858 specific complexes not binding CHOP or c/EBPβ. N.s.: non-specific. Shown are representative blots (n=2-4 of each).

Fig. 3
209x297mm (300 x 300 DPI)

Figure 4

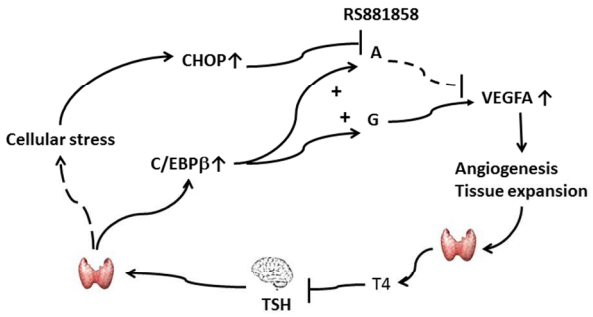

Figure 4: A model illustrating the possible involvement of VEGFA rs881858 in regulating thyroid function and the set point of TSH. The rs881858 A-allele is repressed by CHOP, which is activated by the cellular stress, resulting in less VEGFA enhancer activity, with predicted less thyrocyte VEGF produced. The result is predicted to be reduced angiogenesis and less thyroid compensatory expansion. This result will be less T4 production, less feedback inhibition of TRH and TSH release and therefore increased circulating TSH levels. A higher TSH level will result in increased stimulation of the TSH receptor and a higher degree of activation of the ER-stress response. Dashed lines illustrate rs881858 A-allele related effects.
Fig. 4
338x190mm (96 x 96 DPI)

Figure S1

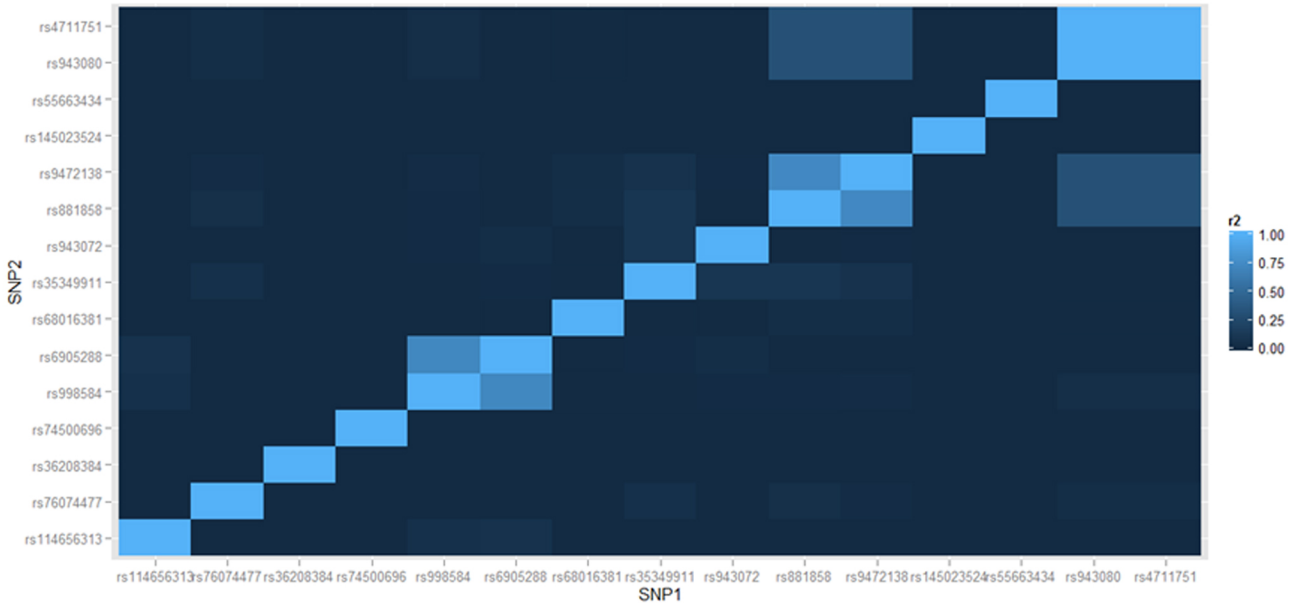
rs4711751
rs943080
rs55663434
rs145023524
rs9472138
rs881858
rs943072
rs35349911
rs68016381
rs6905288
rs998584
rs74500696
rs36208384
rs76074477
rs114656313
SNP2
rs114656313 rs76074477 rs36208384 rs74500696 rs998584 rs6905288 rs68016381 rs35349911 rs943072 rs881858 rs9472138 rs145023524 rs55663434 rs943080 rs4711751
SNP1
r2
1.00
0.75
0.50
0.25
0.00

Figure S2

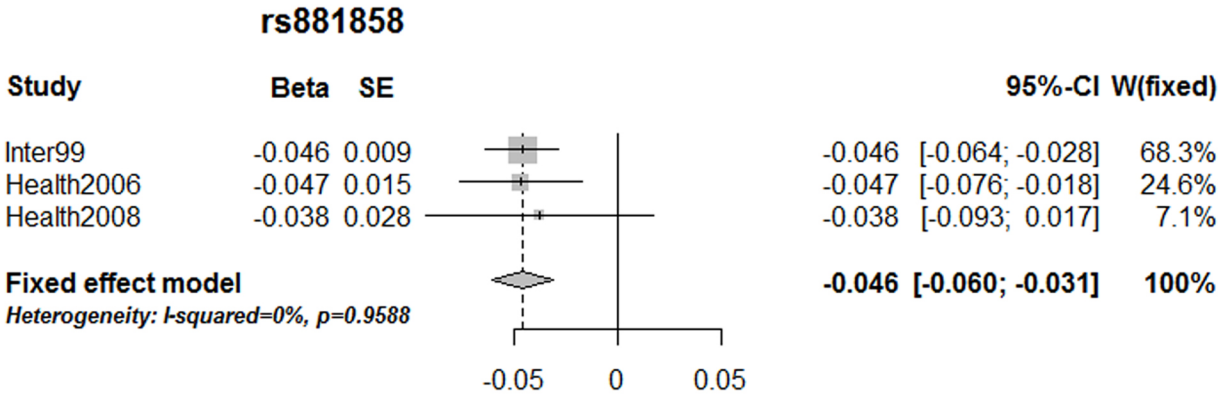
rs881858
Study
Beta
SE
95%-CI
W(fixed)
Inter99 -0.046 0.009 -0.046 [-0.064; -0.028] 68.3%
Health2006 -0.047 0.015 -0.047 [-0.076; -0.018] 24.6%
Health2008 -0.038 0.028 -0.038 [-0.093; 0.017] 7.1%
Fixed effect model -0.046 [-0.060; -0.031] 100%
Heterogeneity: I-squared=0%, p=0.9588
-0.05
0
0.05

Figure S3

Journal of Medical Genetics
Essential Gene Predictions in Human Genome Wide Association Studies
rs729761
https://mc.manuscriptcentral.com/jmedgenet

Journal of Medical Genetics

rs10223666

Scale
chr6:
20 bases
hg19
43,805,470 43,805,475 43,805,480 43,805,485 43,805,490 43,805,495 43,805,500 43,805,505 43,805,510 43,805,515 43,805,520 43,805,525 43,805,530 43,805,535 43,805,540
A A C C T G A G C T G T A G A T A A A C C A A C C A G C T G A A T C G T G C C G C A T C T G T G G G G A G C T G A G A T G G G A C A G C A G C A A G A G G C T T

Ensembl Genes Predictions - Jun 17, 2014
SNPs in Publications
Human mRNAs from GenBank
Human ESTs That Have Been Spliced
H3K27Ac Mark (Often Found Near Active Regulatory Elements) on 7 cell lines from ENCODE
DNaseI Hypersensitivity Clusters in 125 cell types from ENCODE (V3)
Transcription Factor ChIP-seq (161 factors) from ENCODE with Factorbook Motifs
DNaseI Hypersensitive Site Master List (125 cell types) from ENCODE/Analysis

GM12878 DNaseI HS Uniform Peaks from ENCODE/Analysis
H1-hESC DNaseI HS Uniform Peaks from ENCODE/Analysis
K562 DNaseI HS Uniform Peaks from ENCODE/Analysis
HUVEC DNaseI HS Uniform Peaks from ENCODE/Analysis
HeLa-S3 DNaseI HS Uniform Peaks from ENCODE/Analysis
HepG2 DNaseI HS Uniform Peaks from ENCODE/Analysis
A549 DNaseI HS Uniform Peaks from ENCODE/Analysis
CD20+ B cell DNaseI HS Uniform Peaks from ENCODE/Analysis
MCF-7 DNaseI HS Uniform Peaks from ENCODE/Analysis
Monocytes-CD14+ DNaseI HS Uniform Peaks from ENCODE/Analysis
NHEK DNaseI HS Uniform Peaks from ENCODE/Analysis
GM12878 TFBS Uniform Peaks of CTCF from ENCODE/UT-A/Analysis
GM12878 TFBS Uniform Peaks of Pol2-4H8 from ENCODE/HudsonAlpha/Analysis
GM12878 TFBS Uniform Peaks of SP1 from ENCODE/HudsonAlpha/Analysis
H1-hESC TFBS Uniform Peaks of CTCF from ENCODE/UT-A/Analysis
H1-hESC TFBS Uniform Peaks of NANOG_(SC-33759) from ENCODE/HudsonAlpha/Analysis
H1-hESC TFBS Uniform Peaks of Pol2-4H8 from ENCODE/HudsonAlpha/Analysis
K562 TFBS Uniform Peaks of CTCF from ENCODE/UT-A/Analysis
K562 TFBS Uniform Peaks of NF-YA from ENCODE/Stanford/Analysis
K562 TFBS Uniform Peaks of Pol2-4H8 from ENCODE/HudsonAlpha/Analysis
HeLa-S3 TFBS Uniform Peaks of CTCF from ENCODE/UT-A/Analysis
HeLa-S3 TFBS Uniform Peaks of HA-E2F1 from ENCODE/USC/Analysis
HeLa-S3 TFBS Uniform Peaks of Pol2 from ENCODE/HudsonAlpha/Analysis
HepG2 TFBS Uniform Peaks of CTCF from ENCODE/UT-A/Analysis
HepG2 TFBS Uniform Peaks of p300_(SC-584) from ENCODE/Stanford/Analysis
HepG2 TFBS Uniform Peaks of Pol2-4H8 from ENCODE/HudsonAlpha/Analysis
HUVEC TFBS Uniform Peaks of CTCF from ENCODE/UT-A/Analysis
HUVEC TFBS Uniform Peaks of c-Fos from ENCODE/USC/Analysis
HUVEC TFBS Uniform Peaks of Pol2-4H8 from ENCODE/HudsonAlpha/Analysis
A549 (DEX_100nM) TFBS Uniform Peaks of CTCF_(SC-5916) ENCODE/HudsonAlpha/Analysis
A549 (DEX_100nM) TFBS Uniform Peaks of GR from ENCODE/HudsonAlpha/Analysis
IMR90 TFBS Uniform Peaks of CEBPB from ENCODE/Stanford/Analysis
IMR90 TFBS Uniform Peaks of CTCF_(SC-15914) from ENCODE/Stanford/Analysis
IMR90 TFBS Uniform Peaks of Pol2 from ENCODE/Stanford/Analysis
MCF-7 (serum_stimulated) TFBS Uniform Peaks of CTCF from ENCODE/UT-A/Analysis
MCF-7 (serum_stimulated) TFBS Uniform Peaks of c-Myc from ENCODE/UT-A/Analysis
MCF-7 (serum_stimulated) TFBS Uniform Peaks of Pol2 from ENCODE/UT-A/Analysis
DNaseI/FAIRE/ChIP Synthesis from ENCODE/OpenChrom(Duke/UNC/UTA)

GM12878 Syn Pk
H1-hESC Syn Pk
K562 Syn Pk

Histone Modifications by ChIP-seq from ENCODE/Broad Institute

GM12878 H3K4m1
GM12878 H3K4m3
GM12878 H3K27ac
GM12878 H3K27ac
H1-hESC H3K4m1
H1-hESC H3K4m1
H1-hESC H3K27ac
H1-hESC H3K27ac
K562 H3K4m1
K562 H3K4m1
K562 H3K27ac
K562 H3K27ac
A549 DEX H3K4m1
A549 DEX H3K4m1
A549 EtOH H3K4m1
A549 EtOH H3K4m1
A549 DEX H3K27ac
A549 DEX H3K27ac
A549 EtOH H3K27ac
A549 EtOH H3K27ac
CD20+ H3K27ac
CD20+ H3K27ac
HeLa-S3 H3K4m1
HeLa-S3 H3K4m1
HeLa-S3 H3K27ac
HeLa-S3 H3K27ac
HepG2 H3K4m1
HepG2 H3K4m1
HepG2 H3K27ac
HepG2 H3K27ac
HUVEC H3K4m1
HUVEC H3K4m1
HUVEC H3K27ac
HUVEC H3K27ac
CD14+ H3K4m1
CD14+ H3K4m1
CD14+ H3K27ac
CD14+ H3K27ac

Open Chromatin by DNaseI HS from ENCODE/OpenChrom(Duke University)

GM12878 Pk
GM12878 DS
GM12878 DS
H1hESC Pk
H1hESC DS
H1hESC OS
K562 Pk
K562 DS
K562 OS

GM12878 GABP PCR2x ChIP-seq Peaks Rep 1 from ENCODE/HAIB
GM12878 GABP PCR2x ChIP-seq Raw Signal Rep 1 from ENCODE/HAIB
GM78 GABP PCR2 1
GM12878 GABP PCR2x ChIP-seq Peaks Rep 2 from ENCODE/HAIB
GM12878 GABP PCR2x ChIP-seq Raw Signal Rep 2 from ENCODE/HAIB
GM78 GABP PCR2 2
GM12878 Pol2-4H8 PCR1x ChIP-seq Peaks Rep 1 from ENCODE/HAIB
GM12878 Pol2-4H8 PCR1x ChIP-seq Raw Signal Rep 1 from ENCODE/HAIB
GM78 Pol2-4H8 PCR1 1
GM12878 Pol2-4H8 PCR1x ChIP-seq Peaks Rep 2 from ENCODE/HAIB
GM12878 Pol2-4H8 PCR1x ChIP-seq Raw Signal Rep 2 from ENCODE/HAIB
GM78 Pol2-4H8 PCR1 2
GM12878 USF-1 PCR2x ChIP-seq Peaks Rep 1 from ENCODE/HAIB
GM12878 USF-1 PCR2x ChIP-seq Raw Signal Rep 1 from ENCODE/HAIB
GM78 USF1 PCR2 1
GM12878 USF-1 PCR2x ChIP-seq Peaks Rep 2 from ENCODE/HAIB
GM12878 USF-1 PCR2x ChIP-seq Raw Signal Rep 2 from ENCODE/HAIB
GM78 USF1 PCR2 2
H1-hESC GABP PCR1x ChIP-seq Peaks Rep 1 from ENCODE/HAIB
H1-hESC GABP PCR1x ChIP-seq Raw Signal Rep 1 from ENCODE/HAIB
hESC GABP PCR1 1
H1-hESC GABP PCR1x ChIP-seq Peaks Rep 2 from ENCODE/HAIB
H1-hESC GABP PCR1x ChIP-seq Raw Signal Rep 2 from ENCODE/HAIB
hESC GABP PCR1 2
H1-hESC Pol2-4H8 v041610.2 ChIP-seq Peaks Rep 1 from ENCODE/HAIB
H1-hESC Pol2-4H8 v041610.2 ChIP-seq Raw Signal Rep 1 from ENCODE/HAIB
hESC Pol2-4H8 V102 1
H1-hESC Pol2-4H8 v041610.2 ChIP-seq Peaks Rep 2 from ENCODE/HAIB
H1-hESC Pol2-4H8 v041610.2 ChIP-seq Raw Signal Rep 2 from ENCODE/HAIB
hESC Pol2-4H8 V102 2
H1-hESC USF-1 PCR1x ChIP-seq Peaks Rep 1 from ENCODE/HAIB
H1-hESC USF-1 PCR1x ChIP-seq Raw Signal Rep 1 from ENCODE/HAIB
hESC USF1 PCR1 1
H1-hESC USF-1 PCR1x ChIP-seq Peaks Rep 2 from ENCODE/HAIB
H1-hESC USF-1 PCR1x ChIP-seq Raw Signal Rep 2 from ENCODE/HAIB
hESC USF1 PCR1 2
K562 GABP v041610.1 ChIP-seq Peaks Rep 1 from ENCODE/HAIB
K562 GABP v041610.1 ChIP-seq Raw Signal Rep 1 from ENCODE/HAIB
K562 GABP V101 1
K562 GABP v041610.1 ChIP-seq Peaks Rep 2 from ENCODE/HAIB
K562 GABP v041610.1 ChIP-seq Raw Signal Rep 2 from ENCODE/HAIB
K562 GABP V101 2
K562 Pol2-4H8 v041610.1 ChIP-seq Peaks Rep 1 from ENCODE/HAIB
K562 Pol2-4H8 v041610.1 ChIP-seq Raw Signal Rep 1 from ENCODE/HAIB
K562 Pol2-4H8 V101 1
K562 Pol2-4H8 v041610.1 ChIP-seq Peaks Rep 2 from ENCODE/HAIB
K562 Pol2-4H8 v041610.1 ChIP-seq Raw Signal Rep 2 from ENCODE/HAIB
K562 Pol2-4H8 V101 2
K562 USF-1 v041610.1 ChIP-seq Peaks Rep 1 from ENCODE/HAIB
K562 USF-1 v041610.1 ChIP-seq Raw Signal Rep 1 from ENCODE/HAIB
K562 USF1 V101 1
K562 USF-1 v041610.1 ChIP-seq Peaks Rep 2 from ENCODE/HAIB
K562 USF-1 v041610.1 ChIP-seq Raw Signal Rep 2 from ENCODE/HAIB
K562 USF1 V101 2
GM12878 CHD2 IgG-mus ChIP-seq Peaks from ENCODE/SYDH
GM12878 CHD2 IgG-mus ChIP-seq Signal from ENCODE/SYDH
GM78 CHD2 IgM
GM12878 Pol2 IgG-mus ChIP-seq Peaks from ENCODE/SYDH
GM12878 Pol2 IgG-mus ChIP-seq Signal from ENCODE/SYDH
GM78 Pol2 IgM
GM12878 Pol2 Standard ChIP-seq Peaks from ENCODE/SYDH
GM12878 Pol2 Standard ChIP-seq Signal from ENCODE/SYDH
GM78 Pol2 Std
GM12878 Rad21 IgG-rab ChIP-seq Peaks from ENCODE/SYDH
GM12878 Rad21 IgG-rab ChIP-seq Signal from ENCODE/SYDH
GM78 Rad2 IgR
GM12878 TBP IgG-mus ChIP-seq Peaks from ENCODE/SYDH
GM12878 TBP IgG-mus ChIP-seq Signal from ENCODE/SYDH
GM78 TBP IgM
GM12878 ZNF274 Standard ChIP-seq Peaks from ENCODE/SYDH
GM12878 ZNF274 Standard ChIP-seq Signal from ENCODE/SYDH
GM78 Z274 Std
K562 CHD2 IgG-rab ChIP-seq Peaks from ENCODE/SYDH
K562 CHD2 IgG-rab ChIP-seq Signal from ENCODE/SYDH
K562 CHD2 IgR
K562 Pol2 IgG-mus ChIP-seq Peaks from ENCODE/SYDH
K562 Pol2 IgG-mus ChIP-seq Signal from ENCODE/SYDH
K562 Pol2 IgM
K562 Pol2 Standard IFNa 30min ChIP-seq Peaks from ENCODE/SYDH
K562 Pol2 Standard IFNa 30min ChIP-seq Signal from ENCODE/SYDH
K562 IFa3 Pol2 Sd
K562 Pol2 Standard IFNa 6hrs ChIP-seq Peaks from ENCODE/SYDH
K562 Pol2 Standard IFNa 6hrs ChIP-seq Signal from ENCODE/SYDH
K562 IFa6 Pol2 Sd
K562 Pol2 Standard IFNg 30min ChIP-seq Peaks from ENCODE/SYDH
K562 Pol2 Standard IFNg 30min ChIP-seq Signal from ENCODE/SYDH
K562 IFg3 Pol2 Sd
K562 Pol2 Standard IFNg 6hrs ChIP-seq Peaks from ENCODE/SYDH
K562 Pol2 Standard IFNg 6hrs ChIP-seq Signal from ENCODE/SYDH
K562 IFg6 Pol2 Sd
K562 Pol2 Standard ChIP-seq Peaks from ENCODE/SYDH
K562 Pol2 Standard ChIP-seq Signal from ENCODE/SYDH
K562 Pol2 Std
K562 Rad21 Standard ChIP-seq Peaks from ENCODE/SYDH
K562 Rad21 Standard ChIP-seq Signal from ENCODE/SYDH
K562 Rad2 Std
K562 TBP IgG-mus ChIP-seq Peaks from ENCODE/SYDH
K562 TBP IgG-mus ChIP-seq Signal from ENCODE/SYDH
K562 TBP IgM
K562 ZNF274 UC Davis ChIP-seq Peaks from ENCODE/SYDH
K562 ZNF274 UC Davis ChIP-seq Signal from ENCODE/SYDH
K562 Z274 UCD
K562 FOS GFP-tag TFBS Peaks from ENCODE/UChicago
K562 FOS GFP-tag TFBS Signal from ENCODE/UChicago
K562 FOS/GFP Sg
K562 GATA2 GFP-tag TFBS Peaks from ENCODE/UChicago
K562 GATA2 GFP-tag TFBS Signal from ENCODE/UChicago
K562 GATA2/GFP Sg
K562 HDAC8 GFP-tag TFBS Peaks from ENCODE/UChicago
K562 HDAC8 GFP-tag TFBS Signal from ENCODE/UChicago
K562 HDAC8/GFP Sg
K562 JunB GFP-tag TFBS Peaks from ENCODE/UChicago
K562 JunB GFP-tag TFBS Signal from ENCODE/UChicago
K562 JunB/GFP Sg
K562 JunD GFP-tag TFBS Peaks from ENCODE/UChicago
K562 JunD GFP-tag TFBS Signal from ENCODE/UChicago
K562 JunD/GFP Sg
K562 NR4A1 GFP-tag TFBS Peaks from ENCODE/UChicago
K562 NR4A1 GFP-tag TFBS Signal from ENCODE/UChicago
K562 NR4A1/GFP Sg

Open Chromatin by FAIRE from ENCODE/OpenChrom(UNC Chapel Hill)

GM12878 FAIRE Pk
GM12878 FAIRE DS
GM12878 FAIRE OS
H1-hESC FAIRE Pk
H1-hESC FAIRE DS
H1-hESC FAIRE OS
K562 FAIRE Pk
K562 FAIRE DS
K562 FAIRE OS

GM12878 cMyc TFBS ChIP-seq Peaks from ENCODE/OpenChrom-UTA
GM12878 cMyc TFBS ChIP-seq Density Signal ENCODE/OpenChrom-UTA
GM12878 cMyc DS
GM12878 cMyc TFBS ChIP-seq Overlap Signal ENCODE/OpenChrom-UTA
GM12878 cMyc OS
GM12878 CTCF TFBS ChIP-seq Peaks from ENCODE/OpenChrom-UTA
GM12878 CTCF TFBS ChIP-seq Density Signal ENCODE/OpenChrom-UTA
GM12878 CTCF DS
GM12878 CTCF TFBS ChIP-seq Overlap Signal ENCODE/OpenChrom-UTA
GM12878 CTCF OS
GM12878 Pol2 TFBS ChIP-seq Peaks from ENCODE/OpenChrom-UTA
GM12878 Pol2 TFBS ChIP-seq Density Signal ENCODE/OpenChrom-UTA
GM12878 Pol2 DS
GM12878 Pol2 TFBS ChIP-seq Overlap Signal ENCODE/OpenChrom-UTA
GM12878 Pol2 OS
GM12878 Input TFBS ChIP-seq Density Signal ENCODE/OpenChrom-UTA
GM12878 Input DS
H1-hESC cMyc TFBS ChIP-seq Peaks from ENCODE/OpenChrom-UTA
H1-hESC cMyc TFBS ChIP-seq Density Signal ENCODE/OpenChrom-UTA
H1-hESC cMyc DS
H1-hESC cMyc TFBS ChIP-seq Overlap Signal ENCODE/OpenChrom-UTA
H1-hESC cMyc OS
H1-hESC CTCF TFBS ChIP-seq Peaks from ENCODE/OpenChrom-UTA
H1-hESC CTCF TFBS ChIP-seq Density Signal ENCODE/OpenChrom-UTA
H1-hESC CTCF DS
H1-hESC CTCF TFBS ChIP-seq Overlap Signal ENCODE/OpenChrom-UTA
H1-hESC CTCF OS
H1-hESC Pol2 TFBS ChIP-seq Peaks from ENCODE/OpenChrom-UTA
H1-hESC Pol2 TFBS ChIP-seq Density Signal ENCODE/OpenChrom-UTA
H1-hESC Pol2 DS
H1-hESC Pol2 TFBS ChIP-seq Overlap Signal ENCODE/OpenChrom-UTA
H1-hESC Pol2 OS
K562 cMyc TFBS ChIP-seq Peaks from ENCODE/OpenChrom-UTA
K562 cMyc TFBS ChIP-seq Density Signal ENCODE/OpenChrom-UTA
K562 cMyc DS
K562 cMyc TFBS ChIP-seq Overlap Signal ENCODE/OpenChrom-UTA
K562 cMyc OS
K562 CTCF TFBS ChIP-seq Peaks from ENCODE/OpenChrom-UTA
K562 CTCF TFBS ChIP-seq Density Signal ENCODE/OpenChrom-UTA
K562 CTCF DS
K562 CTCF TFBS ChIP-seq Overlap Signal ENCODE/OpenChrom-UTA
K562 CTCF OS
K562 Pol2 TFBS ChIP-seq Peaks from ENCODE/OpenChrom-UTA
K562 Pol2 TFBS ChIP-seq Density Signal ENCODE/OpenChrom-UTA
K562 Pol2 DS
K562 Pol2 TFBS ChIP-seq Overlap Signal ENCODE/OpenChrom-UTA
K562 Pol2 OS
K562 Input TFBS ChIP-seq Density Signal ENCODE/OpenChrom-UTA
K562 Input DS

DNaseI Digital Genomic Footprinting from ENCODE/University of Washington
K562 Sig
HepG2 Sig
HUVEC Sig
DNaseI Hypersensitivity by Digital DNaseI from ENCODE/University of Washington
GM12878 Ht 1
GM12878 Pk 1
GM12878 Sg 1
GM12878 Ht 2
GM12878 Pk 2
GM12878 Sg 2
H1hESC Ht 1
H1hESC Pk 1
H1hESC Sg 1
K562 Ht 1
K562 Pk 1
K562 Sg 1
K562 Ht 2
K562 Pk 2
K562 Sg 2

100 vertebrates Basewise Conservation by PhyloP
100 Vert. Cons
Multiz Alignments of 100 Vertebrates
Gaps
Human
Rhesus
Mouse
Dog
Elephant
Chicken
X_tropicalis
Zebrafish
Lamprey
Opossum (Oct. 2006 (Broad/monDom5)) Alignment Net
chr3 - 31433k
Chicken (May 2006 (WUGSC 2.1/galGal3)) Chained Alignments
Chicken (May 2006 (WUGSC 2.1/galGal3)) Alignment Net
X. tropicalis (Nov. 2009 (JGI 4.2/xenTro3)) Alignment Net
Zebrafish (Jul. 2010 (Zv9/danRer7)) Alignment Net

Common SNPs(144)
Simple Nucleotide Polymorphisms (dbSNP 144) Found in >= 1% of Samples
Simple Nucleotide Polymorphisms (dbSNP 142) Found in >= 1% of Samples
rs10223666
RepeatMasker
Repeating Elements by RepeatMasker

Journal of Medical Genetics
Page 42 of 57
rs13179831
Human mRNAs
Spliced ESTs
H3K27Ac Mark (Often Found Near Active Regulatory Elements) on 7 cell lines from ENCODE
Human ESTs That Have Been Spliced
Transcription Factor ChIP-seq (161 factors) from ENCODE with Factorbook Motifs
DNaseI Hypersensitivity Clusters in 125 cell types from ENCODE (V3)
DNaseI Hypersensitive Site Master List (125 cell types) from ENCODE/Analysis
Open Chromatin by DNaseI HS from ENCODE/OpenChrom(Duke University)
Histone Modifications by ChIP-seq from ENCODE/Broad Institute
Open Chromatin by FAIRE from ENCODE/OpenChrom(UNC Chapel Hill)
100 Vert. Cons
Multiz Alignments of 100 Vertebrates
100 vertebrates Basewise Conservation by PhyloP
Oposs/un (Oct. 2006 (Broad/monDom5)) Alignment Net
Chicken (May 2006 (WUGSC 2.1/galGal3)) Chained Alignments
Chicken (May 2006 (WUGSC 2.1/galGal3)) Alignment Net
X. tropicalis (Nov. 2009 (JGI 4.2/xenTro3)) Alignment Net
Zebrafish (Mar. 2013 (GRCz10/danRer7)) Alignment Net
https://mc.manuscriptcentral.com/jmedgenet
Simple Nucleotide Polymorphisms (dbSNP 144) Found in >= 1% of Samples
Simple Nucleotide Polymorphisms (dbSNP 142) Found in >= 1% of Samples
Repeating Elements by RepeatMasker
RepeatMasker
Common SNP(144)
rs58758521
rs13179831
Scale
chr6:
43,806,300
43,806,310
43,806,320
43,806,330
43,806,340
43,806,350
43,806,360
43,806,370
43,806,380
43,806,390
50 bases
hg19

Journal of Medical Genetics

Scale
chr6:
200 bases
43,806,500
43,806,600
43,806,700
43,806,800
hg19
UCSC Genes (RefSeq, GenBank, CCDS, Rfam, tRNAs & Comparative Genomics)
RefSeq Genes
RefSeq Genes
rs881858
Publications: Sequences in Scientific Articles
Sequences
SNPs
NHGRI Catalog of Published Genome-Wide Association Studies
rs881858
Human mRNAs from GenBank
Human mRNAs
100
Layered H3K27Ac
0
H3K27Ac Mark (Often Found Near Active Regulatory Elements) on 7 cell lines from ENCODE
DNase Clusters
DNaseI Hypersensitivity Clusters in 125 cell types from ENCODE (V3)
Transcription Factor ChIP-seq (161 factors) from ENCODE with Factorbook Motifs
HDAC8
TFAP2C
MAZ
CTCF
JUND
MAX
BHLHE40
EP300
MAFF
RCOR1
MAFK
REST
FOSL1
JUN
CEBPB
HDAC2
CEBPD
FOSL2
Master DNaseI HS
DNaseI Hypersensitive Site Master List (125 cell types) from ENCODE/Analysis
DNaseI Hypersensitivity Uniform Peaks from ENCODE/Analysis
GM12878 DNase
H1-hESC DNase
K562 DNase
HUVEC DNase
HeLa-S3 DNase
HepG2 DNase
A549 DNase
CD20+ DNase
MCF-7 DNase
Myocyte-CD14+ DNase
NHEK DNase
Transcription Factor ChIP-seq Uniform Peaks from ENCODE/Analysis
GM12878 CTCF t
GM12878 POLR2A h
GM12878 SP1
H1-hESC CTCF t
H1-hESC NANOG
H1-hESC POLR2A h
K562 CTCF t
K562 NFYA
K562 POLR2A h
HeLa-S3 CTCF t
HeLa-S3 E2F1 c2
HeLa-S3 POLR2A h
HepG2 CTCF t
HepG2 EP300 s
HepG2 POLR2A h
HUVEC CTCF t
HUVEC FOS
HUVEC POLR2A h
A549+Dx100n CTCF
A549+Dx100n NR3C1
IMR90 CEBPB
IMR90 CTCF
IMR90 POLR2A
MCF-7+stim CTCF
MCF-7+stim MYC
MCF-7+stim POLR2A
DNaseI/FAIRE/ChIP Synthesis from ENCODE/OpenChrom(Duke/UNC/UTA)
GM12878 Syn Pk
H1-hESC Syn Pk
K562 Syn Pk
Histone Modifications by ChIP-seq from ENCODE/Broad Institute
H1-hESC CTCF
H1-hESC CTCF
H1-hESC H3K4m1
H1-hESC H3K4m1
H1-hESC H3K4m3
H1-hESC H3K4m3
H1-hESC H3K27ac
H1-hESC H3K27ac
H1-hESC H3K27m3
H1-hESC H3K27m3
H1-hESC H3K36m3
H1-hESC H3K36m3
K562 CTCF
K562 CTCF
K562 H3K4m1
K562 H3K4m1
K562 H3K4m3
K562 H3K4m3
K562 H3K27ac
K562 H3K27ac
K562 H3K27m3
K562 H3K27m3
K562 H3K36m3
K562 H3K36m3
Open Chromatin by DNaseI HS from ENCODE/OpenChrom(Duke University)
GM12878 Pk
GM12878 DS
GM12878 OS
H1hESC Pk
H1hESC DS
H1hESC OS
K562 Pk
K562 DS
K562 OS
Histone Modifications by ChIP-seq from ENCODE/Stanford/Yale/USC/Harvard
K562 H3K4me1
K562 H3K4me1
K562 H3K4me3
K562 H3K4me3
K562 H3K9ac
K562 H3K9ac
K562 H3K27me3
K562 H3K27me3
NT2-D1 H3K4me1
NT2-D1 H3K4me1
NT2-D1 H3K4me3
NT2-D1 H3K4me3
NT2-D1 H3K9ac
NT2-D1 H3K9ac
NT2-D1 H3K27me3
NT2-D1 H3K27me3
NT2-D1 H3K36me3
NT2-D1 H3K36me3
U2OS H3K9me3
U2OS H3K9me3
U2OS H3K36me3
U2OS H3K36me3
HMR Conserved Transcription Factor Binding Sites
V$CHOP_01
V$HLF_01
V$E4BP4_01
V$CEBPB_01
Open Chromatin by FAIRE from ENCODE/OpenChrom(UNC Chapel Hill)
GM12878 FAIRE Pk
GM12878 FAIRE DS
GM12878 FAIRE OS
H1-hESC FAIRE Pk
H1-hESC FAIRE DS
H1-hESC FAIRE OS
K562 FAIRE Pk
K562 FAIRE DS
K562 FAIRE OS
DNaseI Digital Genomic Footprinting from ENCODE/University of Washington
K562 Sig
HepG2 Sig
HUVEC Sig
DNaseI Hypersensitivity by Digital DNaseI from ENCODE/University of Washington
GM12878 Ht 1
GM12878 Pk 1
GM12878 Sg 1
GM12878 Ht 2
GM12878 Pk 2
GM12878 Sg 2
H1hESC Ht 1
H1hESC Pk 1
H1hESC Sg 1
K562 Ht 1
K562 Pk 1
K562 Sg 1
K562 Ht 2
K562 Pk 2
K562 Sg 2
Histone Modifications by ChIP-seq from ENCODE/University of Washington
GM78 H3K4M3 Ht 1
GM78 H3K4M3 Pk 1
GM78 H3K4M3 Sg 1
GM78 H3K4M3 Ht 2
GM78 H3K4M3 Pk 2
GM78 H3K4M3 Sg 2
GM78 H3K27M3 Ht 1
GM78 H3K27M3 Pk 1
GM78 H3K27M3 Sg 1
GM78 H3K27M3 Ht 2
GM78 H3K27M3 Pk 2
GM78 H3K27M3 Sg 2
GM78 H3K36M3 Ht 1
GM78 H3K36M3 Pk 1
GM78 H3K36M3 Sg 1
GM78 H3K36M3 Ht 2
GM78 H3K36M3 Pk 2
GM78 H3K36M3 Sg 2
GM78 In Sg 1
K562 H3K4M3 Ht 1
K562 H3K4M3 Pk 1
K562 H3K4M3 Sg 1
K562 H3K4M3 Ht 2
K562 H3K4M3 Pk 2
K562 H3K4M3 Sg 2
rs881858
K562 H3K27M3 Ht 1
K562 H3K27M3 Pk 1
K562 H3K27M3 Sg 1
K562 H3K27M3 Ht 2
K562 H3K27M3 Pk 2
K562 H3K27M3 Sg 2
K562 H3K36M3 Ht 1
K562 H3K36M3 Pk 1
K562 H3K36M3 Sg 1
K562 H3K36M3 Ht 2
K562 H3K36M3 Pk 2
K562 H3K36M3 Sg 2
K562 In Sg 1
100 vertebrates Basewise Conservation by PhyloP
4.88
100 Vert. Cons
0
-4.5
Multiz Alignments of 100 Vertebrates
Rhesus
Mouse
Dog
Elephant
Chicken
X_tropicalis
Zebrafish
Lamprey
Simple Nucleotide Polymorphisms (dbSNP 144) Found in >= 1% of Samples
rs79479645
rs881858
rs57588234
rs13201802
rs114595802
Repeating Elements by RepeatMasker
RepeatMasker

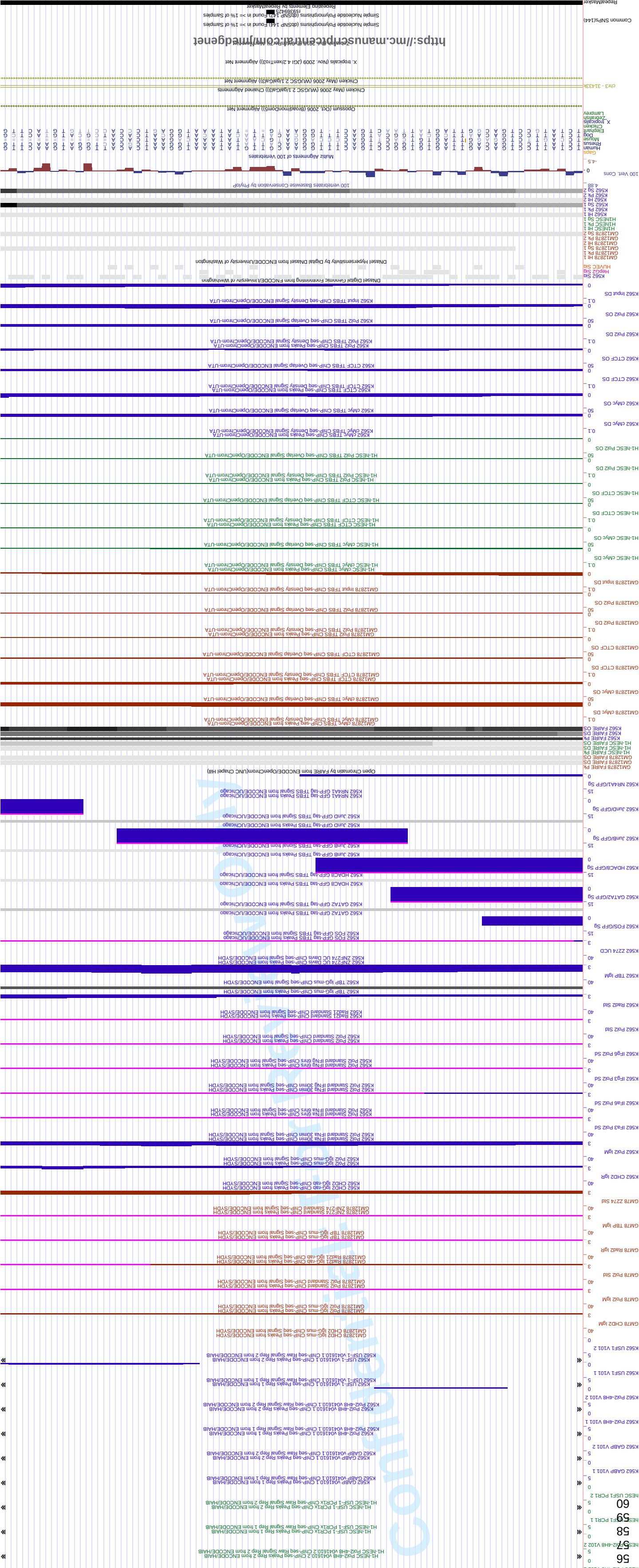
Journal of Medical Genetics
https://mc.manuscriptcentral.com/jmedgenet
rs936942 5
Page 46 of 57

Journal of Medical Genetics

Scale
chr6:
50 bases
hg19
Ensembl Genes Predictions pseudo 71
SNPs in Publications
Human mRNAs from GenBank
Human mRNAs
Human ESTs That Have Been Spliced
Spliced ESTs
H3K27Ac Mark (Often Found Near Active Regulatory Elements) on 7 cell lines from ENCODE
Layered H3K27Ac
DNaseI Hypersensitivity Clusters in 125 cell types from ENCODE (V3)
Transcription Factor ChIP-seq (161 factors) from ENCODE with Factorbook Motifs
POLR2A
GATA2
HDAC1
MYC
IRF1
CCNT2
GATA1
MAZ
DNaseI Hypersensitive Site Master List (125 cell types) from ENCODE/Analysis
Master DNaseI HS
GM12878 DNaseI HS Uniform Peaks from ENCODE/Analysis
H1-hESC DNaseI HS Uniform Peaks from ENCODE/Analysis
K562 DNaseI HS Uniform Peaks from ENCODE/Analysis
HUVEC DNaseI HS Uniform Peaks from ENCODE/Analysis
HeLa-S3 DNaseI HS Uniform Peaks from ENCODE/Analysis
HepG2 DNaseI HS Uniform Peaks from ENCODE/Analysis
A549 DNaseI HS Uniform Peaks from ENCODE/Analysis
CD20+ B cell DNaseI HS Uniform Peaks from ENCODE/Analysis
MCF-7 DNaseI HS Uniform Peaks from ENCODE/Analysis
Monocytes-CD14+ DNaseI HS Uniform Peaks from ENCODE/Analysis
NHEK DNaseI HS Uniform Peaks from ENCODE/Analysis
GM12878 TFBS Uniform Peaks of CTCF from ENCODE/UT-A/Analysis
GM12878 TFBS Uniform Peaks of Pol2-4H8 from ENCODE/HudsonAlpha/Analysis
GM12878 TFBS Uniform Peaks of SP1 from ENCODE/HudsonAlpha/Analysis
H1-hESC TFBS Uniform Peaks of CTCF from ENCODE/UT-A/Analysis
H1-hESC TFBS Uniform Peaks of NANOG_(SC-33759) from ENCODE/HudsonAlpha/Analysis
H1-hESC TFBS Uniform Peaks of Pol2-4H8 from ENCODE/HudsonAlpha/Analysis
K562 TFBS Uniform Peaks of CTCF from ENCODE/UT-A/Analysis
K562 TFBS Uniform Peaks of NF-YA from ENCODE/Stanford/Analysis
K562 TFBS Uniform Peaks of Pol2-4H8 from ENCODE/HudsonAlpha/Analysis
HeLa-S3 TFBS Uniform Peaks of CTCF from ENCODE/UT-A/Analysis
HeLa-S3 TFBS Uniform Peaks of HA-E2F1 from ENCODE/USC/Analysis
HeLa-S3 TFBS Uniform Peaks of Pol2 from ENCODE/HudsonAlpha/Analysis
HepG2 TFBS Uniform Peaks of CTCF from ENCODE/UT-A/Analysis
HepG2 TFBS Uniform Peaks of p300_(SC-584) from ENCODE/Stanford/Analysis
HepG2 TFBS Uniform Peaks of Pol2-4H8 from ENCODE/HudsonAlpha/Analysis
HUVEC TFBS Uniform Peaks of CTCF from ENCODE/UT-A/Analysis
HUVEC TFBS Uniform Peaks of c-Fos from ENCODE/USC/Analysis
HUVEC TFBS Uniform Peaks of Pol2-4H8 from ENCODE/HudsonAlpha/Analysis
A549 (DEX_100nM) TFBS Uniform Peaks of CTCF_(SC-5916) ENCODE/HudsonAlpha/Analysis
A549 (DEX_100nM) TFBS Uniform Peaks of GR from ENCODE/HudsonAlpha/Analysis
IMR90 TFBS Uniform Peaks of CEBPB from ENCODE/Stanford/Analysis
IMR90 TFBS Uniform Peaks of CTCF_(SC-15914) from ENCODE/Stanford/Analysis
IMR90 TFBS Uniform Peaks of Pol2 from ENCODE/Stanford/Analysis
MCF-7 (serum_stimulated) TFBS Uniform Peaks of CTCF from ENCODE/UT-A/Analysis
MCF-7 (serum_stimulated) TFBS Uniform Peaks of c-Myc from ENCODE/UT-A/Analysis
MCF-7 (serum_stimulated) TFBS Uniform Peaks of Pol2 from ENCODE/UT-A/Analysis
DNaseI/FAIRE/ChIP Synthesis from ENCODE/OpenChrom(Duke/UNC/UTA)
GM12878 Syn Pk
H1-hESC Syn Pk
K562 Syn Pk
Histone Modifications by ChIP-seq from ENCODE/Broad Institute
GM12878 H3K4m1
GM12878 H3K4m1
GM12878 H3K27ac
GM12878 H3K27ac
H1-hESC H3K4m1
H1-hESC H3K4m1
H1-hESC H3K27ac
H1-hESC H3K27ac
K562 H3K4m1
K562 H3K4m1
K562 H3K27ac
K562 H3K27ac
A549 DEX H3K4m1
A549 DEX H3K4m1
A549 EtOH H3K4m1
A549 EtOH H3K4m1
A549 DEX H3K27ac
A549 DEX H3K27ac
A549 EtOH H3K27ac
A549 EtOH H3K27ac
CD20+ H3K27ac
CD20+ H3K27ac
HeLa-S3 H3K4m1
HeLa-S3 H3K4m1
HeLa-S3 H3K27ac
HeLa-S3 H3K27ac
HepG2 H3K4m1
HepG2 H3K4m1
HepG2 H3K27ac
HepG2 H3K27ac
HUVEC H3K4m1
HUVEC H3K4m1
HUVEC H3K27ac
HUVEC H3K27ac
CD14+ H3K4m1
CD14+ H3K4m1
CD14+ H3K27ac
CD14+ H3K27ac
Open Chromatin by DNaseI HS from ENCODE/OpenChrom(Duke University)
GM12878 Pk
GM12878 DS
GM12878 OS
H1hESC Pk
H1hESC DS
H1hESC OS
K562 Pk
K562 DS
K562 OS
GM78 GABP PCR2 1
GM12878 GABP PCR2x ChIP-seq Peaks Rep 1 from ENCODE/HAIB
GM12878 GABP PCR2x ChIP-seq Raw Signal Rep 1 from ENCODE/HAIB
GM78 GABP PCR2 2
GM12878 GABP PCR2x ChIP-seq Peaks Rep 2 from ENCODE/HAIB
GM12878 GABP PCR2x ChIP-seq Raw Signal Rep 2 from ENCODE/HAIB
GM78 Pol2-4H8 PCR1 1
GM12878 Pol2-4H8 PCR1x ChIP-seq Peaks Rep 1 from ENCODE/HAIB
GM12878 Pol2-4H8 PCR1x ChIP-seq Raw Signal Rep 1 from ENCODE/HAIB
GM78 Pol2-4H8 PCR1 2
GM12878 Pol2-4H8 PCR1x ChIP-seq Peaks Rep 2 from ENCODE/HAIB
GM12878 Pol2-4H8 PCR1x ChIP-seq Raw Signal Rep 2 from ENCODE/HAIB
GM78 USF1 PCR2 1
GM12878 USF-1 PCR2x ChIP-seq Peaks Rep 1 from ENCODE/HAIB
GM12878 USF-1 PCR2x ChIP-seq Raw Signal Rep 1 from ENCODE/HAIB
GM78 USF1 PCR2 2
GM12878 USF-1 PCR2x ChIP-seq Peaks Rep 2 from ENCODE/HAIB
GM12878 USF-1 PCR2x ChIP-seq Raw Signal Rep 2 from ENCODE/HAIB
hESC GABP PCR1 1
H1-hESC GABP PCR1x ChIP-seq Peaks Rep 1 from ENCODE/HAIB
H1-hESC GABP PCR1x ChIP-seq Raw Signal Rep 1 from ENCODE/HAIB
hESC GABP PCR1 2
H1-hESC GABP PCR1x ChIP-seq Peaks Rep 2 from ENCODE/HAIB
H1-hESC GABP PCR1x ChIP-seq Raw Signal Rep 2 from ENCODE/HAIB
hESC Pol2-4H8 V102 1
H1-hESC Pol2-4H8 v041610.2 ChIP-seq Peaks Rep 1 from ENCODE/HAIB
H1-hESC Pol2-4H8 v041610.2 ChIP-seq Raw Signal Rep 1 from ENCODE/HAIB
hESC Pol2-4H8 V102 2
H1-hESC Pol2-4H8 v041610.2 ChIP-seq Peaks Rep 2 from ENCODE/HAIB
H1-hESC Pol2-4H8 v041610.2 ChIP-seq Raw Signal Rep 2 from ENCODE/HAIB
hESC USF1 PCR1 1
H1-hESC USF-1 PCR1x ChIP-seq Peaks Rep 1 from ENCODE/HAIB
H1-hESC USF-1 PCR1x ChIP-seq Raw Signal Rep 1 from ENCODE/HAIB
hESC USF1 PCR1 2
H1-hESC USF-1 PCR1x ChIP-seq Peaks Rep 2 from ENCODE/HAIB
H1-hESC USF-1 PCR1x ChIP-seq Raw Signal Rep 2 from ENCODE/HAIB
K562 GABP V101 1
K562 GABP v041610.1 ChIP-seq Peaks Rep 1 from ENCODE/HAIB
K562 GABP v041610.1 ChIP-seq Raw Signal Rep 1 from ENCODE/HAIB
K562 GABP V101 2
K562 GABP v041610.1 ChIP-seq Peaks Rep 2 from ENCODE/HAIB
K562 GABP v041610.1 ChIP-seq Raw Signal Rep 2 from ENCODE/HAIB
K562 Pol2-4H8 V101 1
K562 Pol2-4H8 v041610.1 ChIP-seq Peaks Rep 1 from ENCODE/HAIB
K562 Pol2-4H8 v041610.1 ChIP-seq Raw Signal Rep 1 from ENCODE/HAIB
K562 Pol2-4H8 V101 2
K562 Pol2-4H8 v041610.1 ChIP-seq Peaks Rep 2 from ENCODE/HAIB
K562 Pol2-4H8 v041610.1 ChIP-seq Raw Signal Rep 2 from ENCODE/HAIB
K562 USF1 V101 1
K562 USF-1 v041610.1 ChIP-seq Peaks Rep 1 from ENCODE/HAIB
K562 USF-1 v041610.1 ChIP-seq Raw Signal Rep 1 from ENCODE/HAIB
K562 USF1 V101 2
K562 USF-1 v041610.1 ChIP-seq Peaks Rep 2 from ENCODE/HAIB
K562 USF-1 v041610.1 ChIP-seq Raw Signal Rep 2 from ENCODE/HAIB
GM78 CHD2 IgM
GM12878 CHD2 IgG-mus ChIP-seq Peaks from ENCODE/SYDH
GM12878 CHD2 IgG-mus ChIP-seq Signal from ENCODE/SYDH
GM78 Pol2 IgM
GM12878 Pol2 IgG-mus ChIP-seq Peaks from ENCODE/SYDH
GM12878 Pol2 IgG-mus ChIP-seq Signal from ENCODE/SYDH
GM78 Pol2 Std
GM12878 Pol2 Standard ChIP-seq Peaks from ENCODE/SYDH
GM12878 Pol2 Standard ChIP-seq Signal from ENCODE/SYDH
GM78 Rad2 IgR
GM12878 Rad21 IgG-rab ChIP-seq Peaks from ENCODE/SYDH
GM12878 Rad21 IgG-rab ChIP-seq Signal from ENCODE/SYDH
GM78 TBP IgM
GM12878 TBP IgG-mus ChIP-seq Peaks from ENCODE/SYDH
GM12878 TBP IgG-mus ChIP-seq Signal from ENCODE/SYDH
GM78 Z274 Std
GM12878 ZNF274 Standard ChIP-seq Peaks from ENCODE/SYDH
GM12878 ZNF274 Standard ChIP-seq Signal from ENCODE/SYDH
K562 CHD2 IgR
K562 CHD2 IgG-rab ChIP-seq Peaks from ENCODE/SYDH
K562 CHD2 IgG-rab ChIP-seq Signal from ENCODE/SYDH
K562 Pol2 IgM
K562 Pol2 IgG-mus ChIP-seq Peaks from ENCODE/SYDH
K562 Pol2 IgG-mus ChIP-seq Signal from ENCODE/SYDH
K562 IFa3 Pol2 Sd
K562 Pol2 Standard IFNa 30min ChIP-seq Peaks from ENCODE/SYDH
K562 Pol2 Standard IFNa 30min ChIP-seq Signal from ENCODE/SYDH
K562 IFa6 Pol2 Sd
K562 Pol2 Standard IFNa 6hrs ChIP-seq Peaks from ENCODE/SYDH
K562 Pol2 Standard IFNa 6hrs ChIP-seq Signal from ENCODE/SYDH
K562 IFg3 Pol2 Sd
K562 Pol2 Standard IFNg 30min ChIP-seq Peaks from ENCODE/SYDH
K562 Pol2 Standard IFNg 30min ChIP-seq Signal from ENCODE/SYDH
K562 IFg6 Pol2 Sd
K562 Pol2 Standard IFNg 6hrs ChIP-seq Peaks from ENCODE/SYDH
K562 Pol2 Standard IFNg 6hrs ChIP-seq Signal from ENCODE/SYDH
K562 Pol2 Std
K562 Pol2 Standard ChIP-seq Peaks from ENCODE/SYDH
K562 Pol2 Standard ChIP-seq Signal from ENCODE/SYDH
K562 Rad2 Std
K562 Rad21 Standard ChIP-seq Peaks from ENCODE/SYDH
K562 Rad21 Standard ChIP-seq Signal from ENCODE/SYDH
K562 TBP IgM
K562 TBP IgG-mus ChIP-seq Peaks from ENCODE/SYDH
K562 TBP IgG-mus ChIP-seq Signal from ENCODE/SYDH
K562 Z274 UCD
K562 ZNF274 UC Davis ChIP-seq Peaks from ENCODE/SYDH
K562 ZNF274 UC Davis ChIP-seq Signal from ENCODE/SYDH
K562 FOS/GFP Sg
K562 FOS GFP-tag TFBS Peaks from ENCODE/UChicago
K562 FOS GFP-tag TFBS Signal from ENCODE/UChicago
K562 GATA2/GFP Sg
K562 GATA2 GFP-tag TFBS Peaks from ENCODE/UChicago
K562 GATA2 GFP-tag TFBS Signal from ENCODE/UChicago
K562 HDAC8/GFP Sg
K562 HDAC8 GFP-tag TFBS Peaks from ENCODE/UChicago
K562 HDAC8 GFP-tag TFBS Signal from ENCODE/UChicago
K562 JunB/GFP Sg
K562 JunB GFP-tag TFBS Peaks from ENCODE/UChicago
K562 JunB GFP-tag TFBS Signal from ENCODE/UChicago
K562 JunD/GFP Sg
K562 JunD GFP-tag TFBS Peaks from ENCODE/UChicago
K562 JunD GFP-tag TFBS Signal from ENCODE/UChicago
K562 NR4A1/GFP Sg
K562 NR4A1 GFP-tag TFBS Peaks from ENCODE/UChicago
K562 NR4A1 GFP-tag TFBS Signal from ENCODE/UChicago
GM12878 FAIRE Pk
Open Chromatin by FAIRE from ENCODE/OpenChrom(UNC Chapel Hill)
GM12878 FAIRE DS
GM12878 FAIRE OS
H1-hESC FAIRE Pk
H1-hESC FAIRE DS
H1-hESC FAIRE OS
K562 FAIRE Pk
K562 FAIRE DS
K562 FAIRE OS
GM12878 cMyc DS
GM12878 cMyc TFBS ChIP-seq Peaks from ENCODE/OpenChrom-UTA
GM12878 cMyc TFBS ChIP-seq Density Signal ENCODE/OpenChrom-UTA
GM12878 cMyc OS
GM12878 cMyc TFBS ChIP-seq Overlap Signal ENCODE/OpenChrom-UTA
GM12878 CTCF DS
GM12878 CTCF TFBS ChIP-seq Peaks from ENCODE/OpenChrom-UTA
GM12878 CTCF TFBS ChIP-seq Density Signal ENCODE/OpenChrom-UTA
GM12878 CTCF OS
GM12878 CTCF TFBS ChIP-seq Overlap Signal ENCODE/OpenChrom-UTA
GM12878 Pol2 DS
GM12878 Pol2 TFBS ChIP-seq Peaks from ENCODE/OpenChrom-UTA
GM12878 Pol2 TFBS ChIP-seq Density Signal ENCODE/OpenChrom-UTA
GM12878 Pol2 OS
GM12878 Pol2 TFBS ChIP-seq Overlap Signal ENCODE/OpenChrom-UTA
GM12878 Input DS
GM12878 Input TFBS ChIP-seq Density Signal ENCODE/OpenChrom-UTA
H1-hESC cMyc DS
H1-hESC cMyc TFBS ChIP-seq Peaks from ENCODE/OpenChrom-UTA
H1-hESC cMyc TFBS ChIP-seq Density Signal ENCODE/OpenChrom-UTA
H1-hESC cMyc OS
H1-hESC cMyc TFBS ChIP-seq Overlap Signal ENCODE/OpenChrom-UTA
H1-hESC CTCF DS
H1-hESC CTCF TFBS ChIP-seq Peaks from ENCODE/OpenChrom-UTA
H1-hESC CTCF TFBS ChIP-seq Density Signal ENCODE/OpenChrom-UTA
H1-hESC CTCF OS
H1-hESC CTCF TFBS ChIP-seq Overlap Signal ENCODE/OpenChrom-UTA
H1-hESC Pol2 DS
H1-hESC Pol2 TFBS ChIP-seq Peaks from ENCODE/OpenChrom-UTA
H1-hESC Pol2 TFBS ChIP-seq Density Signal ENCODE/OpenChrom-UTA
H1-hESC Pol2 OS
H1-hESC Pol2 TFBS ChIP-seq Overlap Signal ENCODE/OpenChrom-UTA
K562 cMyc DS
K562 cMyc TFBS ChIP-seq Peaks from ENCODE/OpenChrom-UTA
K562 cMyc TFBS ChIP-seq Density Signal ENCODE/OpenChrom-UTA
K562 cMyc OS
K562 cMyc TFBS ChIP-seq Overlap Signal ENCODE/OpenChrom-UTA
K562 CTCF DS
K562 CTCF TFBS ChIP-seq Peaks from ENCODE/OpenChrom-UTA
K562 CTCF TFBS ChIP-seq Density Signal ENCODE/OpenChrom-UTA
K562 CTCF OS
K562 CTCF TFBS ChIP-seq Overlap Signal ENCODE/OpenChrom-UTA
K562 Pol2 DS
K562 Pol2 TFBS ChIP-seq Peaks from ENCODE/OpenChrom-UTA
K562 Pol2 TFBS ChIP-seq Density Signal ENCODE/OpenChrom-UTA
K562 Pol2 OS
K562 Pol2 TFBS ChIP-seq Overlap Signal ENCODE/OpenChrom-UTA
K562 Input DS
K562 Input TFBS ChIP-seq Density Signal ENCODE/OpenChrom-UTA
DNaseI Digital Genomic Footprinting from ENCODE/University of Washington
K562 Sig
HepG2 Sig
HUVEC Sig
DNaseI Hypersensitivity by Digital DNaseI from ENCODE/University of Washington
GM12878 Ht 1
GM12878 Pk 1
GM12878 Sg 1
GM12878 Ht 2
GM12878 Pk 2
GM12878 Sg 2
H1hESC Ht 1
H1hESC Pk 1
H1hESC Sg 1
K562 Ht 1
K562 Pk 1
K562 Sg 1
K562 Ht 2
K562 Pk 2
K562 Sg 2
100 vertebrates Basewise Conservation by PhyloP
100 Vert. Cons
Multiz Alignments of 100 Vertebrates
Gaps
Human
Rhesus
Mouse
Dog
Elephant
Chicken
X_tropicalis
Zebrafish
Lamprey
Opossum (Oct. 2006 (Broad/monDom5)) Alignment Net
chr3 - 31433k
Chicken (May 2006 (WUGSC 2.1/galGal3)) Chained Alignments
Chicken (May 2006 (WUGSC 2.1/galGal3)) Alignment Net
X. tropicalis (Nov. 2009 (JGI 4.2/xenTro3)) Alignment Net
Zebrafish (Oct. 2010 (Zv9/danRer7)) Alignment Net
Common SNPs(144)
Simple Nucleotide Polymorphisms (dbSNP 144) Found in >= 1% of Samples
Simple Nucleotide Polymorphisms (dbSNP 142) Found in >= 1% of Samples
rs9369427
RepeatMasker
Repeating Elements by RepeatMasker

Scale
chr6:
200 bases
hg19
43,811,600
43,811,700
43,811,800
43,811,900
43,812,000
rs9472138
UCSC Genes (RefSeq, GenBank, CCDS, Rfam, tRNAs & Comparative Genomics)
RefSeq Genes
Publications: Sequences in Scientific Articles
Sequences
SNPs
NHGRI Catalog of Published Genome-Wide Association Studies
rs9472138
rs9472138
rs9472138
rs9472138
rs9472138
Human mRNAs from GenBank
Human mRNAs
100
0
H3K27Ac Mark (Often Found Near Active Regulatory Elements) on 7 cell lines from ENCODE
Layered H3K27Ac
DNaseI Hypersensitivity Clusters in 125 cell types from ENCODE (V3)
DNase Clusters
Transcription Factor ChIP-seq (161 factors) from ENCODE with Factorbook Motifs
POLR2A
GATA2
IRF1
MAFK
CEBPB
DNaseI Hypersensitive Site Master List (125 cell types) from ENCODE/Analysis
Master DNaseI HS
DNaseI Hypersensitivity Uniform Peaks from ENCODE/Analysis
GM12878 DNase
H1-hESC DNase
K562 DNase
HUVEC DNase
HeLa-S3 DNase
HepG2 DNase
A549 DNase
CD20+ DNase
MCF-7 DNase
NHEK DNase
Transcription Factor ChIP-seq Uniform Peaks from ENCODE/Analysis
GM12878 CTCF
GM12878 POLR2A
GM12878 SP1
H1-hESC CTCF
H1-hESC NANOG
H1-hESC POLR2A
K562 CTCF
K562 NFYA
K562 POLR2A
HeLa-S3 CTCF
HeLa-S3 E2F1
HeLa-S3 POLR2A
HepG2 CTCF
HepG2 EP300
HepG2 POLR2A
HUVEC CTCF
HUVEC FOS
HUVEC POLR2A
A549+Dx100n CTCF
A549+Dx100n NR3C1
IMR90 CEBPB
IMR90 CTCF
IMR90 POLR2A
MCF-7+stim CTCF
MCF-7+stim MYC
MCF-7+stim POLR2A
DNaseI/FAIRE/ChIP Synthesis from ENCODE/OpenChrom(Duke/UNC/UTA)
GM12878 Syn Pk
H1-hESC Syn Pk
K562 Syn Pk
Histone Modifications by ChIP-seq from ENCODE/Broad Institute
H1-hESC CTCF
H1-hESC H3K4m1
H1-hESC H3K4m3
H1-hESC H3K27ac
H1-hESC H3K27m3
H1-hESC H3K36m3
K562 CTCF
K562 H3K4m1
K562 H3K4m3
K562 H3K27ac
K562 H3K27m3
K562 H3K36m3
Open Chromatin by DNaseI HS from ENCODE/OpenChrom(Duke University)
GM12878 Pk
GM12878 DS
GM12878 OS
H1hESC Pk
H1hESC DS
H1hESC OS
K562 Pk
K562 DS
K562 OS
Histone Modifications by ChIP-seq from ENCODE/Stanford/Yale/USC/Harvard
K562 H3K4me1
K562 H3K4me3
K562 H3K9ac
K562 H3K27me3
NT2-D1 H3K4me1
NT2-D1 H3K4me3
NT2-D1 H3K9ac
NT2-D1 H3K27me3
NT2-D1 H3K36me3
U2OS H3K9me3
U2OS H3K36me3
HMR Conserved Transcription Factor Binding Sites
Open Chromatin by FAIRE from ENCODE/OpenChrom(UNC Chapel Hill)
GM12878 FAIRE Pk
GM12878 FAIRE DS
GM12878 FAIRE OS
H1-hESC FAIRE Pk
H1-hESC FAIRE DS
H1-hESC FAIRE OS
K562 FAIRE Pk
K562 FAIRE DS
K562 FAIRE OS
DNaseI Digital Genomic Footprinting from ENCODE/University of Washington
K562 Sig
HepG2 Sig
HUVEC Sig
DNaseI Hypersensitivity by Digital DNaseI from ENCODE/University of Washington
GM12878 Ht 1
GM12878 Pk 1
GM12878 Sg 1
GM12878 Ht 2
GM12878 Pk 2
GM12878 Sg 2
H1hESC Ht 1
H1hESC Pk 1
H1hESC Sg 1
K562 Ht 1
K562 Pk 1
K562 Sg 1
K562 Ht 2
K562 Pk 2
K562 Sg 2
Histone Modifications by ChIP-seq from ENCODE/University of Washington
GM78 H3K4M3 Ht 1
GM78 H3K4M3 Pk 1
GM78 H3K4M3 Sg 1
GM78 H3K4M3 Ht 2
GM78 H3K4M3 Pk 2
GM78 H3K4M3 Sg 2
GM78 H3K27M3 Ht 1
GM78 H3K27M3 Pk 1
GM78 H3K27M3 Sg 1
GM78 H3K27M3 Ht 2
GM78 H3K27M3 Pk 2
GM78 H3K27M3 Sg 2
GM78 H3K36M3 Ht 1
GM78 H3K36M3 Pk 1
GM78 H3K36M3 Sg 1
GM78 H3K36M3 Ht 2
GM78 H3K36M3 Pk 2
GM78 H3K36M3 Sg 2
GM78 In Sg 1
K562 H3K4M3 Ht 1
K562 H3K4M3 Pk 1
K562 H3K4M3 Sg 1
K562 H3K4M3 Ht 2
K562 H3K4M3 Pk 2
K562 H3K4M3 Sg 2
K562 H3K27M3 Ht 1
K562 H3K27M3 Pk 1
K562 H3K27M3 Sg 1
K562 H3K27M3 Ht 2
K562 H3K27M3 Pk 2
K562 H3K27M3 Sg 2
K562 H3K36M3 Ht 1
K562 H3K36M3 Pk 1
K562 H3K36M3 Sg 1
K562 H3K36M3 Ht 2
K562 H3K36M3 Pk 2
K562 H3K36M3 Sg 2
K562 In Sg 1
rs9472138
100 vertebrates Basewise Conservation by PhyloP
100 Vert. Cons
0
-4.5
Multiz Alignments of 100 Vertebrates
Rhesus
Mouse
Dog
Elephant
Chicken
X_tropicalis
Zebrafish
Lamprey
https://mc.manuscriptcentral.com/jmedgenet
Simple Nucleotide Polymorphisms (dbSNP 144) Found in >= 1% of Samples
rs9472138
Repeating Elements by RepeatMasker
RepeatMasker

rs7758685

Scale
chr6:
50 bases
hg19
43,825,230 43,825,240 43,825,250 43,825,260 43,825,270 43,825,280 43,825,290 43,825,300 43,825,310 43,825,320
---> T G T G A T C A T G C C C T G G G T A G G C T C T G G G T C T T T C C A G A A C C T G G A A A G G T G G A G C G G G T C T G C C C T G G C C C A T G T G A G C C A T T G A C C C C T T G A T G T T C C C

Ensembl Genes Predictions Archive 79 Feb2014
SNPs in Publications
NHGRI Catalog of Published Genome-Wide Association Studies
Human mRNAs from GenBank
Human mRNAs
Human ESTs That Have Been Spliced
Spliced ESTs
H3K27Ac Mark (Often Found Near Active Regulatory Elements) on 7 cell lines from ENCODE
Layered H3K27Ac
DNaseI Hypersensitivity Clusters in 125 cell types from ENCODE (V3)
Transcription Factor ChIP-seq (161 factors) from ENCODE with Factorbook Motifs
DNaseI Hypersensitive Site Master List (125 cell types) from ENCODE/Analysis
Master DNaseI HS
GM12878 DNaseI HS Uniform Peaks from ENCODE/Analysis
H1-hESC DNaseI HS Uniform Peaks from ENCODE/Analysis
K562 DNaseI HS Uniform Peaks from ENCODE/Analysis
HUVEC DNaseI HS Uniform Peaks from ENCODE/Analysis
HeLa-S3 DNaseI HS Uniform Peaks from ENCODE/Analysis
HepG2 DNaseI HS Uniform Peaks from ENCODE/Analysis
A549 DNaseI HS Uniform Peaks from ENCODE/Analysis
CD20+ B cell DNaseI HS Uniform Peaks from ENCODE/Analysis
MCF-7 DNaseI HS Uniform Peaks from ENCODE/Analysis
Monocytes-CD14+ DNaseI HS Uniform Peaks from ENCODE/Analysis
NHEK DNaseI HS Uniform Peaks from ENCODE/Analysis
GM12878 TFBS Uniform Peaks of CTCF from ENCODE/UT-A/Analysis
GM12878 TFBS Uniform Peaks of Pol2-4H8 from ENCODE/HudsonAlpha/Analysis
GM12878 TFBS Uniform Peaks of SP1 from ENCODE/HudsonAlpha/Analysis
H1-hESC TFBS Uniform Peaks of CTCF from ENCODE/UT-A/Analysis
H1-hESC TFBS Uniform Peaks of NANOG (SC-33759) from ENCODE/HudsonAlpha/Analysis
H1-hESC TFBS Uniform Peaks of Pol2-4H8 from ENCODE/HudsonAlpha/Analysis
K562 TFBS Uniform Peaks of CTCF from ENCODE/UT-A/Analysis
K562 TFBS Uniform Peaks of NF-YA from ENCODE/Stanford/Analysis
K562 TFBS Uniform Peaks of Pol2-4H8 from ENCODE/HudsonAlpha/Analysis
HeLa-S3 TFBS Uniform Peaks of CTCF from ENCODE/UT-A/Analysis
HeLa-S3 TFBS Uniform Peaks of HA-E2F1 from ENCODE/USC/Analysis
HeLa-S3 TFBS Uniform Peaks of Pol2 from ENCODE/HudsonAlpha/Analysis
HepG2 TFBS Uniform Peaks of CTCF from ENCODE/UT-A/Analysis
HepG2 TFBS Uniform Peaks of p300 (SC-584) from ENCODE/Stanford/Analysis
HepG2 TFBS Uniform Peaks of Pol2-4H8 from ENCODE/HudsonAlpha/Analysis
HUVEC TFBS Uniform Peaks of CTCF from ENCODE/UT-A/Analysis
HUVEC TFBS Uniform Peaks of c-Fos from ENCODE/USC/Analysis
HUVEC TFBS Uniform Peaks of Pol2-4H8 from ENCODE/HudsonAlpha/Analysis
A549 (DEX_100nM) TFBS Uniform Peaks of CTCF_(SC-5916) ENCODE/HudsonAlpha/Analysis
A549 (DEX_100nM) TFBS Uniform Peaks of GR from ENCODE/HudsonAlpha/Analysis
IMR90 TFBS Uniform Peaks of CEBPB from ENCODE/Stanford/Analysis
IMR90 TFBS Uniform Peaks of CTCF_(SC-15914) from ENCODE/Stanford/Analysis
IMR90 TFBS Uniform Peaks of Pol2 from ENCODE/Stanford/Analysis
MCF-7 (serum_stimulated) TFBS Uniform Peaks of CTCF from ENCODE/UT-A/Analysis
MCF-7 (serum_stimulated) TFBS Uniform Peaks of c-Myc from ENCODE/UT-A/Analysis
MCF-7 (serum_stimulated) TFBS Uniform Peaks of Pol2 from ENCODE/UT-A/Analysis
DNaseI/FAIRE/ChIP Synthesis from ENCODE/OpenChrom(Duke/UNC/UTA)
GM12878 Syn Pk
H1-hESC Syn Pk
K562 Syn Pk
Histone Modifications by ChIP-seq from ENCODE/Broad Institute
GM12878 H3K4me1
GM12878 H3K4me1
GM12878 H3K27ac
GM12878 H3K27ac
H1-hESC H3K4me1
H1-hESC H3K4me1
H1-hESC H3K27ac
H1-hESC H3K27ac
K562 H3K4me1
K562 H3K4me1
K562 H3K27ac
K562 H3K27ac
A549 DEX H3K4me1
A549 DEX H3K4me1
A549 EtOH H3K4me1
A549 EtOH H3K4me1
A549 DEX H3K27ac
A549 DEX H3K27ac
A549 EtOH H3K27ac
A549 EtOH H3K27ac
CD20+ H3K4me1
CD20+ H3K27ac
HeLa-S3 H3K4me1
HeLa-S3 H3K4me1
HeLa-S3 H3K27ac
HeLa-S3 H3K27ac
HepG2 H3K4me1
HepG2 H3K4me1
HepG2 H3K27ac
HepG2 H3K27ac
HUVEC H3K4me1
HUVEC H3K4me1
HUVEC H3K27ac
HUVEC H3K27ac
CD14+ H3K4me1
CD14+ H3K4me1
CD14+ H3K27ac
CD14+ H3K27ac
Open Chromatin by DNaseI HS from ENCODE/OpenChrom(Duke University)
GM12878 Pk
GM12878 DS
GM12878 OS
H1hESC Pk
H1hESC DS
H1hESC OS
K562 Pk
K562 DS
K562 OS
GM12878 GABP PCR2x ChIP-seq Peaks Rep 1 from ENCODE/HAIB
GM12878 GABP PCR2x ChIP-seq Raw Signal Rep 1 from ENCODE/HAIB
GM78 GABP PCR2 1
GM12878 GABP PCR2x ChIP-seq Peaks Rep 2 from ENCODE/HAIB
GM12878 GABP PCR2x ChIP-seq Raw Signal Rep 2 from ENCODE/HAIB
GM78 GABP PCR2 2
GM12878 Pol2-4H8 PCR1x ChIP-seq Peaks Rep 1 from ENCODE/HAIB
GM12878 Pol2-4H8 PCR1x ChIP-seq Raw Signal Rep 1 from ENCODE/HAIB
GM78 Pol2-4H8 PCR1 1
GM12878 Pol2-4H8 PCR1x ChIP-seq Peaks Rep 2 from ENCODE/HAIB
GM12878 Pol2-4H8 PCR1x ChIP-seq Raw Signal Rep 2 from ENCODE/HAIB
GM78 Pol2-4H8 PCR1 2
GM12878 USF-1 PCR2x ChIP-seq Peaks Rep 1 from ENCODE/HAIB
GM12878 USF-1 PCR2x ChIP-seq Raw Signal Rep 1 from ENCODE/HAIB
GM78 USF1 PCR2 1
GM12878 USF-1 PCR2x ChIP-seq Peaks Rep 2 from ENCODE/HAIB
GM12878 USF-1 PCR2x ChIP-seq Raw Signal Rep 2 from ENCODE/HAIB
GM78 USF1 PCR2 2
H1-hESC GABP PCR1x ChIP-seq Peaks Rep 1 from ENCODE/HAIB
H1-hESC GABP PCR1x ChIP-seq Raw Signal Rep 1 from ENCODE/HAIB
hESC GABP PCR1 1
H1-hESC GABP PCR1x ChIP-seq Peaks Rep 2 from ENCODE/HAIB
H1-hESC GABP PCR1x ChIP-seq Raw Signal Rep 2 from ENCODE/HAIB
hESC GABP PCR1 2
H1-hESC Pol2-4H8 v041610.2 ChIP-seq Peaks Rep 1 from ENCODE/HAIB
H1-hESC Pol2-4H8 v041610.2 ChIP-seq Raw Signal Rep 1 from ENCODE/HAIB
hESC Pol2-4H8 V102 1
H1-hESC Pol2-4H8 v041610.2 ChIP-seq Peaks Rep 2 from ENCODE/HAIB
H1-hESC Pol2-4H8 v041610.2 ChIP-seq Raw Signal Rep 2 from ENCODE/HAIB
hESC Pol2-4H8 V102 2
H1-hESC USF-1 PCR1x ChIP-seq Peaks Rep 1 from ENCODE/HAIB
H1-hESC USF-1 PCR1x ChIP-seq Raw Signal Rep 1 from ENCODE/HAIB
hESC USF1 PCR1 1
H1-hESC USF-1 PCR1x ChIP-seq Peaks Rep 2 from ENCODE/HAIB
H1-hESC USF-1 PCR1x ChIP-seq Raw Signal Rep 2 from ENCODE/HAIB
hESC USF1 PCR1 2
K562 GABP v041610.1 ChIP-seq Peaks Rep 1 from ENCODE/HAIB
K562 GABP v041610.1 ChIP-seq Raw Signal Rep 1 from ENCODE/HAIB
K562 GABP V101 1
K562 GABP v041610.1 ChIP-seq Peaks Rep 2 from ENCODE/HAIB
K562 GABP v041610.1 ChIP-seq Raw Signal Rep 2 from ENCODE/HAIB
K562 GABP V101 2
K562 Pol2-4H8 v041610.1 ChIP-seq Peaks Rep 1 from ENCODE/HAIB
K562 Pol2-4H8 v041610.1 ChIP-seq Raw Signal Rep 1 from ENCODE/HAIB
K562 Pol2-4H8 V101 1
K562 Pol2-4H8 v041610.1 ChIP-seq Peaks Rep 2 from ENCODE/HAIB
K562 Pol2-4H8 v041610.1 ChIP-seq Raw Signal Rep 2 from ENCODE/HAIB
K562 Pol2-4H8 V101 2
K562 USF-1 v041610.1 ChIP-seq Peaks Rep 1 from ENCODE/HAIB
K562 USF-1 v041610.1 ChIP-seq Raw Signal Rep 1 from ENCODE/HAIB
K562 USF1 V101 1
K562 USF-1 v041610.1 ChIP-seq Peaks Rep 2 from ENCODE/HAIB
K562 USF-1 v041610.1 ChIP-seq Raw Signal Rep 2 from ENCODE/HAIB
K562 USF1 V101 2
GM12878 CHD2 IgG-mus ChIP-seq Peaks from ENCODE/SYDH
GM12878 CHD2 IgG-mus ChIP-seq Signal from ENCODE/SYDH
GM78 CHD2 IgM
GM12878 Pol2 IgG-mus ChIP-seq Peaks from ENCODE/SYDH
GM12878 Pol2 IgG-mus ChIP-seq Signal from ENCODE/SYDH
GM78 Pol2 IgM
GM12878 Pol2 Standard ChIP-seq Peaks from ENCODE/SYDH
GM12878 Pol2 Standard ChIP-seq Signal from ENCODE/SYDH
GM78 Pol2 Std
GM12878 Rad21 IgG-rab ChIP-seq Peaks from ENCODE/SYDH
GM12878 Rad21 IgG-rab ChIP-seq Signal from ENCODE/SYDH
GM78 Rad2 IgR
GM12878 TBP IgG-mus ChIP-seq Peaks from ENCODE/SYDH
GM12878 TBP IgG-mus ChIP-seq Signal from ENCODE/SYDH
GM78 TBP IgM
GM12878 ZNF274 Standard ChIP-seq Peaks from ENCODE/SYDH
GM12878 ZNF274 Standard ChIP-seq Signal from ENCODE/SYDH
GM78 Z274 Std
K562 CHD2 IgG-rab ChIP-seq Peaks from ENCODE/SYDH
K562 CHD2 IgG-rab ChIP-seq Signal from ENCODE/SYDH
K562 CHD2 IgR
K562 Pol2 IgG-mus ChIP-seq Peaks from ENCODE/SYDH
K562 Pol2 IgG-mus ChIP-seq Signal from ENCODE/SYDH
K562 Pol2 IgM
K562 Pol2 Standard IFNa 30min ChIP-seq Peaks from ENCODE/SYDH
K562 Pol2 Standard IFNa 30min ChIP-seq Signal from ENCODE/SYDH
K562 IFa3 Pol2 Sd
K562 Pol2 Standard IFNa 6hrs ChIP-seq Peaks from ENCODE/SYDH
K562 Pol2 Standard IFNa 6hrs ChIP-seq Signal from ENCODE/SYDH
K562 IFa6 Pol2 Sd
K562 Pol2 Standard IFNg 30min ChIP-seq Peaks from ENCODE/SYDH
K562 Pol2 Standard IFNg 30min ChIP-seq Signal from ENCODE/SYDH
K562 IFg3 Pol2 Sd
K562 Pol2 Standard IFNg 6hrs ChIP-seq Peaks from ENCODE/SYDH
K562 Pol2 Standard IFNg 6hrs ChIP-seq Signal from ENCODE/SYDH
K562 IFg6 Pol2 Sd
K562 Pol2 Standard ChIP-seq Peaks from ENCODE/SYDH
K562 Pol2 Standard ChIP-seq Signal from ENCODE/SYDH
K562 Pol2 Std
K562 Rad21 Standard ChIP-seq Peaks from ENCODE/SYDH
K562 Rad21 Standard ChIP-seq Signal from ENCODE/SYDH
K562 Rad2 Std
K562 TBP IgG-mus ChIP-seq Peaks from ENCODE/SYDH
K562 TBP IgG-mus ChIP-seq Signal from ENCODE/SYDH
K562 TBP IgM
K562 ZNF274 UC Davis ChIP-seq Peaks from ENCODE/SYDH
K562 ZNF274 UC Davis ChIP-seq Signal from ENCODE/SYDH
K562 Z274 UCD
K562 FOS GFP-tag TFBS Peaks from ENCODE/UChicago
K562 FOS GFP-tag TFBS Signal from ENCODE/UChicago
K562 FOS/GFP Sg
K562 GATA2 GFP-tag TFBS Peaks from ENCODE/UChicago
K562 GATA2 GFP-tag TFBS Signal from ENCODE/UChicago
K562 GATA2/GFP Sg
K562 HDAC8 GFP-tag TFBS Peaks from ENCODE/UChicago
K562 HDAC8 GFP-tag TFBS Signal from ENCODE/UChicago
K562 HDAC8/GFP Sg
K562 JunB GFP-tag TFBS Peaks from ENCODE/UChicago
K562 JunB GFP-tag TFBS Signal from ENCODE/UChicago
K562 JunB/GFP Sg
K562 JunD GFP-tag TFBS Peaks from ENCODE/UChicago
K562 JunD GFP-tag TFBS Signal from ENCODE/UChicago
K562 JunD/GFP Sg
K562 NR4A1 GFP-tag TFBS Peaks from ENCODE/UChicago
K562 NR4A1 GFP-tag TFBS Signal from ENCODE/UChicago
K562 NR4A1/GFP Sg
Open Chromatin by FAIRE from ENCODE/OpenChrom(UNC Chapel Hill)
GM12878 FAIRE Pk
GM12878 FAIRE DS
GM12878 FAIRE OS
H1-hESC FAIRE Pk
H1-hESC FAIRE DS
H1-hESC FAIRE OS
K562 FAIRE Pk
K562 FAIRE DS
K562 FAIRE OS
GM12878 cMyc TFBS ChIP-seq Peaks from ENCODE/OpenChrom-UTA
GM12878 cMyc TFBS ChIP-seq Density Signal ENCODE/OpenChrom-UTA
GM12878 cMyc DS
GM12878 cMyc TFBS ChIP-seq Overlap Signal ENCODE/OpenChrom-UTA
GM12878 cMyc OS
GM12878 CTCF TFBS ChIP-seq Peaks from ENCODE/OpenChrom-UTA
GM12878 CTCF TFBS ChIP-seq Density Signal ENCODE/OpenChrom-UTA
GM12878 CTCF DS
GM12878 CTCF TFBS ChIP-seq Overlap Signal ENCODE/OpenChrom-UTA
GM12878 CTCF OS
GM12878 Pol2 TFBS ChIP-seq Peaks from ENCODE/OpenChrom-UTA
GM12878 Pol2 TFBS ChIP-seq Density Signal ENCODE/OpenChrom-UTA
GM12878 Pol2 DS
GM12878 Pol2 TFBS ChIP-seq Overlap Signal ENCODE/OpenChrom-UTA
GM12878 Pol2 OS
GM12878 Input TFBS ChIP-seq Density Signal ENCODE/OpenChrom-UTA
GM12878 Input DS
H1-hESC cMyc TFBS ChIP-seq Peaks from ENCODE/OpenChrom-UTA
H1-hESC cMyc TFBS ChIP-seq Density Signal ENCODE/OpenChrom-UTA
H1-hESC cMyc DS
H1-hESC cMyc TFBS ChIP-seq Overlap Signal ENCODE/OpenChrom-UTA
H1-hESC cMyc OS
H1-hESC CTCF TFBS ChIP-seq Peaks from ENCODE/OpenChrom-UTA
H1-hESC CTCF TFBS ChIP-seq Density Signal ENCODE/OpenChrom-UTA
H1-hESC CTCF DS
H1-hESC CTCF TFBS ChIP-seq Overlap Signal ENCODE/OpenChrom-UTA
H1-hESC CTCF OS
H1-hESC Pol2 TFBS ChIP-seq Peaks from ENCODE/OpenChrom-UTA
H1-hESC Pol2 TFBS ChIP-seq Density Signal ENCODE/OpenChrom-UTA
H1-hESC Pol2 DS
H1-hESC Pol2 TFBS ChIP-seq Overlap Signal ENCODE/OpenChrom-UTA
H1-hESC Pol2 OS
K562 cMyc TFBS ChIP-seq Peaks from ENCODE/OpenChrom-UTA
K562 cMyc TFBS ChIP-seq Density Signal ENCODE/OpenChrom-UTA
K562 cMyc DS
K562 cMyc TFBS ChIP-seq Overlap Signal ENCODE/OpenChrom-UTA
K562 cMyc OS
K562 CTCF TFBS ChIP-seq Peaks from ENCODE/OpenChrom-UTA
K562 CTCF TFBS ChIP-seq Density Signal ENCODE/OpenChrom-UTA
K562 CTCF DS
K562 CTCF TFBS ChIP-seq Overlap Signal ENCODE/OpenChrom-UTA
K562 CTCF OS
K562 Pol2 TFBS ChIP-seq Peaks from ENCODE/OpenChrom-UTA
K562 Pol2 TFBS ChIP-seq Density Signal ENCODE/OpenChrom-UTA
K562 Pol2 DS
K562 Pol2 TFBS ChIP-seq Overlap Signal ENCODE/OpenChrom-UTA
K562 Pol2 OS
K562 Input TFBS ChIP-seq Density Signal ENCODE/OpenChrom-UTA
K562 Input DS
DNaseI Digital Genomic Footprinting from ENCODE/University of Washington
K562 Sig
HepG2 Sig
HUVEC Sig
DNaseI Hypersensitivity by Digital DNaseI from ENCODE/University of Washington
GM12878 Ht 1
GM12878 Pk 1
GM12878 Sg 1
GM12878 Ht 2
GM12878 Pk 2
GM12878 Sg 2
H1hESC Ht 1
H1hESC Pk 1
H1hESC Sg 1
K562 Ht 1
K562 Pk 1
K562 Sg 1
K562 Ht 2
K562 Pk 2
K562 Sg 2
100 vertebrates Basewise Conservation by PhyloP
100 Vert. Cons
Gaps
Multiz Alignments of 100 Vertebrates
Human
Rhesus
Mouse
Dog
Elephant
Chicken
X. tropicalis
Zebrafish
Lamprey
Opossum (Oct. 2006 (Broad/monDom5)) Alignment Net
chr3 - 31433k
Chicken (May 2006 (WUGSC 2.1/galGal3)) Chained Alignments
Chicken (May 2006 (WUGSC 2.1/galGal3)) Alignment Net
X. tropicalis (Nov. 2009 (JGI 4.2/xenTro3)) Alignment Net
Zebrafish (Jul. 2010 (Zv9/danRer7)) Alignment Net
Simple Nucleotide Polymorphisms (dbSNP 144) Found in >= 1% of Samples
rs7758685
Simple Nucleotide Polymorphisms (dbSNP 142) Found in >= 1% of Samples
rs7758685
Repeating Elements by RepeatMasker
RepeatMasker

rs9394969


rs9943080
Journal of Medical Genetics
Page 52 of 57
https://mc.manuscriptcentral.com/jmedgenet
Open Chromatin by FAIRE from ENCODE/OpenChrom(UNC Chapel Hill)
Open Chromatin by DNaseI HS from ENCODE/OpenChrom(Duke University)
Histone Modifications by ChIP-seq from ENCODE/Broad Institute
DNaseI Hypersensitivity by Digital DNaseI from ENCODE/University of Washington
Digital Genomic Footprinting from ENCODE/University of Washington
100 vertebrates Basewise Conservation by PhyloP
Multiz Alignments of 100 Vertebrates
Oxygsun (Oct 2006 (Broad/multiZ0mS)) Alignment Net
Chicken (May 2006 (WUGSC 2.1/galGal3)) Chained Alignments
Chicken (May 2006 (WUGSC 2.1/galGal3)) Alignment Net
X. tropicalis (Nov. 2009 (JGI 4.2/xenTro3)) Alignment Net
Simple Nucleotide Polymorphisms (dbSNP 144) Found in >= 1% of Samples
Simple Nucleotide Polymorphisms (dbSNP 142) Found in >= 1% of Samples
Repeating Elements by RepeatMasker
RepeatMasker
Human mRNAs
Spliced ESTs
Labeled H3K27Ac
ZBTB7A
Master DNaseI HS
DNaseI Hypersensitivity Clusters in 125 cell types from ENCODE (V3)
Transcription Factor ChIP-seq (161 factors) from ENCODE with Factorbook Motifs
DNaseI Hypersensitive Site Master List (125 cell types) from ENCODE/Analysis
GM12878 DNaseI HS Uniform Peaks from ENCODE/Analysis
K562 DNaseI HS Uniform Peaks from ENCODE/Analysis
H1-hESC DNaseI HS Uniform Peaks from ENCODE/Analysis
HeLa-S3 DNaseI HS Uniform Peaks from ENCODE/Analysis
HepG2 DNaseI HS Uniform Peaks from ENCODE/Analysis
CD20+ B cell DNaseI HS Uniform Peaks from ENCODE/Analysis
A549 DNaseI HS Uniform Peaks from ENCODE/Analysis
MCF-7 DNaseI HS Uniform Peaks from ENCODE/Analysis
Monocytes-CD14+ DNaseI HS Uniform Peaks from ENCODE/Analysis
GM12878 TFBS Uniform Peaks of CTCF from ENCODE/UT-A/Analysis
GM12878 TFBS Uniform Peaks of Pol2-4H8 from ENCODE/Hudsonalpha/Analysis
H1-hESC TFBS Uniform Peaks of CTCF from ENCODE/UT-A/Analysis
NHEK DNaseI HS Uniform Peaks from ENCODE/Analysis
H1-hESC TFBS Uniform Peaks of NANOG (SC-33759) from ENCODE/Hudsonalpha/Analysis
K562 TFBS Uniform Peaks of NF-YA from ENCODE/Stanford/Analysis
K562 TFBS Uniform Peaks of CTCF from ENCODE/UT-A/Analysis
K562 TFBS Uniform Peaks of Pol2-4H8 from ENCODE/Hudsonalpha/Analysis
HeLa-S3 TFBS Uniform Peaks of NF-E2F1 from ENCODE/USC/Analysis
HeLa-S3 TFBS Uniform Peaks of CTCF from ENCODE/UT-A/Analysis
HepG2 TFBS Uniform Peaks of Rad21 (SC-784) from ENCODE/Stanford/Analysis
HepG2 TFBS Uniform Peaks of Pol2-4H8 from ENCODE/Hudsonalpha/Analysis
HUVEC TFBS Uniform Peaks of c-Fos from ENCODE/USC/Analysis
HUVEC TFBS Uniform Peaks of CTCF from ENCODE/UT-A/Analysis
HUVEC TFBS Uniform Peaks of Pol2-4H8 from ENCODE/Hudsonalpha/Analysis
A549 (DEX 100nM) TFBS Uniform Peaks of CTCF (SC-5916) from ENCODE/Hudsonalpha/Analysis
IMR90 TFBS Uniform Peaks of CTCF from ENCODE/Stanford/Analysis
IMR90 TFBS Uniform Peaks of Pol2 from ENCODE/Hudsonalpha/Analysis
MCF-7 (serum_stimulated) TFBS Uniform Peaks of c-Myc from ENCODE/UT-A/Analysis
MCF-7 (serum_stimulated) TFBS Uniform Peaks of CTCF from ENCODE/UT-A/Analysis
MCF-7 (serum_stimulated) TFBS Uniform Peaks of Pol2 from ENCODE/Stanford/Analysis
DNaseI/FAIRE/ChIP Synthesis from ENCODE/OpenChrom(Duke/UNC/UT-A)
GM12878 FAIRE PK
GM12878 FAIRE DS
K562 NR4A1/GFP Sg
K562 Jund/GFP Sg
K562 HDAC8/GFP Sg
K562 GATA2/GFP Sg
K562 FOS/GFP Sg
K562 Z274 UCD
K562 TBP IgM
K562 Rad2 Std
K562 Pol2 Std
K562 IFg6 Pol2 Sd
K562 IFg3 Pol2 Sd
K562 IFa6 Pol2 Sd
K562 IFa3 Pol2 Sd
K562 Pol2 IgM
K562 CHD2 IgR
GM78 Z274 Std
GM78 TBP IgM
GM78 Rad2 IgR
GM78 Pol2 Std
GM78 Pol2 IgM
GM78 CHD2 IgM
K562 USF1 V101 2
K562 USF1 V101 1
K562 Pol2-4H8 V102 2
K562 Pol2-4H8 V102 1
K562 GABP V101 2
K562 GABP V101 1
K562 USF1 PCR1 2
K562 FAIRE PK
K562 FAIRE DS
H1-hESC FAIRE PK
H1-hESC FAIRE DS
H1-hESC FAIRE OS
GM12878 FAIRE PK
GM12878 FAIRE DS
GM12878 cMyc Sig
GM12878 cMyc TFBS ChIP-seq Peaks from ENCODE/OpenChrom-UTA
GM12878 cMyc TFBS ChIP-seq Density Signal from ENCODE/OpenChrom-UTA
GM12878 cMyc DS
GM12878 cMyc OS
GM12878 CTCF TFBS ChIP-seq Peaks from ENCODE/OpenChrom-UTA
GM12878 CTCF TFBS ChIP-seq Density Signal from ENCODE/OpenChrom-UTA
GM12878 CTCF DS
GM12878 CTCF OS
GM12878 Pol2 TFBS ChIP-seq Peaks from ENCODE/OpenChrom-UTA
GM12878 Pol2 TFBS ChIP-seq Density Signal from ENCODE/OpenChrom-UTA
GM12878 Pol2 DS
GM12878 Pol2 OS
GM12878 Input TFBS ChIP-seq Density Signal from ENCODE/OpenChrom-UTA
GM12878 Input DS
H1-hESC cMyc TFBS ChIP-seq Peaks from ENCODE/OpenChrom-UTA
H1-hESC cMyc TFBS ChIP-seq Density Signal from ENCODE/OpenChrom-UTA
H1-hESC cMyc DS
H1-hESC cMyc OS
H1-hESC CTCF TFBS ChIP-seq Peaks from ENCODE/OpenChrom-UTA
H1-hESC CTCF TFBS ChIP-seq Density Signal from ENCODE/OpenChrom-UTA
H1-hESC CTCF DS
H1-hESC CTCF OS
H1-hESC Pol2 TFBS ChIP-seq Peaks from ENCODE/OpenChrom-UTA
H1-hESC Pol2 TFBS ChIP-seq Density Signal from ENCODE/OpenChrom-UTA
H1-hESC Pol2 DS
H1-hESC Pol2 OS
K562 cMyc TFBS ChIP-seq Peaks from ENCODE/OpenChrom-UTA
K562 cMyc TFBS ChIP-seq Density Signal from ENCODE/OpenChrom-UTA
K562 cMyc DS
K562 cMyc OS
K562 CTCF TFBS ChIP-seq Peaks from ENCODE/OpenChrom-UTA
K562 CTCF TFBS ChIP-seq Density Signal from ENCODE/OpenChrom-UTA
K562 CTCF DS
K562 CTCF OS
K562 Pol2 TFBS ChIP-seq Peaks from ENCODE/OpenChrom-UTA
K562 Pol2 TFBS ChIP-seq Density Signal from ENCODE/OpenChrom-UTA
K562 Pol2 DS
K562 Pol2 OS
K562 Input TFBS ChIP-seq Density Signal from ENCODE/OpenChrom-UTA
K562 Input DS
K562 HepG2 HuVEC Sig
GM12878 HeLa-S3 K562 HepG2 HuVEC Sig
GM12878 Pk 1
GM12878 Sig 1
GM12878 Pk 2
GM12878 Sig 2
H1hESC Pk 1
H1hESC Sig 1
K562 Pk 1
K562 Sig 1
K562 Pk 2
K562 Sig 2
100 Vert. Cons
Human Rhesus Mouse Elephant Chicken X. tropicalis Zebrafish Lamprey
Gaps
Scale
chr3 - 31433k
chr3 - 31434k

rs4711751

Scale
chr6:
20 bases
hg19
Ensembl Genes Predicted Genes Refseq Genes
SNPs in Publications
NHGRI Catalog of Published Genome-Wide Association Studies
rs4711751
Human mRNAs from GenBank
Human ESTs That Have Been Spliced
H3K27Ac Mark (Often Found Near Active Regulatory Elements) on 7 cell lines from ENCODE
DNaseI Hypersensitivity Clusters in 125 cell types from ENCODE (V3)
Transcription Factor ChIP-seq (161 factors) from ENCODE with Factorbook Motifs
DNaseI Hypersensitive Site Master List (125 cell types) from ENCODE/Analysis
GM12878 DNaseI HS Uniform Peaks from ENCODE/Analysis
H1-hESC DNaseI HS Uniform Peaks from ENCODE/Analysis
K562 DNaseI HS Uniform Peaks from ENCODE/Analysis
HUVEC DNaseI HS Uniform Peaks from ENCODE/Analysis
HeLa-S3 DNaseI HS Uniform Peaks from ENCODE/Analysis
HepG2 DNaseI HS Uniform Peaks from ENCODE/Analysis
A549 DNaseI HS Uniform Peaks from ENCODE/Analysis
CD20+ B cell DNaseI HS Uniform Peaks from ENCODE/Analysis
MCF-7 DNaseI HS Uniform Peaks from ENCODE/Analysis
Monocytes-CD14+ DNaseI HS Uniform Peaks from ENCODE/Analysis
NHEK DNaseI HS Uniform Peaks from ENCODE/Analysis
GM12878 TFBS Uniform Peaks of CTCF from ENCODE/UT-A/Analysis
GM12878 TFBS Uniform Peaks of Pol2-4H8 from ENCODE/HudsonAlpha/Analysis
GM12878 TFBS Uniform Peaks of SP1 from ENCODE/HudsonAlpha/Analysis
H1-hESC TFBS Uniform Peaks of CTCF from ENCODE/UT-A/Analysis
H1-hESC TFBS Uniform Peaks of NANOG (SC-33759) from ENCODE/HudsonAlpha/Analysis
H1-hESC TFBS Uniform Peaks of Pol2-4H8 from ENCODE/HudsonAlpha/Analysis
K562 TFBS Uniform Peaks of CTCF from ENCODE/UT-A/Analysis
K562 TFBS Uniform Peaks of NF-YA from ENCODE/Stanford/Analysis
K562 TFBS Uniform Peaks of Pol2-4H8 from ENCODE/HudsonAlpha/Analysis
HeLa-S3 TFBS Uniform Peaks of CTCF from ENCODE/UT-A/Analysis
HeLa-S3 TFBS Uniform Peaks of HA-E2F1 from ENCODE/USC/Analysis
HeLa-S3 TFBS Uniform Peaks of Pol2 from ENCODE/HudsonAlpha/Analysis
HepG2 TFBS Uniform Peaks of CTCF from ENCODE/UT-A/Analysis
HepG2 TFBS Uniform Peaks of p300 (SC-584) from ENCODE/Stanford/Analysis
HepG2 TFBS Uniform Peaks of Pol2-4H8 from ENCODE/HudsonAlpha/Analysis
HUVEC TFBS Uniform Peaks of CTCF from ENCODE/UT-A/Analysis
HUVEC TFBS Uniform Peaks of c-Fos from ENCODE/USC/Analysis
HUVEC TFBS Uniform Peaks of Pol2-4H8 from ENCODE/HudsonAlpha/Analysis
A549 (DEX 100nM) TFBS Uniform Peaks of CTCF (SC-5916) ENCODE/HudsonAlpha/Analysis
A549 (DEX 100nM) TFBS Uniform Peaks of GR from ENCODE/HudsonAlpha/Analysis
IMR90 TFBS Uniform Peaks of CEBPB from ENCODE/Stanford/Analysis
IMR90 TFBS Uniform Peaks of CTCF (SC-15914) from ENCODE/Stanford/Analysis
IMR90 TFBS Uniform Peaks of Pol2 from ENCODE/Stanford/Analysis
MCF-7 (serum stimulated) TFBS Uniform Peaks of CTCF from ENCODE/UT-A/Analysis
MCF-7 (serum stimulated) TFBS Uniform Peaks of c-Myc from ENCODE/UT-A/Analysis
MCF-7 (serum stimulated) TFBS Uniform Peaks of Pol2 from ENCODE/UT-A/Analysis
DNaseI/FAIRE/ChIP Synthesis from ENCODE/OpenChrom(Duke/UNC/UTA)
GM12878 Syn Pk
H1-hESC Syn Pk
K562 Syn Pk
Histone Modifications by ChIP-seq from ENCODE/Broad Institute
GM12878 H3K4m1
GM12878 H3K4m1
GM12878 H3K27ac
GM12878 H3K27ac
H1-hESC H3K4m1
H1-hESC H3K4m1
H1-hESC H3K27ac
H1-hESC H3K27ac
K562 H3K4m1
K562 H3K4m1
K562 H3K27ac
K562 H3K27ac
A549 DEX H3K4m1
A549 DEX H3K4m1
A549 EtOH H3K4m1
A549 EtOH H3K4m1
A549 DEX H3K27ac
A549 DEX H3K27ac
A549 EtOH H3K27ac
A549 EtOH H3K27ac
CD20+ H3K27ac
CD20+ H3K27ac
HeLa-S3 H3K4m1
HeLa-S3 H3K4m1
HeLa-S3 H3K27ac
HeLa-S3 H3K27ac
HepG2 H3K4m1
HepG2 H3K4m1
HepG2 H3K27ac
HepG2 H3K27ac
HUVEC H3K4m1
HUVEC H3K4m1
HUVEC H3K27ac
HUVEC H3K27ac
CD14+ H3K4m1
CD14+ H3K4m1
CD14+ H3K27ac
CD14+ H3K27ac
Open Chromatin by DNaseI HS from ENCODE/OpenChrom(Duke University)
GM12878 Pk
GM12878 DS
GM12878 OS
H1hESC Pk
H1hESC DS
H1hESC OS
K562 Pk
K562 DS
K562 OS
GM12878 GABP PCR2x ChIP-seq Peaks Rep 1 from ENCODE/HAIB
GM12878 GABP PCR2x ChIP-seq Raw Signal Rep 1 from ENCODE/HAIB
GM78 GABP PCR2 1
GM12878 GABP PCR2x ChIP-seq Peaks Rep 2 from ENCODE/HAIB
GM12878 GABP PCR2x ChIP-seq Raw Signal Rep 2 from ENCODE/HAIB
GM78 GABP PCR2 2
GM12878 Pol2-4H8 PCR1x ChIP-seq Peaks Rep 1 from ENCODE/HAIB
GM12878 Pol2-4H8 PCR1x ChIP-seq Raw Signal Rep 1 from ENCODE/HAIB
GM78 Pol2-4H8 PCR1 1
GM12878 Pol2-4H8 PCR1x ChIP-seq Peaks Rep 2 from ENCODE/HAIB
GM12878 Pol2-4H8 PCR1x ChIP-seq Raw Signal Rep 2 from ENCODE/HAIB
GM78 Pol2-4H8 PCR1 2
GM12878 USF-1 PCR2x ChIP-seq Peaks Rep 1 from ENCODE/HAIB
GM12878 USF-1 PCR2x ChIP-seq Raw Signal Rep 1 from ENCODE/HAIB
GM78 USF1 PCR2 1
GM12878 USF-1 PCR2x ChIP-seq Peaks Rep 2 from ENCODE/HAIB
GM12878 USF-1 PCR2x ChIP-seq Raw Signal Rep 2 from ENCODE/HAIB
GM78 USF1 PCR2 2
H1-hESC GABP PCR1x ChIP-seq Peaks Rep 1 from ENCODE/HAIB
H1-hESC GABP PCR1x ChIP-seq Raw Signal Rep 1 from ENCODE/HAIB
hESC GABP PCR1 1
H1-hESC GABP PCR1x ChIP-seq Peaks Rep 2 from ENCODE/HAIB
H1-hESC GABP PCR1x ChIP-seq Raw Signal Rep 2 from ENCODE/HAIB
hESC GABP PCR1 2
H1-hESC Pol2-4H8 v041610.2 ChIP-seq Peaks Rep 1 from ENCODE/HAIB
H1-hESC Pol2-4H8 v041610.2 ChIP-seq Raw Signal Rep 1 from ENCODE/HAIB
hESC Pol2-4H8 V102 1
H1-hESC Pol2-4H8 v041610.2 ChIP-seq Peaks Rep 2 from ENCODE/HAIB
H1-hESC Pol2-4H8 v041610.2 ChIP-seq Raw Signal Rep 2 from ENCODE/HAIB
hESC Pol2-4H8 V102 2
H1-hESC USF-1 PCR1x ChIP-seq Peaks Rep 1 from ENCODE/HAIB
H1-hESC USF-1 PCR1x ChIP-seq Raw Signal Rep 1 from ENCODE/HAIB
hESC USF1 PCR1 1
H1-hESC USF-1 PCR1x ChIP-seq Peaks Rep 2 from ENCODE/HAIB
H1-hESC USF-1 PCR1x ChIP-seq Raw Signal Rep 2 from ENCODE/HAIB
hESC USF1 PCR1 2
K562 GABP v041610.1 ChIP-seq Peaks Rep 1 from ENCODE/HAIB
K562 GABP v041610.1 ChIP-seq Raw Signal Rep 1 from ENCODE/HAIB
K562 GABP V101 1
K562 GABP v041610.1 ChIP-seq Peaks Rep 2 from ENCODE/HAIB
K562 GABP v041610.1 ChIP-seq Raw Signal Rep 2 from ENCODE/HAIB
K562 GABP V101 2
K562 Pol2-4H8 v041610.1 ChIP-seq Peaks Rep 1 from ENCODE/HAIB
K562 Pol2-4H8 v041610.1 ChIP-seq Raw Signal Rep 1 from ENCODE/HAIB
K562 Pol2-4H8 V101 1
K562 Pol2-4H8 v041610.1 ChIP-seq Peaks Rep 2 from ENCODE/HAIB
K562 Pol2-4H8 v041610.1 ChIP-seq Raw Signal Rep 2 from ENCODE/HAIB
K562 Pol2-4H8 V101 2
K562 USF-1 v041610.1 ChIP-seq Peaks Rep 1 from ENCODE/HAIB
K562 USF-1 v041610.1 ChIP-seq Raw Signal Rep 1 from ENCODE/HAIB
K562 USF1 V101 1
K562 USF-1 v041610.1 ChIP-seq Peaks Rep 2 from ENCODE/HAIB
K562 USF-1 v041610.1 ChIP-seq Raw Signal Rep 2 from ENCODE/HAIB
K562 USF1 V101 2
GM12878 CHD2 IgG-mus ChIP-seq Peaks from ENCODE/SYDH
GM12878 CHD2 IgG-mus ChIP-seq Signal from ENCODE/SYDH
GM78 CHD2 IgM
GM12878 Pol2 IgG-mus ChIP-seq Peaks from ENCODE/SYDH
GM12878 Pol2 IgG-mus ChIP-seq Signal from ENCODE/SYDH
GM78 Pol2 IgM
GM12878 Pol2 Standard ChIP-seq Peaks from ENCODE/SYDH
GM12878 Pol2 Standard ChIP-seq Signal from ENCODE/SYDH
GM78 Pol2 Std
GM12878 Rad21 IgG-rab ChIP-seq Peaks from ENCODE/SYDH
GM12878 Rad21 IgG-rab ChIP-seq Signal from ENCODE/SYDH
GM78 Rad2 IgR
GM12878 TBP IgG-mus ChIP-seq Peaks from ENCODE/SYDH
GM12878 TBP IgG-mus ChIP-seq Signal from ENCODE/SYDH
GM78 TBP IgM
GM12878 ZNF274 Standard ChIP-seq Peaks from ENCODE/SYDH
GM12878 ZNF274 Standard ChIP-seq Signal from ENCODE/SYDH
GM78 Z274 Std
K562 CHD2 IgG-rab ChIP-seq Peaks from ENCODE/SYDH
K562 CHD2 IgG-rab ChIP-seq Signal from ENCODE/SYDH
K562 CHD2 IgR
K562 Pol2 IgG-mus ChIP-seq Peaks from ENCODE/SYDH
K562 Pol2 IgG-mus ChIP-seq Signal from ENCODE/SYDH
K562 Pol2 IgM
K562 Pol2 Standard IFNa 30min ChIP-seq Peaks from ENCODE/SYDH
K562 Pol2 Standard IFNa 30min ChIP-seq Signal from ENCODE/SYDH
K562 IFa3 Pol2 Sd
K562 Pol2 Standard IFNa 6hrs ChIP-seq Peaks from ENCODE/SYDH
K562 Pol2 Standard IFNa 6hrs ChIP-seq Signal from ENCODE/SYDH
K562 IFa6 Pol2 Sd
K562 Pol2 Standard IFNg 30min ChIP-seq Peaks from ENCODE/SYDH
K562 Pol2 Standard IFNg 30min ChIP-seq Signal from ENCODE/SYDH
K562 IFg3 Pol2 Sd
K562 Pol2 Standard IFNg 6hrs ChIP-seq Peaks from ENCODE/SYDH
K562 Pol2 Standard IFNg 6hrs ChIP-seq Signal from ENCODE/SYDH
K562 IFg6 Pol2 Sd
K562 Pol2 Standard ChIP-seq Peaks from ENCODE/SYDH
K562 Pol2 Standard ChIP-seq Signal from ENCODE/SYDH
K562 Pol2 Std
K562 Rad21 Standard ChIP-seq Peaks from ENCODE/SYDH
K562 Rad21 Standard ChIP-seq Signal from ENCODE/SYDH
K562 Rad2 Std
K562 TBP IgG-mus ChIP-seq Peaks from ENCODE/SYDH
K562 TBP IgG-mus ChIP-seq Signal from ENCODE/SYDH
K562 TBP IgM
K562 ZNF274 UC Davis ChIP-seq Peaks from ENCODE/SYDH
K562 ZNF274 UC Davis ChIP-seq Signal from ENCODE/SYDH
K562 Z274 UCD
K562 FOS GFP-tag TFBS Peaks from ENCODE/UChicago
K562 FOS GFP-tag TFBS Signal from ENCODE/UChicago
K562 FOS/GFP Sg
K562 GATA2 GFP-tag TFBS Peaks from ENCODE/UChicago
K562 GATA2 GFP-tag TFBS Signal from ENCODE/UChicago
K562 GATA2/GFP Sg
K562 HDAC8 GFP-tag TFBS Peaks from ENCODE/UChicago
K562 HDAC8 GFP-tag TFBS Signal from ENCODE/UChicago
K562 HDAC8/GFP Sg
K562 JunB GFP-tag TFBS Peaks from ENCODE/UChicago
K562 JunB GFP-tag TFBS Signal from ENCODE/UChicago
K562 JunB/GFP Sg
K562 JunD GFP-tag TFBS Peaks from ENCODE/UChicago
K562 JunD GFP-tag TFBS Signal from ENCODE/UChicago
K562 JunD/GFP Sg
K562 NR4A1 GFP-tag TFBS Peaks from ENCODE/UChicago
K562 NR4A1 GFP-tag TFBS Signal from ENCODE/UChicago
K562 NR4A1/GFP Sg
Open Chromatin by FAIRE from ENCODE/OpenChrom(UNC Chapel Hill)
GM12878 FAIRE Pk
GM12878 FAIRE DS
GM12878 FAIRE OS
H1-hESC FAIRE Pk
H1-hESC FAIRE DS
H1-hESC FAIRE OS
K562 FAIRE Pk
K562 FAIRE DS
K562 FAIRE OS
GM12878 cMyc TFBS ChIP-seq Peaks from ENCODE/OpenChrom-UTA
GM12878 cMyc TFBS ChIP-seq Density Signal ENCODE/OpenChrom-UTA
GM12878 cMyc DS
GM12878 cMyc TFBS ChIP-seq Overlap Signal ENCODE/OpenChrom-UTA
GM12878 cMyc OS
GM12878 CTCF TFBS ChIP-seq Peaks from ENCODE/OpenChrom-UTA
GM12878 CTCF TFBS ChIP-seq Density Signal ENCODE/OpenChrom-UTA
GM12878 CTCF DS
GM12878 CTCF TFBS ChIP-seq Overlap Signal ENCODE/OpenChrom-UTA
GM12878 CTCF OS
GM12878 Pol2 TFBS ChIP-seq Peaks from ENCODE/OpenChrom-UTA
GM12878 Pol2 TFBS ChIP-seq Density Signal ENCODE/OpenChrom-UTA
GM12878 Pol2 DS
GM12878 Pol2 TFBS ChIP-seq Overlap Signal ENCODE/OpenChrom-UTA
GM12878 Pol2 OS
GM12878 Input TFBS ChIP-seq Density Signal ENCODE/OpenChrom-UTA
GM12878 Input DS
H1-hESC cMyc TFBS ChIP-seq Peaks from ENCODE/OpenChrom-UTA
H1-hESC cMyc TFBS ChIP-seq Density Signal ENCODE/OpenChrom-UTA
H1-hESC cMyc DS
H1-hESC cMyc TFBS ChIP-seq Overlap Signal ENCODE/OpenChrom-UTA
H1-hESC cMyc OS
H1-hESC CTCF TFBS ChIP-seq Peaks from ENCODE/OpenChrom-UTA
H1-hESC CTCF TFBS ChIP-seq Density Signal ENCODE/OpenChrom-UTA
H1-hESC CTCF DS
H1-hESC CTCF TFBS ChIP-seq Overlap Signal ENCODE/OpenChrom-UTA
H1-hESC CTCF OS
H1-hESC Pol2 TFBS ChIP-seq Peaks from ENCODE/OpenChrom-UTA
H1-hESC Pol2 TFBS ChIP-seq Density Signal ENCODE/OpenChrom-UTA
H1-hESC Pol2 DS
H1-hESC Pol2 TFBS ChIP-seq Overlap Signal ENCODE/OpenChrom-UTA
H1-hESC Pol2 OS
K562 cMyc TFBS ChIP-seq Peaks from ENCODE/OpenChrom-UTA
K562 cMyc TFBS ChIP-seq Density Signal ENCODE/OpenChrom-UTA
K562 cMyc DS
K562 cMyc TFBS ChIP-seq Overlap Signal ENCODE/OpenChrom-UTA
K562 cMyc OS
K562 CTCF TFBS ChIP-seq Peaks from ENCODE/OpenChrom-UTA
K562 CTCF TFBS ChIP-seq Density Signal ENCODE/OpenChrom-UTA
K562 CTCF DS
K562 CTCF TFBS ChIP-seq Overlap Signal ENCODE/OpenChrom-UTA
K562 CTCF OS
K562 Pol2 TFBS ChIP-seq Peaks from ENCODE/OpenChrom-UTA
K562 Pol2 TFBS ChIP-seq Density Signal ENCODE/OpenChrom-UTA
K562 Pol2 DS
K562 Pol2 TFBS ChIP-seq Overlap Signal ENCODE/OpenChrom-UTA
K562 Pol2 OS
K562 Input TFBS ChIP-seq Density Signal ENCODE/OpenChrom-UTA
K562 Input DS
DNaseI Digital Genomic Footprinting from ENCODE/University of Washington
K562 Sig
HepG2 Sig
HUVEC Sig
DNaseI Hypersensitivity by Digital DNaseI from ENCODE/University of Washington
GM12878 Ht 1
GM12878 Pk 1
GM12878 Sg 1
GM12878 Ht 2
GM12878 Pk 2
GM12878 Sg 2
H1hESC Ht 1
H1hESC Pk 1
H1hESC Sg 1
K562 Ht 1
K562 Pk 1
K562 Sg 1
K562 Ht 2
K562 Pk 2
K562 Sg 2
100 vertebrates Basewise Conservation by PhyloP
100 Vert. Cons
Multiz Alignments of 100 Vertebrates
Gaps
Human
Rhesus
Mouse
Dog
Elephant
Chicken
X_tropicalis
Zebrafish
Lamprey
Opossum (Oct. 2006 (Broad/monDom5)) Alignment Net
chr3 - 31433k
Chicken (May 2006 (WUGSC 2.1/galGal3)) Chained Alignments
Chicken (May 2006 (WUGSC 2.1/galGal3)) Alignment Net
X. tropicalis (Nov. 2009 (JGI 4.2/xenTro3)) Alignment Net
Zebrafish (Jul. 2010 (Zv9/danRer7)) Alignment Net
Simple Nucleotide Polymorphisms (dbSNP 144) Found in >= 1% of Samples
rs9462935
rs4711751
Simple Nucleotide Polymorphisms (dbSNP 142) Found in >= 1% of Samples
rs9462935
rs4711751
Repeating Elements by RepeatMasker
RepeatMasker

Supplementary Figure S4: Thyroid eQTL data (GTEX portal.org)

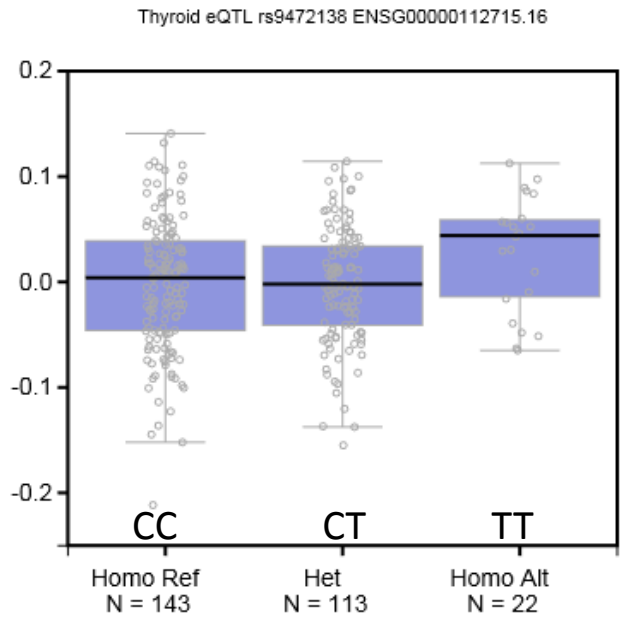

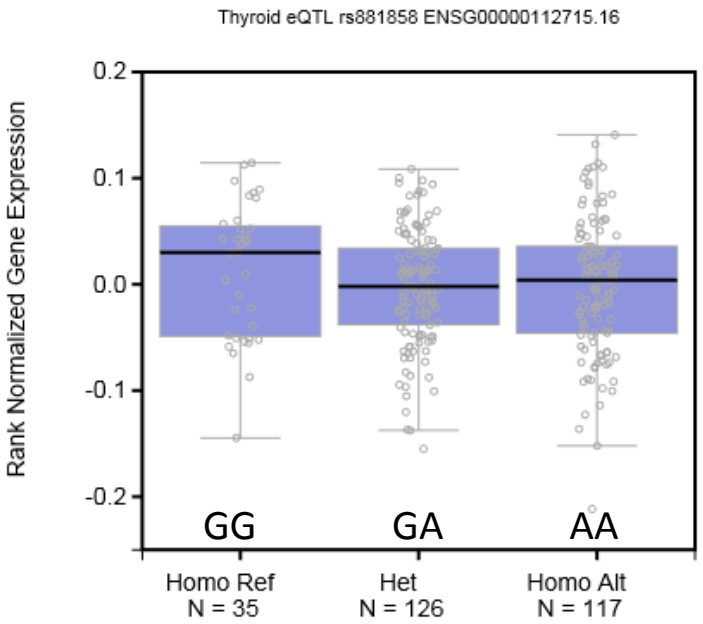

SNP	P-Value	Effect Size
rs9472138	0,15	0,067
rs881858	0,22	-0,058
rs943080	0,24	0,049
rs4711751	0,26	-0,047

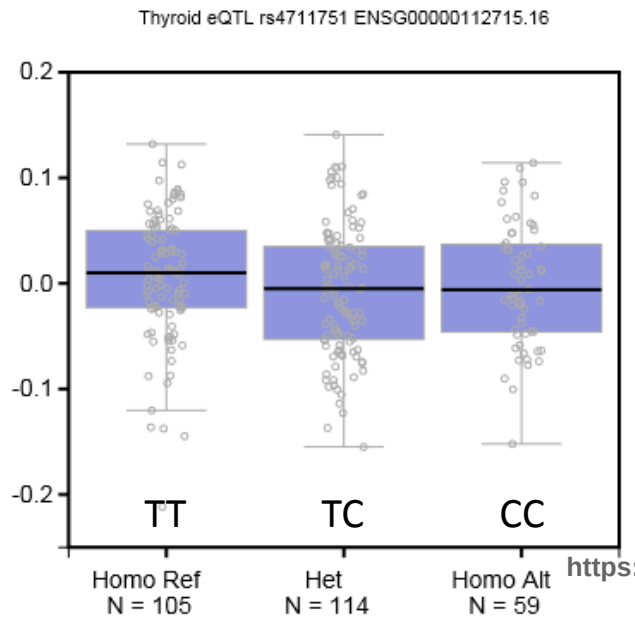

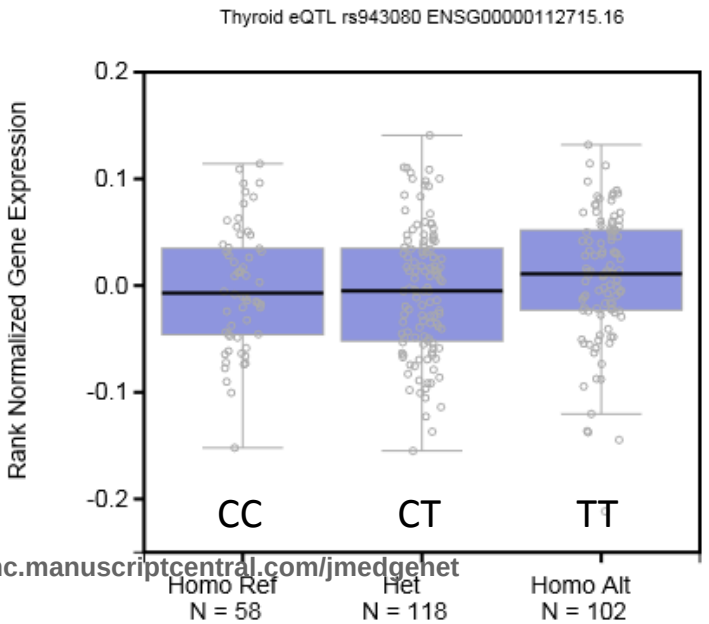

Supplementary tables

Table S1: Baseline characteristics of the three Danish cohorts participating in discovery analyses.

	Inter99	Health2006	Health2008
N	5645	2711	601
Men (%)	50.1	44.8	43.7
Age (yrs)	46.1 ± 7.9	48.9 ± 13.1	46.4 ± 8.1
BMI (kg/m^2)	26.2 ± 4.5	25.8 ± 4.6	25.6 ± 4.3
TSH (mIU/L)	1.39 ± 0.67	1.53 ± 0.73	1.15 ± 0.55

Data are mean ± standard deviation.

Table S2: Study population characteristics at baseline and at five years follow-up in the Inter99 normal glucose tolerant (NGT) participants.

Characteristics	Baseline	Follow up	Changes from baseline to follow-up
n (%men)	4,374 (46.3%)	Up to 3,467 (46.4%)	
Age (years)	45.1 ± 7.8	50.5 ± 7.8	5.38 ± 2.3
BMI (kg/m^2)	25.5 ± 4.0	25.7 ± 4.0	0.44 ± 1.7
HbA1c (%)	5.7 ± 0.3	5.7 ± 0.3	-0.038 ± 0.26
Leptin (ng/ml)	5.3 (2.4-11.1)	-	-
T4 (pmol/L)	15 (13.9-16.3)	14.7 (13.6-15.9)	-0.3 (-1.3-0.6)
TSH (mU/L)	1.26 (0.91-1.75)	1.41 (1.0-1.99)	0.14 (-0.15-0.5)
Fasting plasma glucose (mmol/L)	5.3 ± 0.4	5.2 ± 0.5	-0.046 ± 0.49
2hr glucose (mmol/L)	5.4 ± 1.1	5.5 ± 1.4	0.016 ± 1.48
Fasting serum insulin (pmol/L)	31.0 (22.0 - 45.0)	28.0 (21.0 - 41.0)	-1.0 (-11.0-8.0)
Insulin sensitivity index ($ISI_{MATSUDA}$)	3.16 (2.24-4.44)	3.12 (2.18-4.40)	-
Insulinogenic index	77.1 (49.1-128.0)	77.1 (50.0-124.2)	-
HOMA-IR	1.21 (0.83-1.80)	1.09 (0.77-1.65)	-0.05 (-0.46-0.34)
Disposition index	229.2 (161.7-348.2)	230.8 (161.6-337.2)	-

We use interquartile range for insulin and related measures as the distribution may be skewed. Data are mean ± SD or median (interquartile range)

Table S3: Oligonucleotides used for cloning *VEGFA* promoter-enhancer constructs and electrophoretic mobility shift assays

Name	Sequence (italics: tail for fill-in labeling, bold CHOP10 site, red: rs881858)	Purpose
RS881858 G sense >hg19_dna range=chr6:43806593-43806628	*agct*TGCTG**TTATGCAAT*G*ATC**CCGC	Fill-in labeled probe
RS881858 G a-sense	*agct*GCGG**GATCATTGCATAA**CAGCA	Fill-in labeled probe
RS881858 A sense	*agct*TGCTG**TTATGCAAT*A*ATC**CCGC	Fill-in labeled probe
RS881858 A a-sense	*agct*GCGG**GAT*T*ATTGCATAA**CAGCA	Fill-in labeled probe
c/EBPβ sense	*agct*GCGTTGCGCCACGATCTCTC	Fill-in labeled probe
c/EBPβ a-sense	*agctGAGAGATCGTGGCGCAACGC*	Fill-in labeled probe
RS881858 G sense f	*agct*TGCTG**TTATGCAAT*G*ATC**CCGC*agct*	Full length probe for competition assays
RS881858 G a-sense f	*agct*GCGG**GATCATTGCATAA**CAGCA*agct*	Full length probe for competition assays
RS881858 A sense f	*agct*TGCTG**TTATGCAAT*A*ATC**CCGC*agct*	Full length probe for competition assays
RS8818 58 A a-sense f	*agct*GCGG**GAT*T*ATTGCATAA**CAGCA*agct*	Full length probe for competition assays
c/EBPβ sense f	*agct*GCGTTGCGCCACGATCTCTC*agct*	Full length probe for competition assays
c/EBPβ a-sense f	*agct*GAGAGATCGTGGCGCAACGC*agct*	Full length probe for competition assays
CHOP10 sense	*agct*TTCTGATGCAACTGGCTGAG	Fill-in labeled probe
CHOP10 a-sense	*agct*CTCAGCCAGTTGCATCAGAA	Fill-in labeled probe
CHOP10 sense f	*agct*TTCTGATGCAACTGGCTGAG*agct*	Full length probe for competition assays
CHOP10 a-sense f	*agct*CTCAGCCAGTTGCATCAGAA*agct*	Full length probe for competition assays
VEGFA pro F	CTAACTGGCCGGTACCTTCCCAAAGGAC CCCAGTC	Cloning: PCR primer VEGFA promoter-exon 1, sense
VEGFA pro R	TATCCTCGAGGCTAGGCCCGATTCAAGT GGGGAAT	Cloning: PCR primer VEGFA promoter-exon 1, a-sense
RS881858 sense	AAATCGATAAGGATCCTCTTCCACAGAA GTCAGAGTGC	Cloning: PCR primer RS881858 region, sense
RS881858 a-sense	AAGGGCATCGGTCGACCAAAGCCCCTTG CCTCCC	Cloning: PCR primer RS881858 region, a-sense
RS9472138 sense	AAATCGATAAGGATCCACCCTAAGCACG TTCTCCTC	Cloning: PCR primer RS9472138 region, sense
RS9472138 a-sense	AAGGGCATCGGTCGACACAACCTACTGA TACATGCCACA	Cloning: PCR primer RS9472138 region, a-sense

Table S4: *VEGFA* SNPs not reaching study-wide significance for association with circulating levels of thyroid stimulating hormone (TSH)

SNP name	Position (build 37/hg19)	Location wrt *VEGFA*	Alleles (effect/ other)	EAF	Inter99 *n*=5,420		Health2006 *n*=-2,442		Health2008 *n*=583		Combined		
					Effect	*P*	Effect	*P*	Effect	*P*	*N*	*P*	I^2 (P_{HET})
rs114656313	43,692,999	Upstream	A/C	0.026	-0.012	0.65	0.03	0.45	0.0007	0.99	8,445	0.95	0 (0.69)
rs76074477	43,713,214	Upstream	A/G	0.043	0.056	0.0098	-0.047	0.63	-0.081	0.21	8,445	0.12	67 (0.05)
rs36208384	43,737,909	5' region	A/C	0.016	0.018	0.56	0.003	0.57	-0.087	0.47	8,440	0.54	0 (0.67)
rs74500696	43,748,845	Intron	A/G	0.012	-0.037	0.36	-0.026	0.95	0.008	0.94	8,445	0.49	0 (0.83)
rs998584	43,757,896	Downstream	G/T	0.45	-0.004	0.62	0.016	0.86	-0.007	0.78	8,426	0.57	0 (0.99)
rs6905288	43,758,873	Downstream	A/G	0.55	-0.004	0.62	-0.016	0.25	-0.008	0.74	8,444	0.27	0 (0.79)
rs68016381	43,761,645	Downstream	T/C	0.047	-0.048	0.021	-0.013	0.12	-0.050	0.46	8,445	0.004	0 (1.0)
rs35349911	43,785,255	Downstream	T/C	0.43	-0.001	0.90	0.028	0.23	-0.013	0.62	8,445	0.54	0 (0.52)
rs943072	43,795,968	Downstream	A/C	0.09	-0.003	0.82	0.003	0.88	-0.016	0.73	8,445	0.86	0 (0.92)
rs145023524	43,819,046	Downstream	A/G	0.006	-0.006	0.91	-0.002	0.55	0.12	0.40	8,445	0.62	0 (0.66)
rs55663434	43,820,609	Downstream	A/G	0.015	-0.031	0.39	-0.015	0.59	0.034	0.73	8,445	0.38	0 (0.83)

[#]SNPs in LD (r^2>0.4). EAF: Effect allele frequency. I^2: heterogeneity at meta-analyses level. P_{HET}: P value for heterogeneity

Table S5: Evaluation of possible regulatory variants in the *VEGFA* locus.

SNP	Position (hg19/chr 6)	Open chromatin (DNase seq)	Conser-vation	H3K27 acetylation marks	H3K4Me1 marks	Chip-Seq signal	SNP located in TFX BS
rs729761 G>T	43804571	+	-	-	+	+ (RCOR1, NR2F2, TEAD4, GATA2, TAL1)	-
rs2396083 G>C	43804808	(+)	-	-	+	-	-
rs2396084 G>A	43804825	(+)	-	-	+	-	-
rs744103 A>T	43805362	-	-	-	(+)	+ (CMYC)	-
rs10223666 C>G	43805502	(+)	+	-	(+)	-	-
rs1317983* C>T	43806335	-	-	+	+	+ (RAD21, CTCF)	-
rs881858 G>A	43806609	+	+	+	+	+ (CEBPB)	+ (CEBPB & CHOP)
rs9472135 T>C	43809802	-	-	-	-	-	-
rs9472137 T>C	43810469	-	-	-	-	-	-
rs9369425 G>A	43810974	+	-	+	+	+ (MAFF)	-
rs9369427 A>C	43811430	-	-	(+)	+	+ (POLR2R, GATA2)	-
rs9472138 C>T	43811762	-	-	-	+	+ (MAFK, CEBPB)	-
rs1536304 T>C	43817837	-	-	-	+	+ (FOXA1)	-#
rs7758685 G>A	43825266	-	-	-	-	-	-
rs9394969 G>T	43825459	-	-	-	-	-	-
rs943080 T>C	43826627	-	+	-	+	-	-
rs4711751 T>C	43828582	-	-	-	-	-	-

*rs1317983 is located just 274nt 5' of rs881858 and these SNPs share peak for H3K27Ac and H3K4Me1 marks. #FOXA1 site is 2 nt 3' of SNP, but position is not important for binding. TFX BS: Transcription factor binding site. This table was compiled based on data in Fig. S3.

Table S6: Changes from baseline to follow-up (5yr) in the Inter99 cohort among normal glucose tolerant subjects at baseline for GG, GA and AA genotypes of *VEGFA* rs881858

***VEGFA* rs881858**	**GG**	**GA**	**AA**	**N total**	***Effect**	**SE**	***P***
Δ TSH (mIU/L)	0.16 (-0.08, 0.47)	0.12 (-0.17, 0.46)	0.14 (-0.17, 0.53)	2843	-0.024	0.088	0.78
Δ Free T4 (pmol/L)	-0.5 (-1.4, 0.4)	-0.3 (-1.2, 0.8)	-0.3 (-1.3, 0.6)	2856	-0.027	0.067	0.68
Δ BMI (kg/m^2)	0.61 ± 1.6	0.41 ± 1.8	0.43 ± 1.6	3466	0.033	0.046	0.47
Δ HbA1c (%)	-0.05 (-0.17, 0.13)	-0.05 (-0.16, 0.13)	-0.06 (-0.17, 0.13)	2991	0.002	0.007	0.69
Δ Fasting plasma glucose (mmol/L)	-0.1 (-0.3, 0.2)	-0.1 (-0.3, 0.2)	-0.1 (-0.3, 0.2)	2985	0.005	0.014	0.69
Δ 2-hour glucose during OGTT (mmol/L)	-0.1 (-0.8, 0.7)	0 (-0.9, 0.8)	-0.1 (-1.0, 0.8)	2965	0.072	0.042	0.091
Δ Fasting serum insulin (pmol/L)	-2.0 (-12.7, 8)	-1.0 (-11, 9)	-1.0 (-11, 8)	2981	-0.72	0.68	0.28
Δ HOMA-IR	-0.09 (-0.50, 0.31)	-0.05 (-0.46, 0.34)	-0.04 (-0.46, 0.33)	2979	-0.025	0.028	0.36

* G allele of *VEGFA* as the effect allele assuming an additive genetic model. N total is the number of normal glucose tolerant subjects at baseline who had genotype and phenotype information available during follow-up as well. Values correspond to median (interquartile range) in non-transformed traits

Table S7. Formulas used for calculating insulinogenic index, the Matsuda insulin sensitivity index, the disposition index and HOMA-IR

Trait	Measurement or calculation
Insulinogenic index	(Serum insulin at 30-min (pmol/l) - fasting serum insulin (pmol/l)) / (plasma glucose at 30-min (mmol/l) - fasting plasma glucose (mmol/l))
$ISI_{Matsuda}$	(10,000/√(fasting plasma glucose (mmol/l)×18 × fasting serum insulin (pmol/l)/6) × (mean plasma glucose (mmol/l)×18 × mean serum insulin (pmol/l)/6 during OGTT))
Disposition index	The insulinogenic index × $ISI_{Matsuda}$
HOMA-IR	((fasting serum insulin (pmol/l)/ 6)*(fasting plasma glucose (mmol/l)))/22.5